August 1985

EUROPEAN ORGANISATION FOR EXPERIMENTAL PHOTOGRAMMETRIC RESEARCH

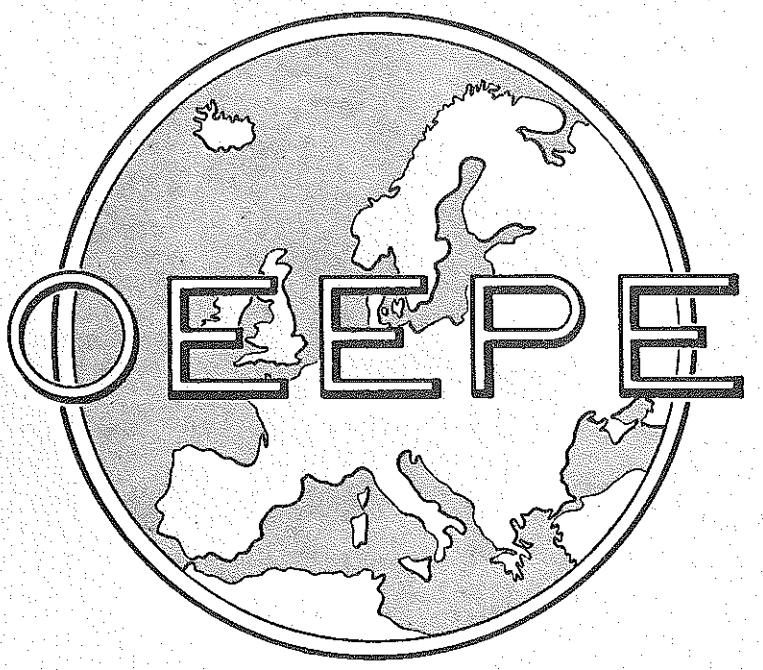

OFFICIAL PUBLICATION

N° 15

Wir bitten, die vorgedruckte Empfangsbestätigung auf der unteren Hälfte dieses Blattes herauszutrennen, Ihre Adresse, bei Änderung auch die frühere, einzutragen und die Karte zurückzusenden. Bei mehreren Heften in einer Lieferung genügt es, nur eine Karte zurückzusenden, wenn die Nummern der anderen Hefte auf dieser notiert sind. *Sollten die Bestätigungskarten ausbleiben, müssen wir annehmen, daß Sie am Tauschverkehr mit uns nicht mehr interressiert sind, und weitere Lieferungen einstellen.*

Please detach the acknowledgement of receipt attached below, enter your address, in case of change enter your former address, too, and return the card.
If a shipment comprises several volumes, please return one card only listing all numbers. *If the receipt is not acknowledged we understand that you are no longer interested in our exchange of publications and that you wish to be cancelled from our mailing list.*

Ayez la bontē de dētacher l'accusē de rēception que vous trouvez sur la partie inférieure de cette page, d'y inscrire votre adresse et, le cas échéant, votre ancienne adresse et de retourner la carte.
Si la livraison se compose de plusieurs fascicules, il suffit de ne retourner qu'une seule carte portant ēgalement les numēros des autres fascicules. *Le fait d'avoir expēdiē un envois sans avoir reçu la carte de rēception nous donnera raison à supposer que vous n'êtes plus intéressés à continuer l'échange de publications et que vous approuverez l'arrêt de nos envois.*

Le rogamos sacar el acuse de recibo figurando en la parte inferior de esta pāgina, inscribir su dirección y si ha cambiado, inscribir la dirección anterior, y retornar esta tarjeta.
Si el envío se compone de varios fascículos es bastante retornarnos una sola tarjeta indicando también los nūmeros de los otros fascículos. *Si quedamos sin acuses de recibo tenemos que suponer que ya no tiene Vd interēs en nuestro cambio de publicaciones y que desea Vd suspender otros envíos.*

Absender:
Sender:
Expēditeur:
Expedidor:

Es sind hier eingegangen:
We received:
Nous avons reçu:
Han llegado en nuestras manos:

OEEPE
Publ. off. No. 15

Institut für Angewandte Geodäsie
Richard-Strauss-Allee 11
D-6000 Frankfurt am Main 70
Germany · Allemagne · Alemania

August 1985

EUROPEAN ORGANISATION FOR EXPERIMENTAL PHOTOGRAMMETRIC RESEARCH

OFFICIAL PUBLICATION

N° 15

ISSN 0257-0505

Printed and published by the Institut für Angewandte Geodäsie, Frankfurt a. M.

EUROPEAN ORGANISATION
for
EXPERIMENTAL PHOTOGRAMMETRIC RESEARCH

STEERING COMMITTEE

(composed of Representatives of the Governments of the Member Countries)

President:	Director General P. Mc MASTER Ordnance Survey Romsey Road Maybush Southampton S09 4DH	United Kingdom
Members:	w. Hofrat Dr. techn. J. BERNHARD Bundesamt für Eich- und Vermessungswesen Krotenthallergasse 3 A-1080 Wien	Austria
	Administrateur-Général J. DE SMET Institut Géographique National 13, Abbaye de la Cambre B-1050 Bruxelles	Belgium
	Ir. J. VEREECKEN Director of the Dept. of Photogrammetry Institut Géographique National 13, Abbaye de la Cambre B-1050 Bruxelles	
	Mr. O. BRANDE-LAVRIDSEN Laboratoret for Fotogrammetri og Landmåling Ålborg Universitets Center Fibigerstraede 11 DK-9220 Ålborg Ø	Denmark
	Mr. J. KRUEGER Matrikeldirektoratet Opmalingsafdelingen Titangade 13 DK-2200 Copenhagen N	
	Prof. Dr.-Ing. F. ACKERMANN Institut für Photogrammetrie der Universität Stuttgart Keplerstrasse 11 D-7000 Stuttgart 1	Federal Republic of Germany
	Prof. Dr.-Ing. G. HAMPEL Präsident des LVA Baden-Württemberg Büchsenstrasse 54 D-7000 Stuttgart 1	
	Direktor Dr.-Ing. W. SATZINGER Institut für Angewandte Geodäsie Richard-Strauss-Allee 11 D-6000 Frankfurt a. M. 70	

Finland

Mr. M. JAAKKOLA
National Board of Survey
Box 84
SF-00521 Helsinki 52

Prof. Dr. E. KILPELÄ
Institute of Photogrammetry Helsinki
University of Technology
SF-02150 Espoo 15

France

Mr. J. DESUDDE
Institut Géographique National
Aérodrome de Creil
F-60107 Creil

Mr. G. DUCHER
Directeur de la Recherche
Institut Géographique National
2, Avenue Pasteur
F-94160 Saint Mandé

Italy

Prof. Dr. M. CUNIETTI
Istituto Topografia, Fotogrammetria e Geofisica
Piazza Leonardo da Vinci 32
I-20133 Milano

Dr. Eng. L. SURACE
Geographical Military Institute
Via Cesare Battista 8—10
I-50122 Firence

Netherlands

Prof. Ir. A. J. VAN DER WEELE
International Institute for Aerospace Survey
and Earth Sciences (ITC)
350 Boulevard 1945, P. O. Box 6
NL-7500 AA Enschede

Ir. C. J. REMYNSE
Hoofdirekteur Hoofdirektie
v. h. Kadaster en de Openbare Registers
Waltersingel 1
NL-7300 GH Apeldoorn

Norway

Director E. O. DAHLE
Norges Geografiske Oppmåling
N-3500 Hønefoss

Mr. Ø. BRANDSÆTER
Deputy Director
Mapping Division
Norges Geografiske Oppmåling
N-3500 Hønefoss

Sweden

Prof. K. TORLEGÅRD
Royal Institute of Technology
Dept. of Photogrammetry
S-10044 Stockholm 70

Mr. L. OTTOSON
National Land Survey of Sweden
S-80112 Gävle

Switzerland

Prof. Dr. O. KÖLBL
Institut de Photogrammétrie, EPFL
GR-Ecublens
CH-1015 Lausanne

Director R. SCHOLL
Schweizerische Schule für
Photogrammetrie-Operateure
Rosenbergstrasse 16
CH-9000 St. Gallen

Dr. I. J. DOWMAN
Dept. of Photogrammetry and Surveying
University College London
Gower Street 6
London WC 1E BT

United Kingdom

EXECUTIVE BUREAU

Mr. J. KURE
Secretary General of the OEEPE
International Institute for Aerospace Survey
and Earth Sciences (ITC)
350 Boulevard 1945, P. O. Box 6
NL-7500 AA Enschede (Netherlands)

Prof. Dr. H. G. JERIE
International Institute for Aerospace Survey
and Earth Sciences (ITC)
350 Boulevard 1945, P. O. Box 6
NL-7500 AA Enschede (Netherlands)

Prof. Ir. J. VISSER
International Institute for Aerospace Survey
and Earth Sciences (ITC)
350 Boulevard 1945, P. O. Box 6
NL-7500 AA Enschede (Netherlands)

HONORARY SECRETARY GENERAL

Ir. R. VERLAINE
Secretaire General Honoraire
36 Avenue E, Digneffe
Liège (Belgium)

SCIENTIFIC COMMISSIONS

Commission A — **Aerotriangulation**

President: Mrs. P. NOUKKA
National Board of Survey
Box 84
SF-00521 Helsinki 52

Commission B — **Digital Elevation Models**

President: Dr. K. TEMPFLI
International Institute for Aerospace Survey
and Earth Sciences (ITC)
350 Boulevard 1945, P. O. Box 6
NL-7500 AA Enschede

Commission C — **Large scale Restitution**

President: Prof. Dr. O. KÖLBL
Institut de Photogrammétrie, EPFL
GR-Ecublens
CH-1015 Lausanne

Commission D — **Photogrammetry and Cartography**

President: Major General C. THOMPSON
Directorate of Military Survey
Ministry of Defense
Elmwood Avenue
Feltham Middlesex TW13 7AE

Commission E — **Topographic Interpretation**

President: Prof. Dr.-Ing. W. HOFMANN
Heinrich-Vogl-Strasse 7
D-8000 München 71

Commission F — **Fundamental Problems of Photogrammetry**

President: Prof. Dr. G. LIGTERINK
Technical University Delft
Thijsseweg 11
NL-2600 GA Delft

APPLICATION COMMISSIONS

Commission I — **Topographic Mapping**

President: Prof. Ir. L. VAN ZUYLEN
Topographic Service
Westvest 9
NL-2613 AX Delft

Commission II — **Cadastral Mapping**

President: Mr. J. KRUEGER
Matrikeldirektoratet Opmalingsafdelingen
Titangade 13
DK-2200 Copenhagen N

Commission III — **Engineering Surveys**

Commission IV — **Environmental/Thematic Surveys**

President: Mr. B. FOLLESTAD
Deputy Director Geological Survey of Norway
Leif Erikssonsvei 59, Postboks 3006
N-700 Trondheim

Commission V — **Land Information Systems**

President: Prof. Dr.-Ing. G. EICHHORN
Technische Hochschule Darmstadt
Hochschulstrasse 61
D-6100 Darmstadt

DK 528.711.1:771.53

Optimal Emulsions for Large-Scale Mapping

(Test of "Steinwedel")

Commission C of the OEEPE 1981—84

(with 53 Figures)

By Matti Jaakkola, Wolfgang Brindöpke, Otto Kölbl, Pirkko Noukka

Table of Contents

After page 102:
List of OEEPE publications

Optimal Emulsions for Large-Scale Mapping

(Test of "Steinwedel")

1 Introduction

The planimetric accuracy of photogrammetric methods in large-scale mapping was examined thoroughly in the previous test programmes of Commission C/OEEPE. As a result, a good understanding has been gained of the applicability and limitations of the photogrammetric survey method from the point of view of geometrical quality. The tests to which I refer are those by Oberriet, Reichenbach, Dordrecht and Vienna.

Another basic question in the photogrammetric survey method is the completeness of the survey. How much field data can be reliably interpreted and measured from the image. The volume of reliable data gathered is mainly of economic and practical importance but this has been a subject of controversy in the test programmes of a purely geometrical nature as well.

Several tools exist with which we can increase the volume and reliability of image data. One of them is targeting of some objects. Use of the correct emulsion is beneficial for some types of interpretation, and proper illumination of the measuring device may be as important in restitution work.

The survey agencies have usually adopted a particular emulsion for standard use in large-scale mapping. At present, however, a great variety of different emulsions are available, both black & white, and colour. In this study an attempt will be made to establish whether there are significant general differences, advantages or disadvantages in the use of different emulsions in large-scale mapping.

The test "Optimal Emulsions for Large-Scale Mapping" was initiated and outlined by Dr. *Brindöpke*. In 1981 both Commission C and the Steering Committee of the OEEPE accepted the test for inclusion in the test programme of Commission C.

The prestudies were made by Prof. *Kölbl* in 1981—82. In 1981 a working group consisting of *Jaakkola, Brindöpke, Kölbl* and *Noukka* was established within Commission C to implement the project.

During planning of the test, three main aspects of the method were identified: image quality, interpretation and accuracy. As stated above, accuracy has already been the principal subject of several tests, and direct repetition of such tests would be very unlikely to give any essentially new information. On the other hand, image quality, and consequently its interpretation, have only very rarely been identified as important, so they were given precedence here and accuracy was considered only so far as was necessary for the experiment. Apart from emulsions the other parameters were identified from the nature of the large-scale mapping.

Three centres were established, one for each of the main aspects,

Functions of the Pilot Centre and analysis of the reliability of interpretation for the various emulsions: Niedersächsisches Landesverwaltungsamt, Hannover, through Dr. *Brindöpke*.

Image Quality, a photographic-physical test of the emulsion, bearing in mind the different target-subsoil combinations: Ecole Polytechnique Fēdērale, Lausanne, through Prof. *Kölbl.*

Geometrical Accuracy, a geometrical test of the numerical restitutions of the highest precision of the signalized points: National Board of Survey, Helsinki, through Tec. Lic. *Noukka.*

Details of test arrangements and the results are presented in Chapters 2—7.

2 Project description

2.1 Objectives of the test

For the test field and the photo flight the following questions were of primary interest:

- what are the absolute accuracies of signalized points for different emulsions?
- what are the optimum combinations of emulsion, target colour and subsoil that can be measured?
- do any of the emulsions provide an especially good acuity, e. g. in the case of eaves?
- are there differences in reliability of interpretation for the different emulsions?

In addition to the above main aims, it should also be possible to investigate other questions about large-scale photography such as:

- what results do the different emulsions give when photo flights are made in cloudy weather?
- how does underexposure or overexposure affect the objects to be photographed, e. g. targets, topographical objects?

2.2 Choice of test frames

2.2.1 Test area

In spring 1982 the Pilot Centre at Hannover chose a test area "Steinwedel" 15 km east of Hannover (Figure 1). It has the following features:

- it covers about 400 x 600 metres;
- part of it is open and free for signalizing without interference;
- there are several different topographical objects (buildings, streets, waterfronts, landmarks, meadows, arable land, etc.);
- differences in height are insignificant.

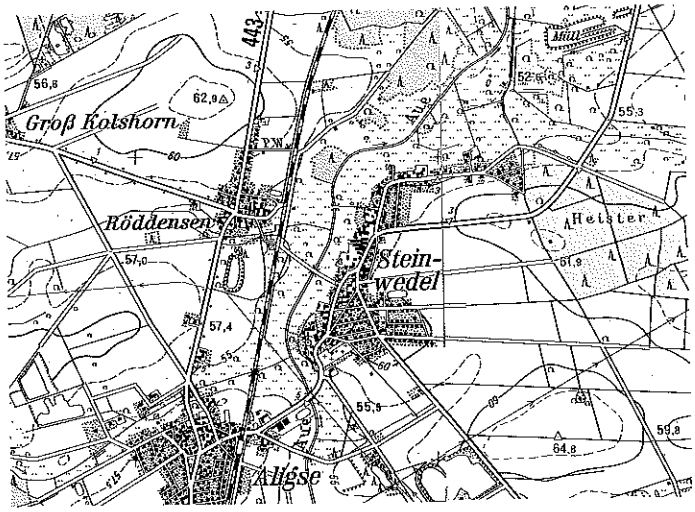

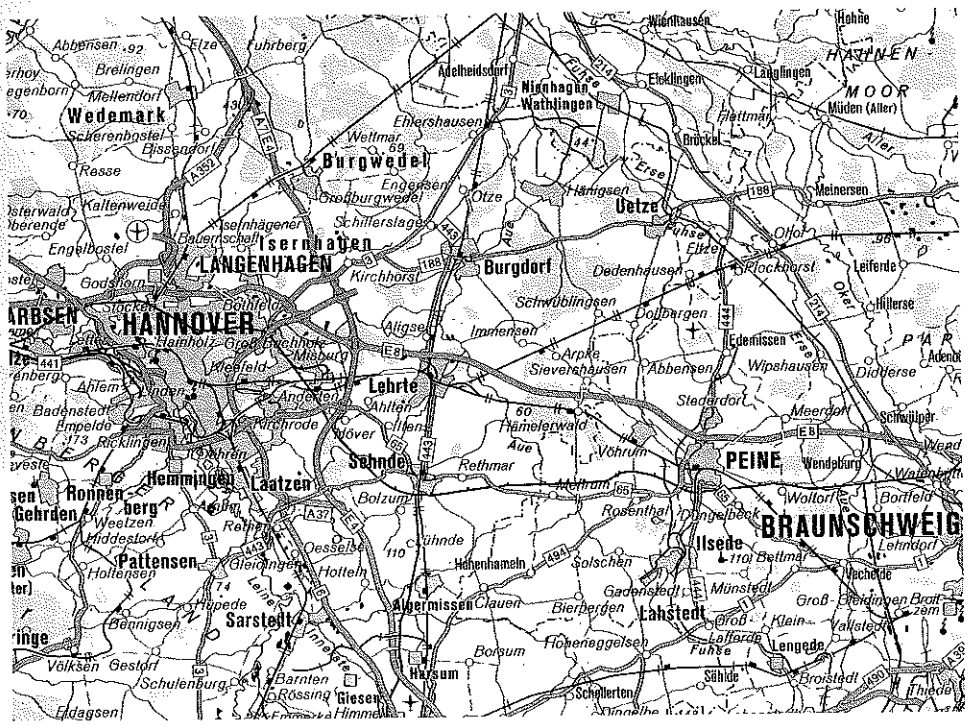

Figure 1 — Location of the test field

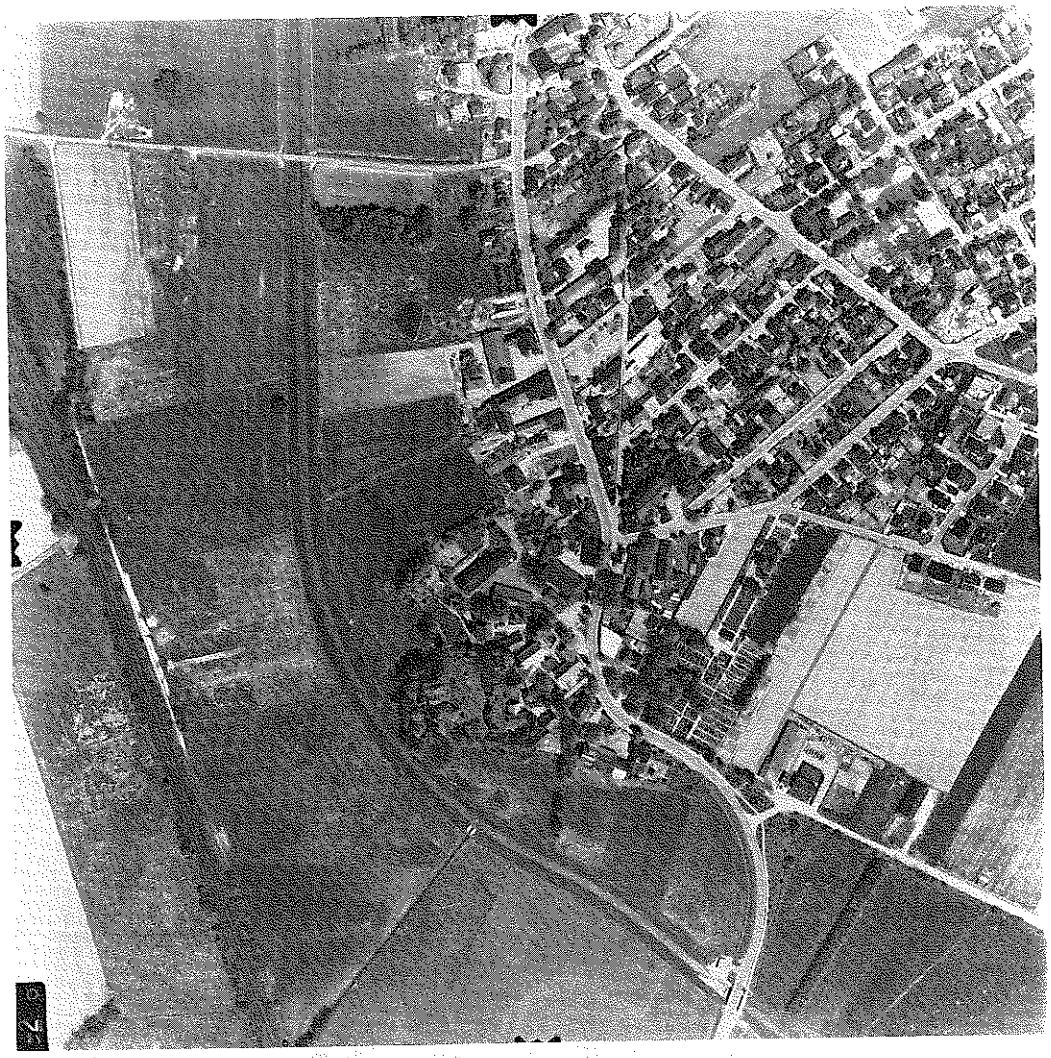

Figure 2 — Aerial photograph of the test field "Steinwedel"

2.2.2 Choice of emulsions

For the test nine emulsions were chosen, which are described in more detail in Figure 5.

2.2.3 Aerial photography

The following parameters were chosen for the aerial photography:

- scale of photography: 1 : 4000;
- camera: Zeiss RMK 30/23 with Topar 5,6 f lens;

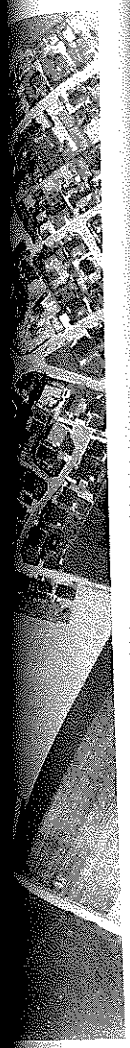

igure 5.

- photography to be completed by: May 9, 1982;
- photo flight companies: Hansa Luftbild and Kirchner & Wolf;
- photo flight conditions:
  - partly clear sky with good visibility;
  - partly clouded sky (under the clouds);
  - altogether 17 "flights" with different emulsions and conditions were planned;
- flight course:
  - each flight should produce at least two models of the test area for each round trip;
  - the test area should be completely covered by one model.

Further information about aerial photography is given in Chapter 2.4.

2.3 Field preparations

2.3.1 Control survey

All ground control measurements were carried out by the National Survey of Lower Saxony, Hannover, and were guided by Dr. *W. Tegeler.*

The ground control included twenty stations altogether which were marked permanently with either steel or plastic pipes (Figure 4). The inserted caps permit all the marks to be identified to an accuracy of 1 mm.

The measurements were carried out with Elta 2 and SM 4 electrooptical tachymeters with automatic centring. The directions were measured with the Elta 2 in two rounds and with the SM 4 in three rounds. The distances were calculated from reciprocal measurements, whereby the zero point and scale corrections were determined from the Hannover calibration line before and after the survey.

The traverse network was computed in free adjustment and orientated to the land coordinate system with a three parameter transformation. The net adjustment included 87 redundant observations and the standard deviations of the coordinates varied from $\pm$ 0.001 to $\pm$ 0.003 metres.

2.3.2 Check point survey

In addition to the ground control stations, the test field included 113 actual check points (Figure 4), of which 87 were determined with a double polar survey. The standard deviations of the check point coordinates were up to $\pm$ 0.013 metres. The rest of the check points were roof points without any coordinates.

2.3.3 Targeting

The twenty ground control stations were signalized with 12 x 12 cm red-orange targets and fitted with 30 x 30 cm black contrast plates and two 10 x 80 cm white identification stripes. All the control stations were visible from the air.

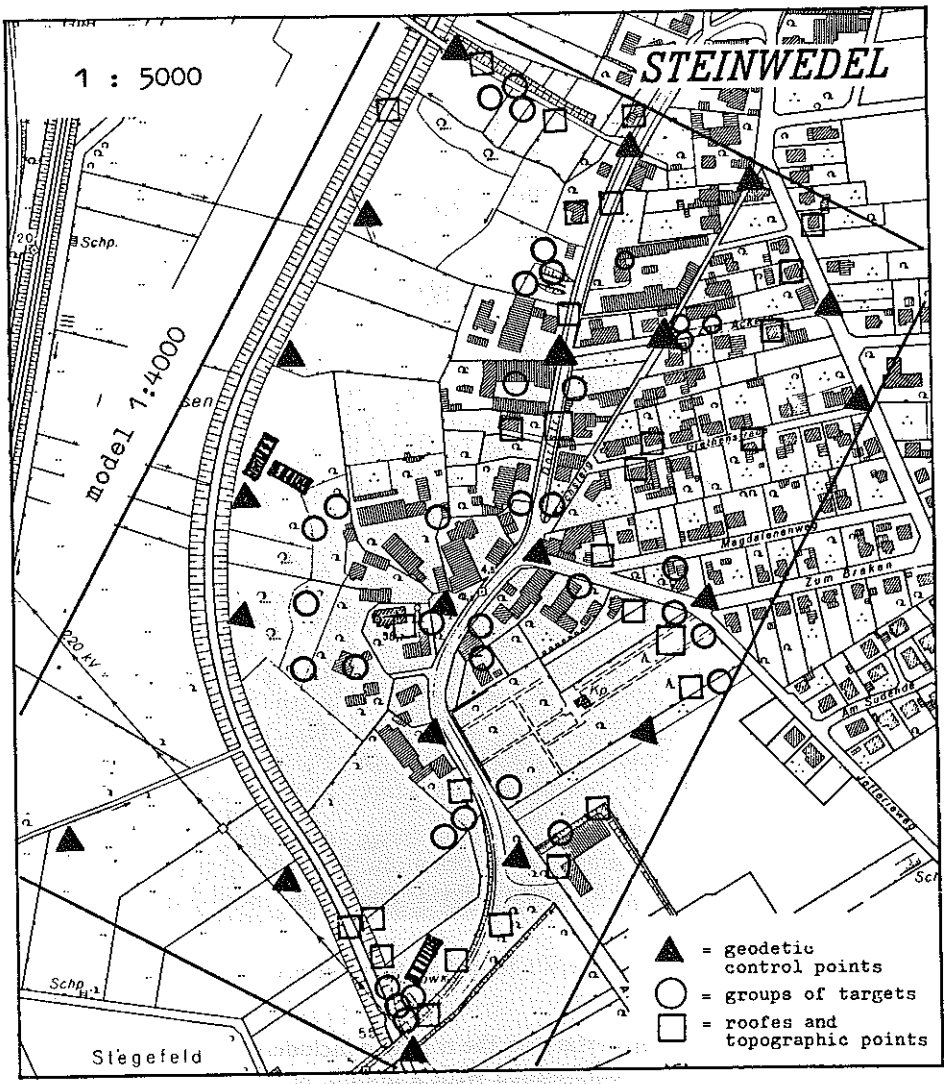

Figure 3 — Points of test field

The 113 check points were signalized with four different colours according to the following table.

Background / Target colour	Grassland	Soil	Asphalt/ Concrete	Roof (red)	Shadow	In total
White	9	9	8	6	4	36
Red	9	9	8	6	4	36
Yellow	9	2	—	6	4	21
Black	—	6	8	6	—	20
in total	27	26	24	24	12	113

The points were arranged in 36 groups, each having 3 to 4 points of different target colour, and spaced evenly over the test area. They were divided as follows:

Grassland	9 groups
Soil	9 groups
Asphalt	8 groups
Roof	6 groups
Shadow	4 groups.

The target size was 12 cm x 12 cm. Unlike the control stations the signalized check points had neither contrast plates nor identification stripes.

In all cases there was effective aerial visibility.

2.3.4 Roof points

The following objects were chosen to test the sharpness of the contours with the various emulsions (Figure 4):

20 roof corners and
2 x 17 roof edge points.

The roof corners, which were easy to identify in the image, had no markings, whereas the roof edge points were given marking stripes for identification. The distances between the marked points of the roof edges were measured terrestrially to an accuracy of ± 1 cm.

2.3.5 Topographical features

Altogether 32 topographical objects were chosen for further tests on the reliability and accuracy of the interpretation. They represent a broad spectrum of different topographical features:

3 slope edge points
2 hedge corners
2 wall corners

4 building corners
3 field corners
2 fence corners
3 stakes
3 pole base points
6 road edge points
4 waterfront points.

A white marking stripe was placed at each point in order to avoid gross identification errors. The positions of all the points were terrestrially determined with an accuracy of about ± 1 cm.

2.3.6 RP test targets

Three targets were placed in the field to determine the resolving power and for the modulation transfer function test. Figure 3 shows the position of the targets in the model.

The targets were 70 x 300 cm resp. 70 x 200 cm. The breadth of the lines varied from 4 to 20 cm, thus a resolution of between 49 L/mm and 9 L/mm could be achieved with photo scale M_b 1 : 4000.

The position of the targets in the field was chosen in the following way:

- two targets were orientated with the bars parallel to the flight direction in order to avoid the influence of image motion (one target — A — in the middle of the model, the second — C — closer to the edge);
- a third target — B — was orientated perpendicular to the flight direction in order to determine the effect of the image motion numerically.

All the targets were photographed in all the 17 flights in the test programme.

The target measurements are analysed in Chapter 3.

2.3.7 Identification of points

For photogrammetric restitution there were 219 points altogether in the test field, including the 20 control stations. After targeting had been completed on May 8, 1982, the test field was watched from the first possible flight day, May 9, until the last flight day, June 18. Although the destruction of about 30 points could not be avoided, some of them could be replaced.

All 219 points, however, could be identified unharmed in the images of the first 11 flights of the first two flight sessions (the "priviliged programme").

All the points used in the test are shown on a map at a scale of 1 : 1000 (Figure 3).

4.1 geodetic control point

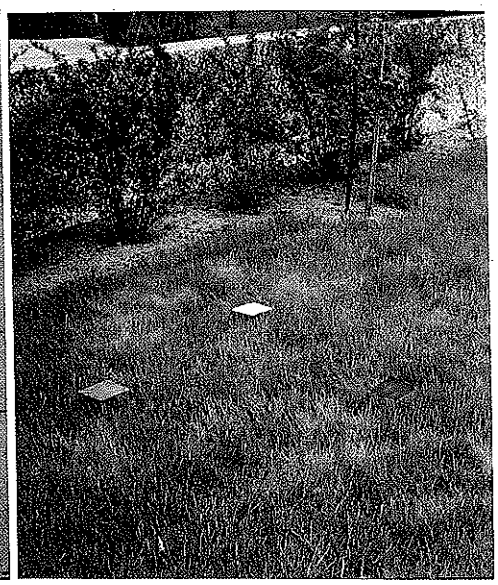

4.2 signalized points

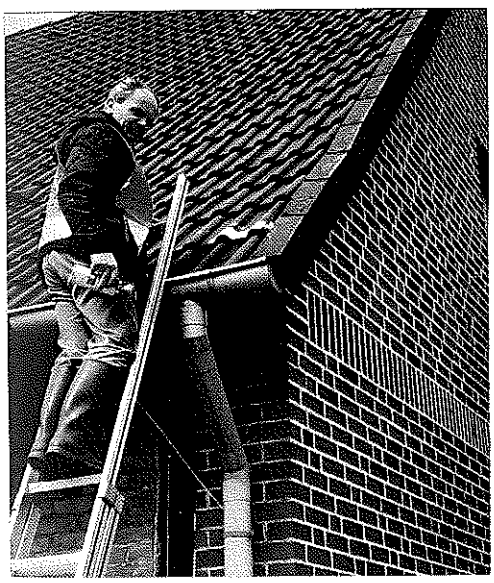

4.3 roof edge

4.4 topographic point

Figure 4 — Examples of points

2.4 Results of the aerial photography

2.4.1 Quantity of photographic material

The 17 planned flights were performed under two different light conditions using the nine planned emulsions (Figure 5), as follows (see also Figure 6):

May 12	9 flights with 9 emulsions	sunny
May 17	2 flights with 2 emulsions	cloudy
May 27	2 additional flights	sunny
June 4	1 additional repetition flight	sunny
June 18	3 additional repetitions flights	cloudy.

The essential image material for the test, namely the results of the first 11 flights, was thus collected during the four resp. nine days after the targeting.

The only purpose of the six additional flights was to test other weather conditions, another camera and different colour filter, with the same film material.

The 11 flights in the privileged programme produced 35 models. Together with the 19 models from the additional aerial photography, there were a total of 54 suitable models for the test work.

2.4.2 Quality of the image material

The quality of the photo material from the first 11 flights can be described as good to very good. The image quality obtained during cloudy weather was definitely inferior, as was expected.

One of the 17 flights (no. 13) was obviously overexposed and proved to be less suitable already in the provisional test. It was, however, included in the test programme for the sake of comparison, as were some models from the first 11 flights which were also overexposed for testing purposes.

The navigation was almost always correct even though some models deviated slightly from the planned flight routes. This resulted in a limited number of control and check points. These models were also included in the test programme.

2.4.3 Representativeness of the photographic material

The 54 available models combine to give photographic source material with good and varied characteristics. If eight models are omitted because of overexposure, there remain 46 models (35 in sunshine, 11 in cloudy weather) are very good and meet the requirements of the test in full.

2.5 Organization of restitution by the participants

After the photographic material had been checked, 54 suitable models were available to all the participants.

By the end of 1982 the National Board of Survey, Helsinki, had finished the precise restitution, and the EPF Lausanne, had done the photographic measurements, so that restitution by participants could start in January 1983. OEEPE members were invited to participate. A total of 18 institutes, authorities and private companies from seven member countries joined the test (see Figure 7).

The participants were instructed to restitute five or ten models each and to send the transformed coordinates to the pilot centre. The participants were to follow the "Instructions for Restitution" (see Appendix 1), which were set up by the working group. By October 1983 all the restitutions were finished and the computational work was done in the pilot centre.

The 54 models were restituted 115 times altogether (Figure 7), i. e., most of the models were restituted twice, several models up to four times.

Photoflights and Restitution

Nr	Emulsion		Manu-fact.	Properties AFS/EASF	L/mm	base mm	Characterization grain	speed	contrast
1	Black+ White	Aviphot PAN 200 PE	Agfa	500	50	0,1	fine	high	good
2		PLUS-X Aerographic 2402	Kodak	200	50	0,1	medium	medium	medium
3		DOUBLE-X Aerographic 2405	Kodak	500	50	0,1	fine	high	good
4		Panatomic-X Aerocon II,3412	Kodak	40	160	0,06	v.fine	less	high
5		High Definition Aerial 3414	Kodak	8	250	0,06	extr.fine	slow	strong
6	Color	Aerochrome MS 2448 \SO-397	Kodak	32	40	0,1	fine	medium	medium
7		Ektachrome EF,Aerographic\	Kodak	64	40	0,1	v.fine	medium	low
8		Aerocolor Negative 2445	Kodak	100	40	0,1	v.fine	high	wide exp.latit.
9		Aerochrome Infrared 2443	Kodak	40	32	0,1	fine	medium	high

Figure 5 — Used Emulsions

Flight Strip-Nr.	Emulsion	Date 1982	Flight Com-pany	Exposure Time	Apert.	Remarks	Number of models	Number of plott. models
1	PAN 200	12.May	HL	1/1000	8	normal, good	3	9
2	PAN 200	18.June	HL	1/600	6.5	overcast sky,good	3	6
3	PLUS X	12.May	KW	1/500	5.6	normal, good	2	6
4	DOUBLE X	12.May	KW	1/700	5.6	normal, good	2	4
5	DOUBLE X	17.May	KW	1/500	5.6	overcast sky,weak	3	6
6	Panatomic	12.May	HL	1/700	5.6	underexposed, sharp	2	6
				1/300	"	normal exposure	3	6
				1/200	"	overexposed, unsharp	1	2
7	High Def.	12.May	KW	1/200	5,6	normal exposed, unsh.	2	3
				1/400	"	underexposed,	2	4
8	C-Dia 2448	12.May	KW	1/500	5,6	normal, good	2	5
9	Dia 2448	27.May	HL	1/400	5,6	normal, optimal	1	3
				1/500	"	underexposed, good	1	2
				1/800	"	overexposed	2	5
10	Dia 2448	17.May	KW	1/300	5,6	overcast sky, good	2	5
11	Dia SO-397	12.May	HL	1/1000	8	normal, good	2	5
				1/1000	11	underexposed	2	3
12	Dia SO-397	27.May	HL	1/1000	8	normal, v.good	2	2
				1/1000	11	underexp.,very good	1	3
13	Dia SO-397	4.June	KW	1/200	5,6	overexposed, bad	3	6
14	Dia SO-397	18.June	HL	1/500	8	overcast sky, dark	1	1
				1/1000	8	underexp.,bad	2	3
15	Dia SO-397	18.June	KW	?	8	overcast sky,bad	3	5
16	C-Negativ	12.May	KW	1/400	5,6	normal,very good	2	6
17	CIR-Infrar	12.May	HL	1/300	5,6	normal	2	3
				1/700	"	underexp.very good	2	4
				1/200	"	overexp., light	1	2
1-7 = black&white 8-17 = color			HL = Hansa Luftbild, Münster KW = Kirchner & Wolf, Hildesheim			Σ=	54	115

Figure 6 — Results of Photo-Flights — Photomaterial available

Country	Nr.	Name	Instruments	Ø-float. mark	number of plotted models
CH	34	Institut Photogram., Zürich	Wild AC 1	25 µm	5
	35	Institut Photogram., Lausanne	Wild BC 1	25	5
D	01	Landesvermessung Hannover	Zeiss-Planicomp	40	21
	02	Inst.Angew.Geodäsie,Frankf.	Zeiss-Planicomp	40	6
	03	Landesvermessungsamt Bonn	Zeiss-Planicomp	40	6
	04	Landesvermessungsamt Kiel	Wild AMH, RAP	45	5
	05	Landesvermessungsamt Wiesbaden	Zeiss-Planicomp	20	5
	06	Landesvermessungsamt München	Zeiss-Planicomp	40	5
	07	LAmt Flurbereinigung Ludwigsbg.	Zeiss-Planicomp	20	5
	08	Fa.Kirchner&Wolf, Hildesheim	Zeiss-Planimat	40	5
	09	Fa. Rheinbraun, Köln	Zeiss-Planimat	40	5
DK	21	Photogram. Labor. Uni Aalborg	Zeiss-Planimat	40	5
F	23	IGN, Paris	Matra-Traster	?	3
GB	24	School Military Survey,Newbury	Wild A 8	70	5
	25	Clyde Surveys Ltd.,Maidenhead	Wild A 8	70	10
	26	Dep.Photogrammetry,Uni London	Kern DSR 1	25	5
I	29	Instituto Topografia, Milano	Zeiss-Planicomp	40	9
NL	22	ITC, Enschede	Wild A 10	40	5

Figure 7 — Participants

3 Analysis of the image quality

In most cases, image quality is characterized by the well-known 3-bar test, with which it is possible to measure how many lines per millimetre can be distinguished for a given contrast. This is an efficient method provided the test is applied under conditions comparable to those when individual components (different films) are analysed or an imaging system as a whole is tested. It is not possible to predict the performance of a complete imaging system even if the resolution of the individual components is known. The 3-line test does not allow either prediction of the level of contrast which will show a small object, for example a signalized point reproduced in an aerial photograph.

A much more powerful tool is the modulation transfer function. A disadvantage of this function might be that one is dealing with a function which cannot in general be characterized by a single value. It is, however, possible, using the bias of the spread function, to define a very few parameters to describe the image quality. In the present study, the spread function was assumed to be a Gauss function needing only one parameter for its description, but it became evident that, in reality, the spread function has a much more complex form.

3.1 Targets for the determination of the modulation transfer function

Special test targets were used for determining the modulation transfer function; these targets showed up bars with gradually diminishing distances (cf. Figures 8 and 9). This special form of test target was suggested after a series of investigations of the test field used by the Institute of Photogrammetry of the Swiss Federal Institute of Technology in Lausanne (cf. [11]). The bar distances adopted for the test on Steinwedel does not, however, allow the determination of the whole range of the modulation transfer function, as will be shown later; the analysis was therefore restricted to the central part of the MTF, between 12 and 40 lines/mm.

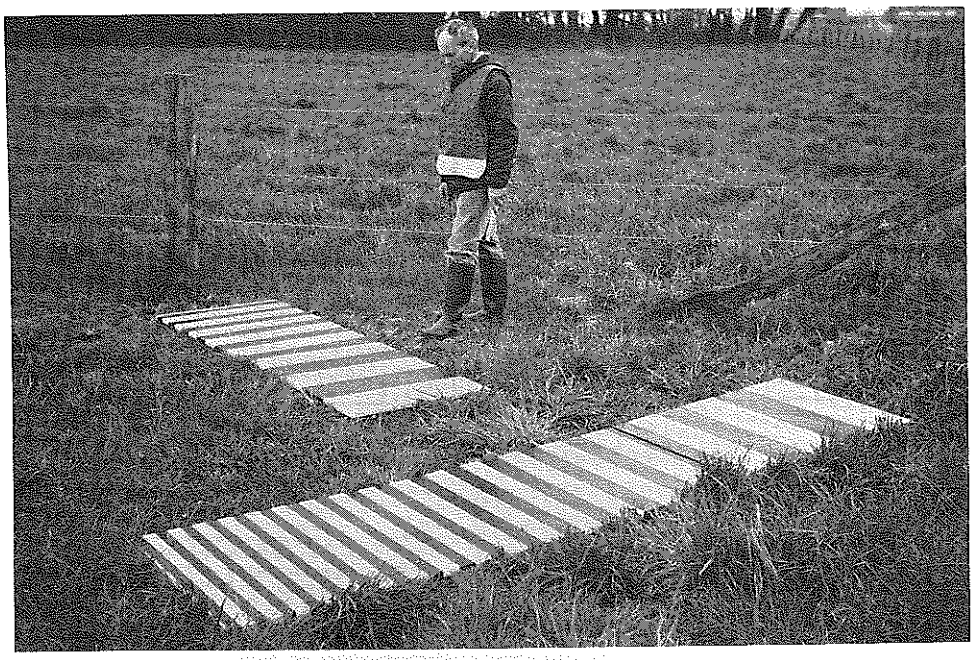

Figure 8 — Photograph of the test targets used for determining the modulation transfer function.

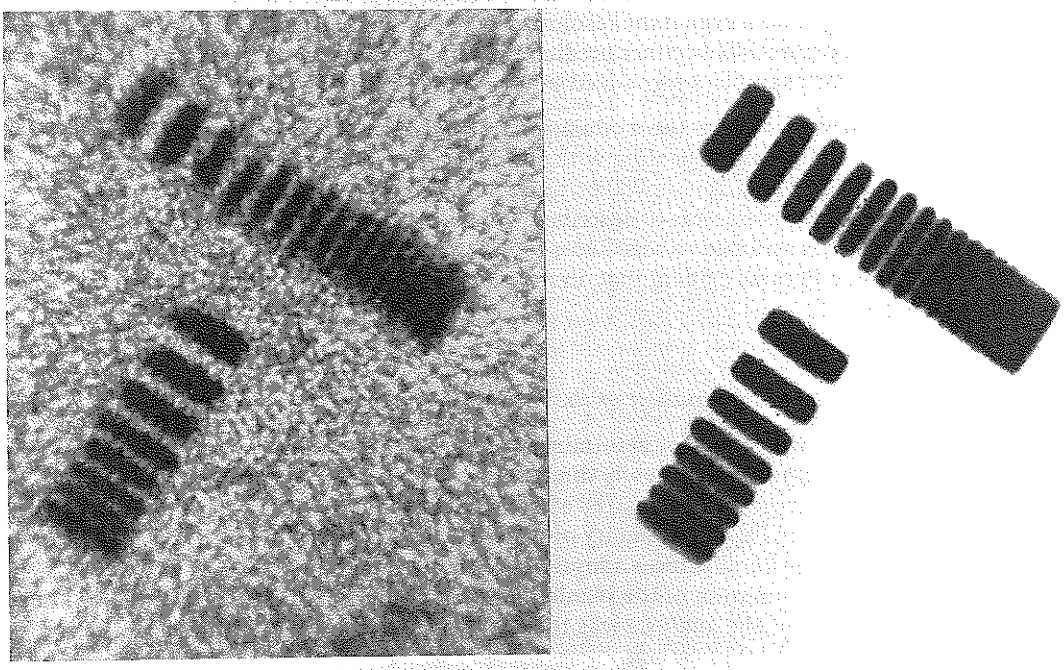

Figure 9 — Microphotographs of a test target on Agfa Pan 200 and Kodak Panatomic-X films

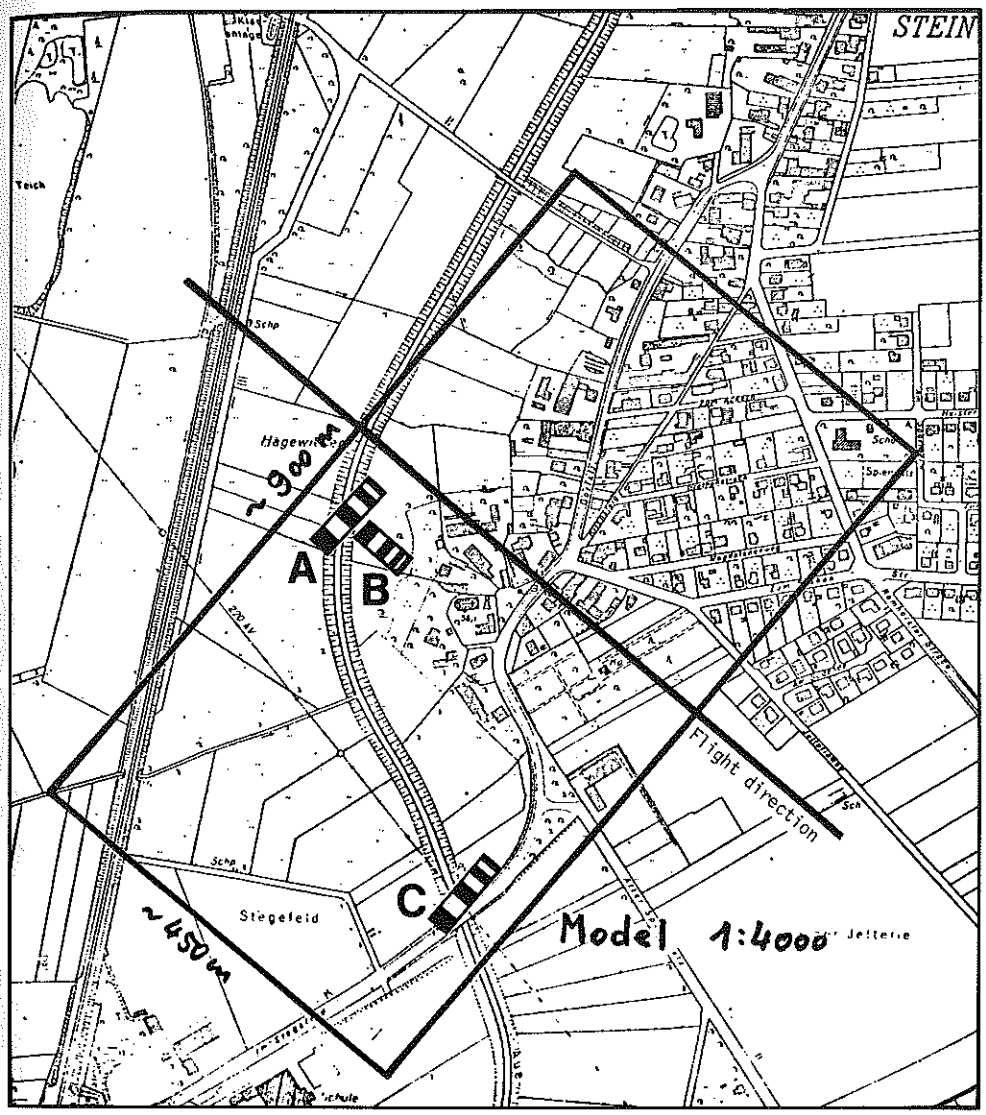

Figure 10 — Overview of the test area with the position of the test targets used for determining the modulation transfer function. Most of the targets were orientated with the bars parallel to the flight direction in order to avoid the influence of image motion; only one target was orientated perpendicular to the flight direction in order to determine the effect of image motion numerically

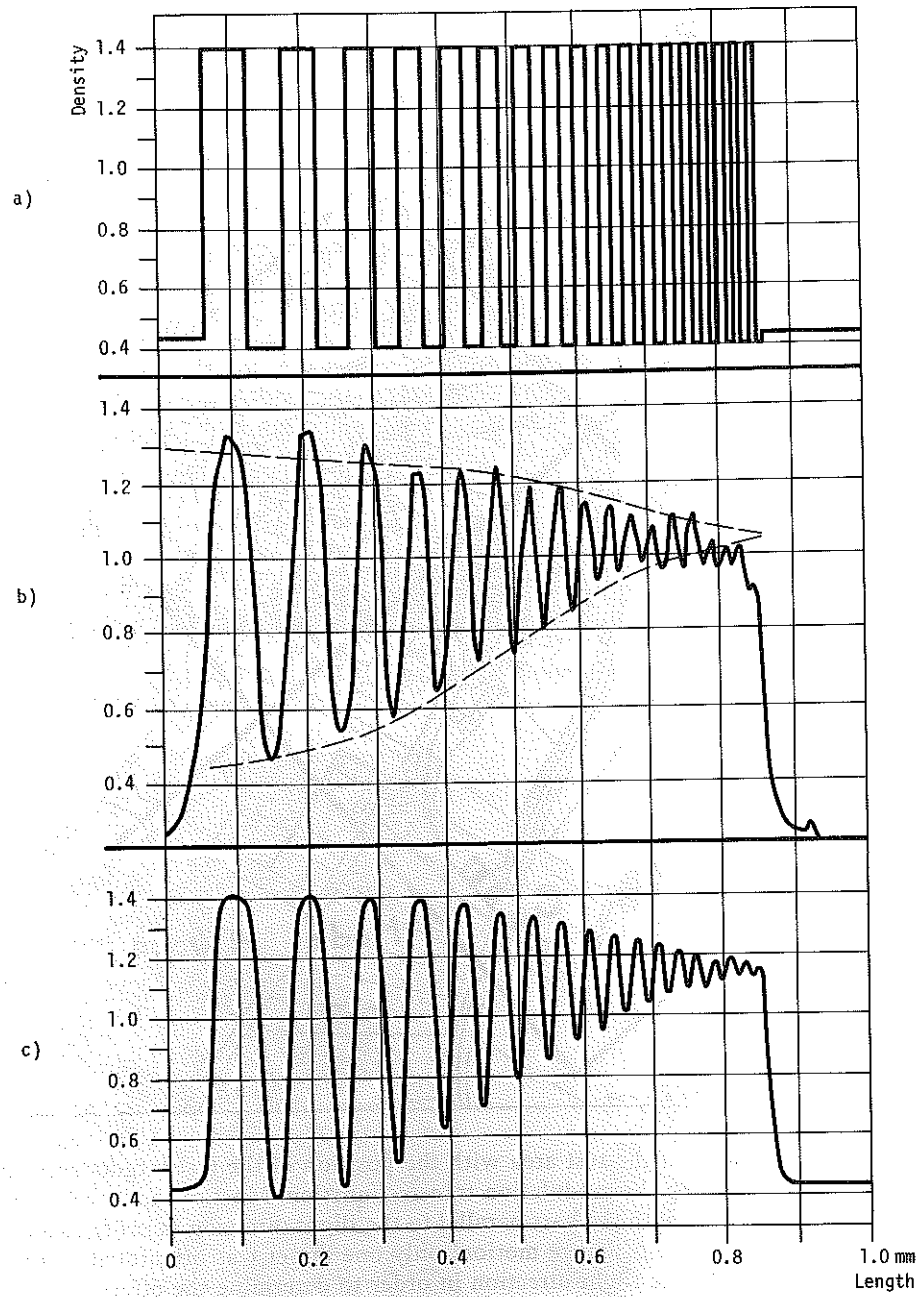

Figure 11 — a) Comparison of the reflectance of the original target, b) the density profile measured on a Kodak Panatomic-X film and c) the computer-simulated density profile for a Gaussian spread function calculated for $\sigma = 22$ µm. The dashed line drawn around the measured density profile shows the extreme values of the simulated curve

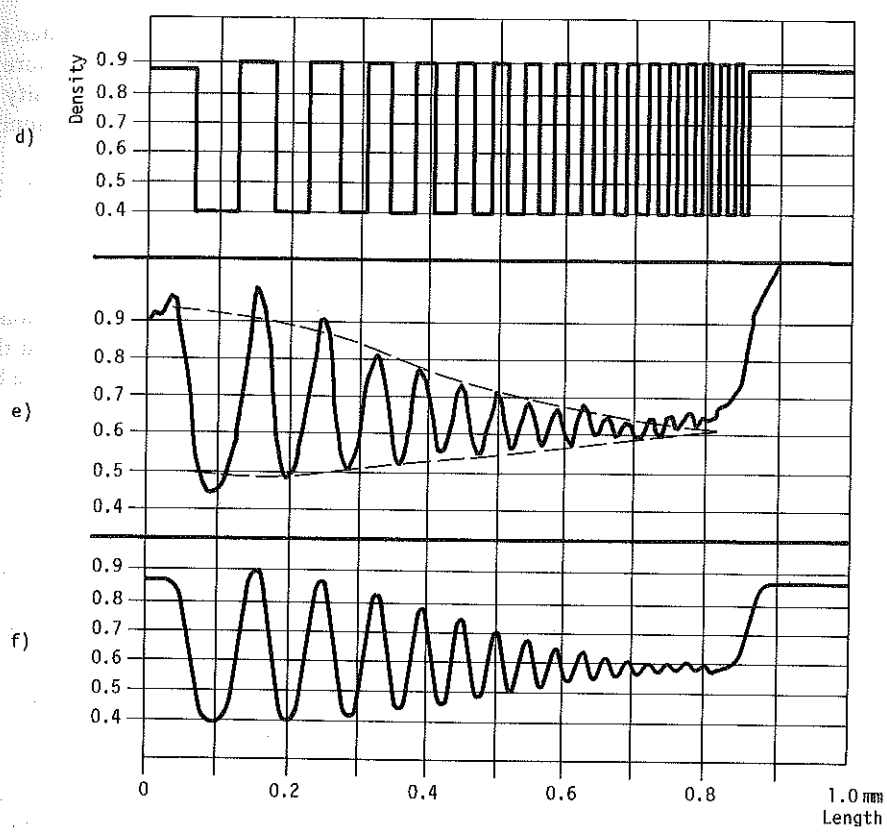

continued Figure 11 — Density profile measured on a Colour film SO 397 (e) and the computer-simulated density profile for a spread function $\sigma = 28\ \mu m$ (f)

Figure 11 shows various density profiles over the test targets; the object contrast of the test target is shown in the upper part of the figure. According to reflectance measurements, the clear parts of the targets reflect about 80 % of the incident light, whereas the dark parts reflect only 10—15 % of the light; this latter value depends mainly on the angle of incidence. The result is a contrast of about 1 : 6 to 1 : 8. In the photographic industry a sinusoidal transition between dark and clear parts of test targets is very often preferred to rectangular targets. Although sinusoidal targets have many advantages it appears that rectangular targets give considerably more information as asymmetric effects, caused for example by a coma of the lens, can also be controlled. Finally, rectangular targets can be produced much more easily than sinusoidal ones.

Different density profiles measured in aerial photographs are shown in Figure 11. The measurements were done on a Joyce-Loebel microdensitometer. As expected, the contrast between the bars diminishes as the bar distance decreases until finally the bars can no longer be distinguished. The density reached at the highest frequencies does not correspond to the mean of the minimum and maximum densities. Nevertheless, it

should be borne in mind that the density is measured on a logarithmic scale. When the density is converted into transparency values, these values correspond in effect more or less to the mean of the two extremes. It is evident that when reconstructing density or transparency values the nature of the characteristic curve of the film, the developing process and the atmospheric conditions have to be taken into account.

3.2 *Application of the spread function*

In principle the modulation transfer function could be deduced by direct comparison of the reflectance curve and the corresponding density profile of the test targets. In this case, it would be sufficient to determine the contrast reduction as a function of the bar distances.

$$R(\nu) = \frac{I^i_{max} - I^i_{min}}{I^0_{max} - I^0_{min}} \quad . \tag{1}$$

In this formula $R(\nu)$ is the contrast reduction factor as a function of the frequency (width of a bright and a dark bar together), I is the transparency (for diapositives) or the opacity (for negatives) in the image space (index i) and the reflectivity in the object space (index 0).

In comparing with a sinusoidal function it would be necessary to adopt a correction value. However, because of the strong granularity of the film and other irregularities, this did not appear useful. Preference was given to a simulation method, whereby the Fourier transform of the modulation transfer function, i. e. the spread function, is needed. Numerically this procedure has considerable advantages, as the form of the spread function can be estimated much more reliably than the modulation transfer function. For the present study, the spread function was assumed to be a Gauss function with a variable exponent (σ); cf. also Figure 12. In the formula below, x is the length of profile $I(x)$, with the dimension inversely proportional to the transparency. N. B. the definition of parameter σ is different from that commonly used in mathematics and statistics.

$$I(x) = \frac{4}{\sigma\sqrt{\pi}}\, e^{-4\left(\frac{x - x_0}{\sigma}\right)^2} \quad . \tag{2}$$

The Fourier transform of the Gauss function is also a Gauss function. Consequently, the form of the modulation transfer function is well defined when the mathematical expression for the spread function is fixed. Figure 13 shows a series of modulation transfer functions corresponding to a Gauss function with varying σ. Characteristic of this modulation transfer function is a rather steep but uniform slope for frequencies between 15 and 30 Hz. Modulation transfer functions with a flatter or steeper slope cannot be approximated by a single Gauss function. In this case it is necessary to choose another mathematical function or to use a composite Gauss function with varying exponent.

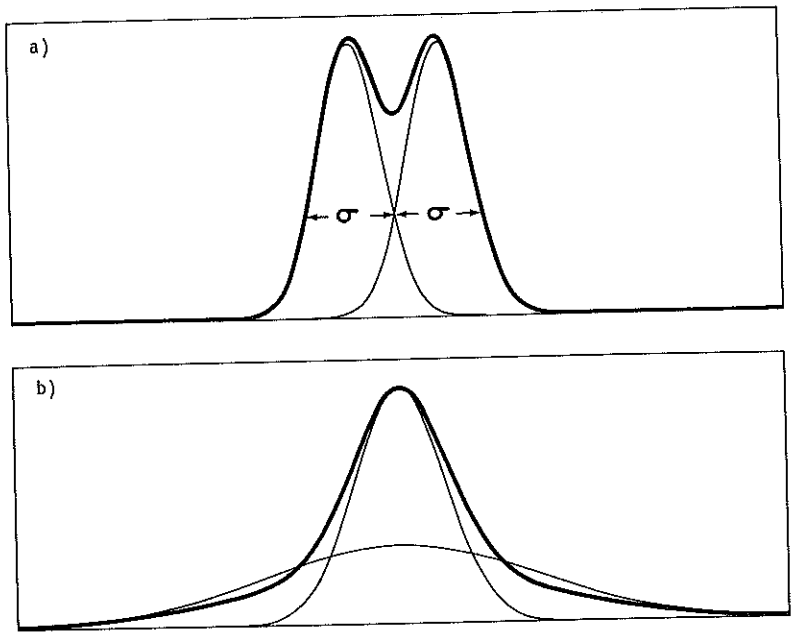

Figure 12 — a) Two narrow bars with high contrast in the object space will show a density profile in the image space corresponding to the sum of two Gauss functions. If the distance between the two bars is σ then it should just be possible to distinguish them on the photographs; the transparency between the two peaks will be 25 % lower than the two maxima

b) Spread function (heavy line) composed of two Gauss functions with different σ values (thin lines). The sum was reduced so that its maximum corresponds to the higher Gauss function

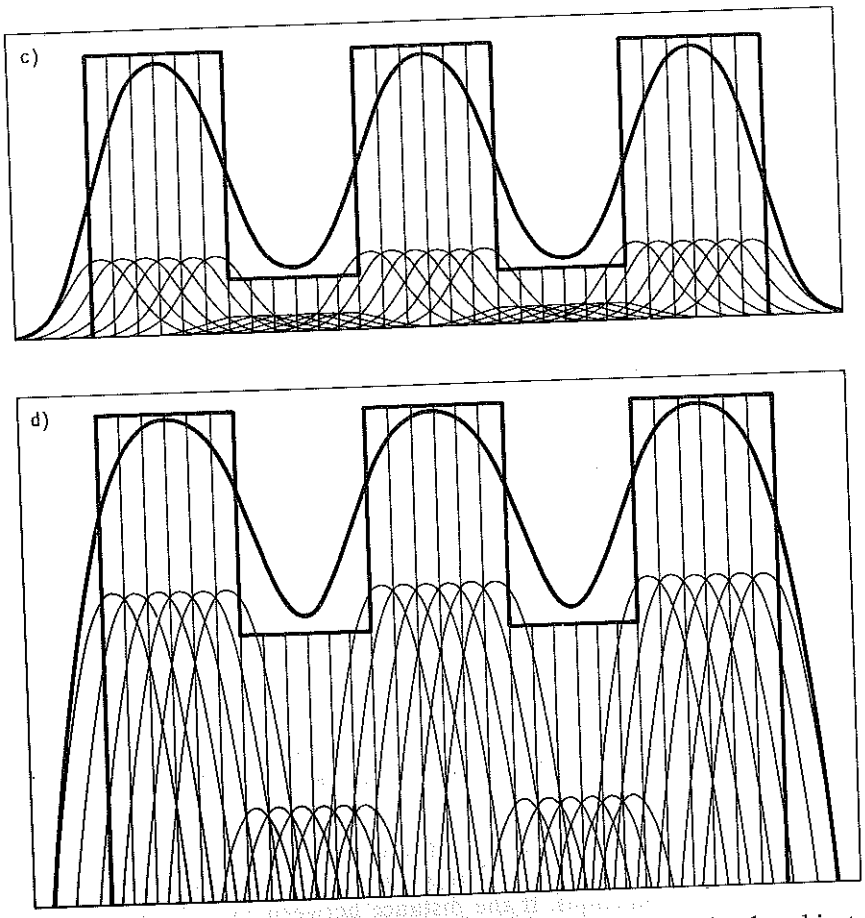

continued Figure 12 — c) Reproduction of a rectangular signal in the object space using individual Gauss spread functions. Each individual small rectangle (fine lines) is reproduced in the image by a spread function, the amplitude of which is defined by the original light intensity. The sum of the individual spread functions (thick lines) gives a curve similar to a sine function which describes the transparency in the image space

d) Same presentation as 12 c) but instead of the transparency τ the density $D = lg\frac{1}{\tau}$ is shown. Note the asymmetric form of the density curve

A modulation transfer function with a flatter slope is obtained when the base of the initial Gauss function is widened by combining it with a larger Gauss function with a considerably lower maximum (cf. Figure 12 b).

$$I(x) = k_1\, e^{-4\left(\frac{x-x_0}{\sigma_1}\right)^2} + k_2\, e^{-4\left(\frac{x-x_0}{\sigma_2}\right)^2} + \ldots \qquad (3)$$

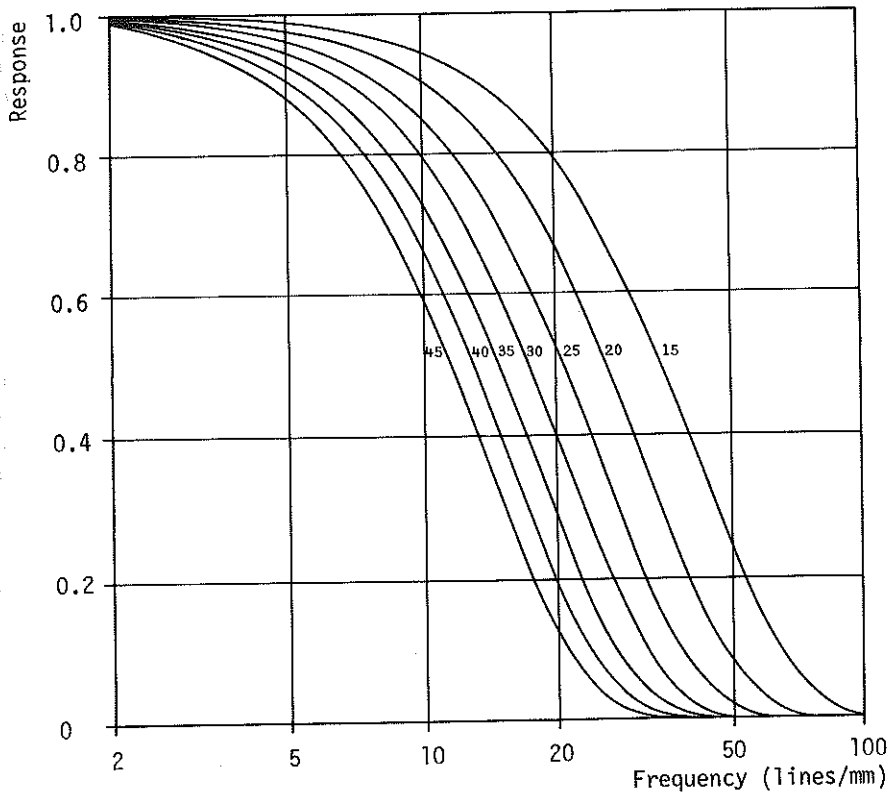

Figure 13 — Modulation transfer functions as spread functions corresponding to various Gauss functions; the values correspond to the sigma of the Gauss function

Purely theoretically it would also be possible to determine the spread function directly from the Fourier transforms of the object function and image function. This procedure, however, would be rather imprecise, as higher frequencies are strongly influenced by the granularity of the film, and so had to be abandoned.

For practical applications, the original object function has been approximated by a series of 1000 points generated by the computer. Subsequently, a series of spread functions with different σ have been used to calculate various image functions which have been presented graphically and plotted. These simulated image functions are then compared with the original density measurements and the function with optimum coincidence is retained (cf. Figure 11).

In formula (1), a σ has been introduced which corresponds to the distance between the inflexion points. This value has a special significance as it can be considered to be a measurement of the resolution. For any 2 bars in the object space, whose images correspond to 2 Gauss functions, the 2 images can just be distinguished provided the

distance between the maxima is equal to the value of σ (cf. Figure 12 a). The minimum of the functions is then 25 % below the two peaks. As the micron was chosen as the unit of σ, the value 1000/σ corresponds to some extent to the resolution in lines per millimetre.

3.3 *Practical results*

Figure 14 shows an overview of the different films for which the spread function was determined; the spread functions are given by their σ values. As expected, black & white film gives a much higher resolution than colour film. The difference is of the order of 20—30 %. The results for the different films however show some irregularities and the values are subject to considerable variation. Some of the variations within an individual picture are due to the different positions of the test targets on the image plane relative to the optical axis of the lens used. Nevertheless the values shown, which represent a mean, should be only slightly affected by these variations.

In order to check the empirically determined modulation transfer function, efforts were made to compare it with laboratory measurements. The Zeiss factory kindly placed at our disposal modulation transfer measurements for a lens type similar to the one used in the test (cf. Figure 15). The modulation transfer function for some of the film material used was taken from Kodak and Agfa publications (cf. Figure 16). The modulation transfer function resulting from these two components is shown in Figure 17. The function was computed for a central part of the image $r = 30$ mm; other components, such as the turbulence of the atmosphere or image motion, have been omitted. Nevertheless, the results of this comparison coincide quite well as can be seen in the figure. This quite good coincidence does not remove the reservations stated earlier. Particularly, it should be kept in mind that the laboratory measurements are also limited to a frequency range of 10—40 Hz and extrapolation is not justified in reality.

An analysis of the modulation transfer function shows that image quality differs considerably from film to film. The highest image quality is obtained with Panatomic-X film, whereas colour IR film gives the lowest image quality; evidently image motion was too high during the test, so the High Definition film could have given reasonable results and seems to confirm these tests. The High Definition film seems useful only for large-scale photography, when the image motion is compensated as shown in other experiments (cf. [2]). Cameras with such equipment would also facilitate the use of the Panatomic-X film.

In Figure 18 some micro-enlargements of different signalized points are reproduced as a better illustration, as the modulation transfer functions represent a rather abstract way of describing image quality. These photographs demonstrate more vividly than figures the high performance of the Panatomic-X film compared for example with Double-X film. However, the measuring results do not seem to be affected by the resolving power of the film. This is quite astonishing at first glance and it seems that the optical system of the measuring instrument and especially the optical enlargement used was, in most cases, inadequate for the high quality of the photographs taken.

Emulsion	Date	Exposure	Survey comp.	Pictures numbers	Ø	t	Filter	Development	σ	Density D_{min} - D_{max}	σ A	σ B	σ C	σ A	σ B	σ C	ΔD A	ΔD B	ΔD C	ΔD A	ΔD B	ΔD C
Pan 200	12.5	n (S)	HL	17/19	8	1/1000		8 feet, 1R 29.5° C	28	1.03 - 1.73	38	24	26	24	20	36	0.64	0.85	0.78	0.67	0.82	0.40
	18.6	+ D (C)	HL	24/26	6.3	1/600		13.5 feet, 2R 29.5° C	25	0.87 - 1.62	22	24	30	22	26	28	0.70	0.84	0.63	0.75	0.86	0.76
Plus-X	12.5	+ D (S)	KW	80/81	5.6	1/500		60 inch, 30° C	26	0.87 - 1.40	26	32	28	22	26	24	0.54	0.46	0.43	0.71	0.63	0.43
Double-X	12.5	n (S)	KW	64/65	5.6	1/750		30 inch, 24° C	27	0.64 - 1.22	28	28	26	28	28	26	0.53	0.49	0.52	0.72	0.74	0.50
	17.5	+ D (C)	KW	8/9	5.6	1/500		15 inch, 22° C	26	0.93 - 1.61	24	26	--	26	30	26	0.73	0.66	--	0.65	0.72	0.62
Panatomic-X	12.5	n (S)	HL	15/17	5.6	1/300		16 feet, 1R 29.5° C	27	0.98- >2.00	24	22	22	26	40	--	0.95	1.03	>1.24	1.03	0.85	--
		- D (S)		28/30	5.6	1/700			22	0.58 - 1.53	22	24	--	20	20	24	0.75	0.75	--	1.17	1.29	0.80
		+ D (S)		34/36	5.6	1/200				> 2.00	34	--	--	34	--	--	--	--	--	1.17	--	--
High defin.	12.5	+ D (S)	KW	130/131	5.6	1/200		15 inch, 30° C	30	1.14- >2.10	26	34	--	26	36	26	1.18	0.70	--	1.50	0.48	0.90
Dia MS 2448	12.5	- D (S)	KW	96/97	5.6	1/500		910, 46.1° C	38	0.34 - 0.77	34	40	38	38	38	38	0.53	0.45	0.24	0.48	0.45	0.44
	27.5	n (S)	HL	40/42	5.6	1/400			37	1.26 - 1.86	34	40	40	34	36	38	0.72	0.57	0.48	0.58	0.60	0.53
		- D (S)		13/15	5.6	1/800			32	1.37- >2.00	32	32	34	28	30	32	>0.52	>0.58	0.70	>0.62	>0.65	0.68
	17.5	n (S)	KW	22/23	5.6	1/300			38	1.12 - 1.46	--	38	--	38	38	40	0.16	0.52	0.14	0.43	0.43	0.37
Dia SO 397	12.5	- 1/3 (S)	HL	24/26	8/11	1/1000	HF 3/4	910, 46.1° C	35	0.42 - 1.04	40	34	32	34	34	38	0.68	0.70	0.59	0.61	0.66	0.49
		n (S)		12/14	8	1/1000			35	0.37 - 0.96	34	34	32	36	36	38	0.65	0.76	0.51	0.67	0.58	0.41
		- 1 D (S)		30/32	11/8	1/1000	HF 3/4		32	0.73 - 1.46	30	32	30	30	30	38	0.77	0.86	0.78	0.75	0.69	0.54
	27.5	n (S)	HL	42/44	8	1/1000	CC 10-C	910, 46.1° C	32	0.43 - 0.99	32	30	28	32	34	36	0.58	0.65	0.55	0.62	0.52	0.43
		- 1 D (S)		13/15	11/8	1/1000	CC 10-C		33	0.82 - 1.49	30	32	36	--	--	34	0.72	0.70	0.54	--	--	0.69
		n (S)		51/53	8	1/1000			36	0.38 - 0.87	34	38	38	34	38	32	0.57	0.51	0.39	0.51	0.50	0.48
	4.6	n (S)	KW	7/8	5.6	1/200			36	<0.25 - 0.45	38	34	34	40	36	36	0.29	0.16	>0.13	>0.25	>0.18	0.23
	18.6	n (C)	HL	87/89	8	1/500		910, 46.1° C	36	0.49 - 0.87	34	38	40	34	36	--	0.41	0.40	0.27	0.40	0.40	--
		- 1 D (C)		67/69	8	1/1000			36	0.85 - 1.33	38	38	32	34	38	36	0.41	0.60	0.39	0.43	0.57	0.45
		- ½ D (C)		75/77	8	1/750			31	0.63 - 1.05	30	32	34	30	30	30	0.38	0.42	0.37	0.47	0.46	0.40
	18.6	n (C)	KW	3/4	5.6				36	~ 0.50	34	40	36	34	--	38	0.22	0.21	0.12	0.10	0.10	0.10
Color neg.	12.5	n (S)	KW	113/114	5.6				34	1.10 - 1.54	30	30	--	34	40	--	0.57	0.51	--	0.40	0.28	--
Color IR	12.5	- 1 D (S)	HL	24/26	5.6	1/700	D	910, 48.9° C	34	<0.25 - 1.07	34	34	34	34	36	32	>1.11	>0.97	0.35	>0.94	>0.98	0.58
		n (S)		18/20	5.6	1/300	D		40	<0.15 - 0.44	38	40	--	40	40	--	>0.39	>0.25	--	>0.33	>0.17	--
		+ 1 D (S)		29/31	5.6	1/200	D		36	~ 0.20	36	--	--	--	--	--	>0.14	--	--	--	--	--

Figure 14 — Analysis of the image quality of the test material with the aid of the modulation transfer function. The modulation transfer function is characterized by the value of the spread function; whereas the spread function has been approximated with a Gauss function. The adjacent column gives the minimum and maximum densities measured on the test target with the microdensitometer. The individual values of σ and the density differences ΔD shown in the following columns under A, B, C refer to the 3 individual test targets, labelled as in Figure 10

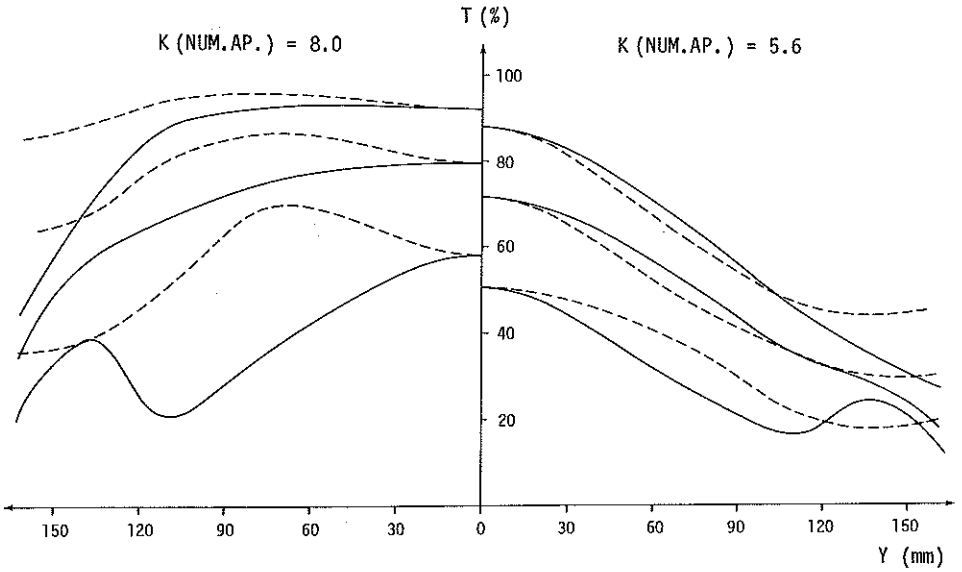

Figure 15 — Modulation transfer function of the lens type used for aerial photography (Zeiss Topar A, $c = 30$ cm). MTF for radial lines (——) and tangential lines (— — —), spectral range: 0.486 to 0.707 µm, spatial frequencies: 10, 20, 40 lines/mm. (Courtesy of Zeiss Oberkochen)

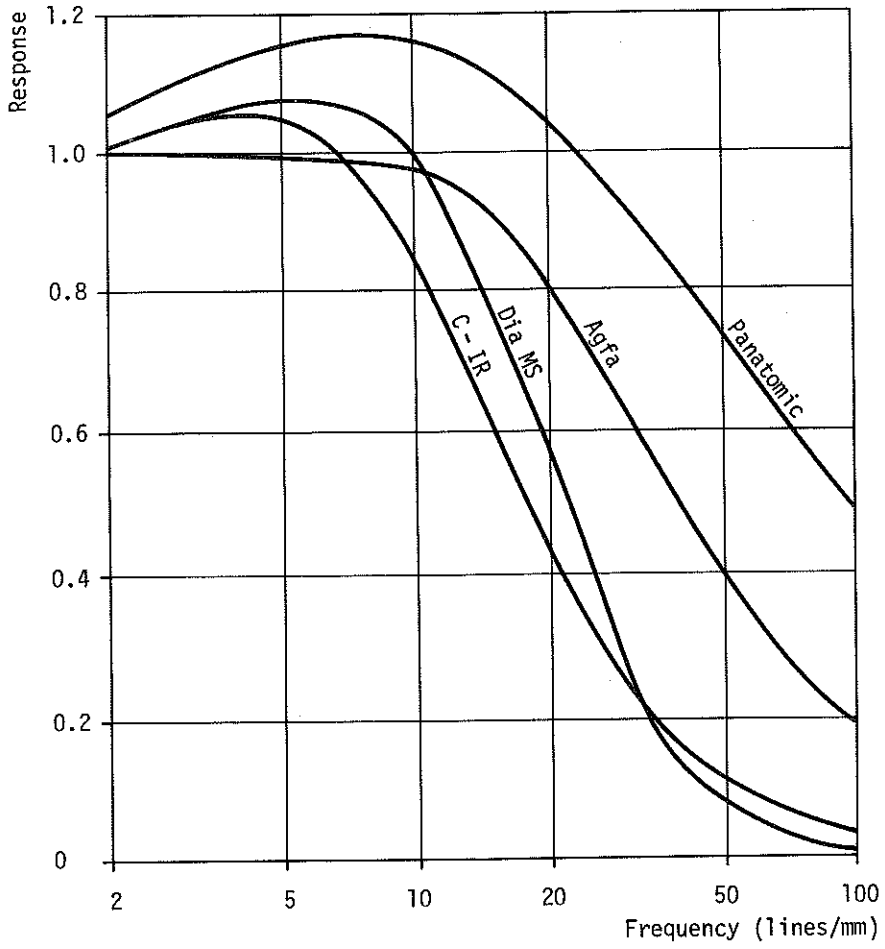

Figure 16 — Modulation transfer function for some of the film material used; curves from manufacturers information (Agfa: Agfa Pan 200, Panatomic: Kodak Panatomic-X 3412, Dia MS: Kodak Dia MS 2448, C-IR: Kodak Color Infrared 2443)

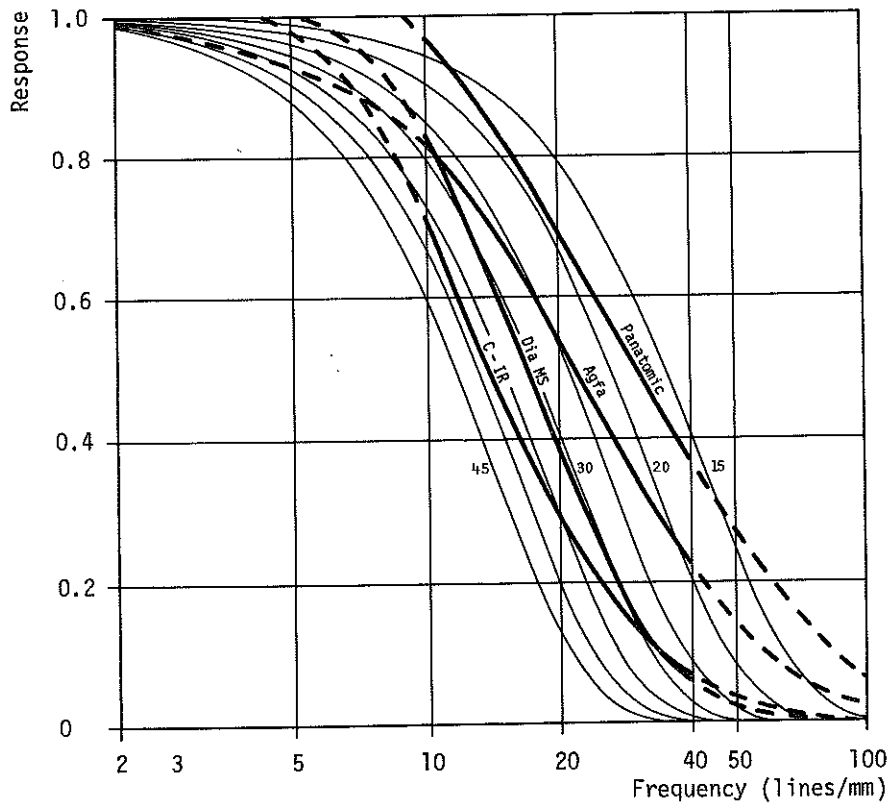

Figure 17 — Expected modulation transfer function according to laboratory measurements on the lens and the film (thick lines) compared with the MTF of Gauss functions (thin lines). According to Figure 14 the following values are expected: Panatomic 20—22 µm, Agfa 22—25 µm, Dia MS 32—34 µm, C-IR 32—36 µm. Laboratory measurements of the MTF of the lens are limited to the range of 10—40 Hz

Figure 18 a)—d)

Comparison of signal reproductions on different aerial films. 8 points groups have been chosen with different undergrounds; the indications on the underground, the number of the points groups and the colour of the signals are given on top of the figure (w = white signal, b = black signal, r = red signal and y = yellow signal). The designations of the films correspond to the indications in Figure 6 of chapter 2.4. The figure shows also the flight numbers and the picture numbers, furthermore particularities of illumination and exposure are given. The micro-enlargements have been reproduced with uniform exposure in order to submit the impression of the operator as for dark or clear parts of the image. The image sections correspond to a size of 1 mm x 1.2 mm on the original negatives

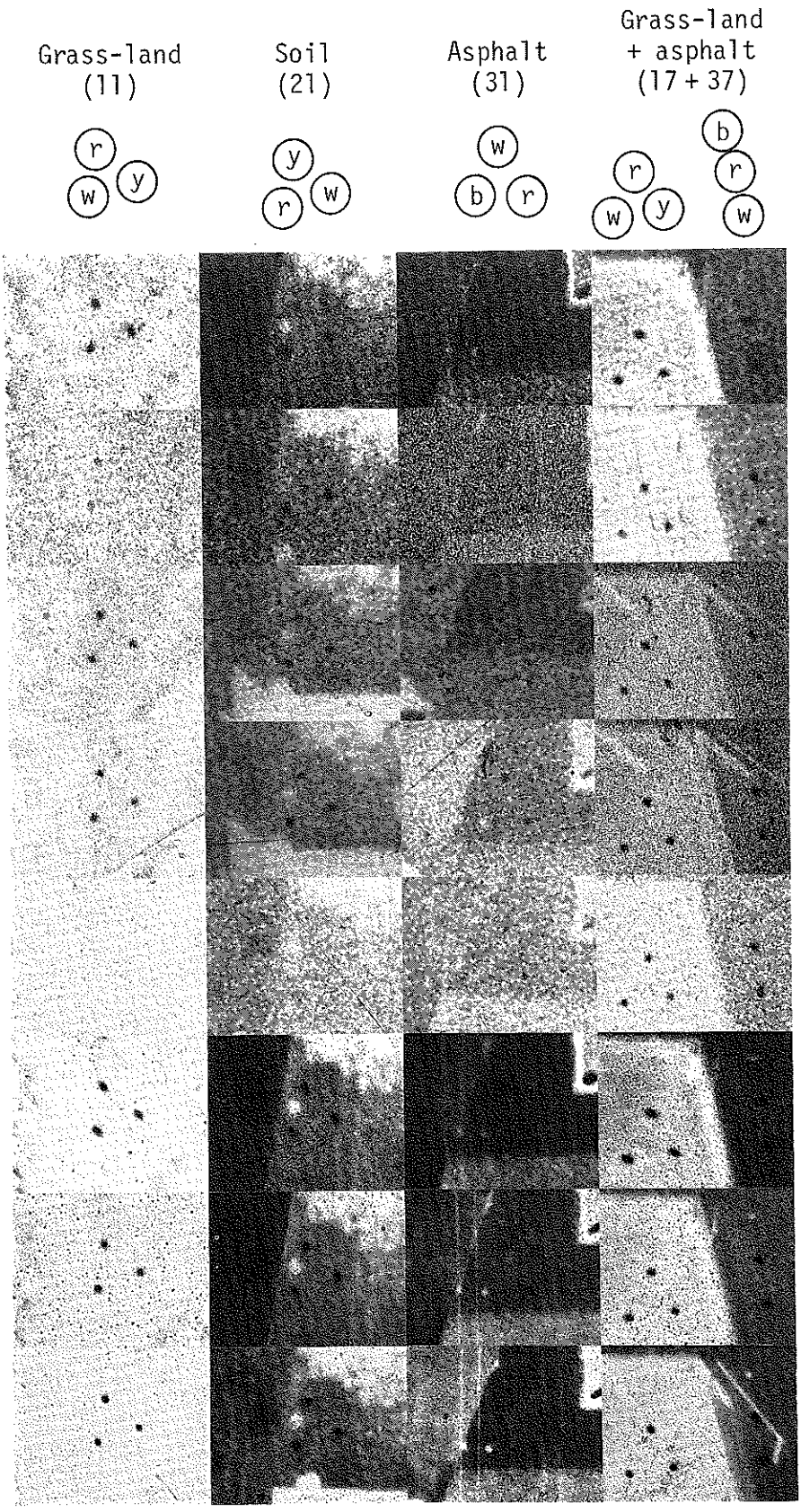
Grass-land (11)
Soil (21)
Asphalt (31)
Grass-land + asphalt (17 + 37)
r w y
y r w
w b r
b r r w y w
Pan 200 1/031
Pan 200 2/026 cloudy
Plus-X 3/081
Double-X 4/067
Double-X 5/006 cloudy
Panatomic-X 6/022
Panatomic-X 6/028 under-exp.
High defin. 7/134 under-exp.

Figure 18 a)

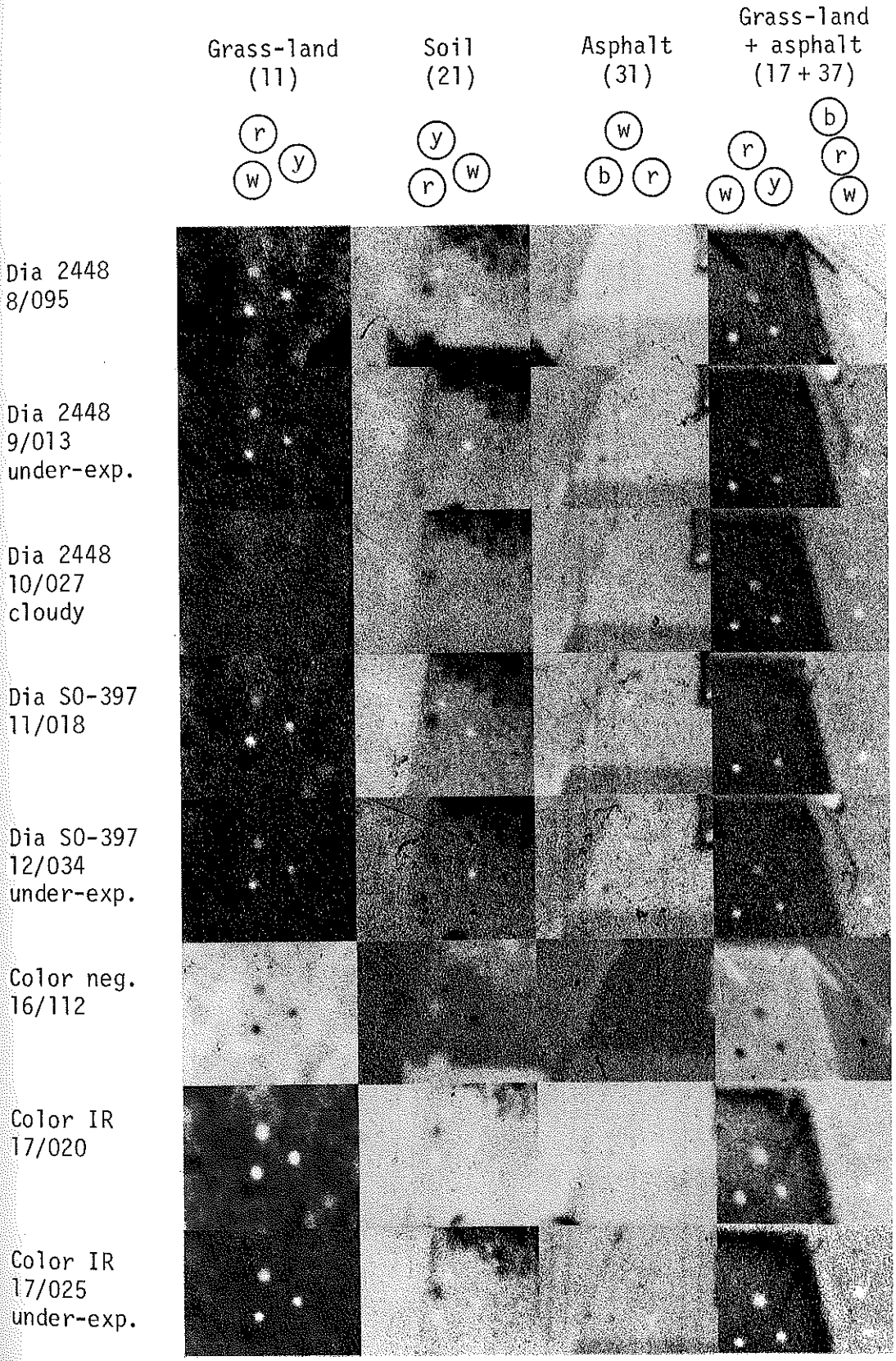
Grass-land
(11)
Soil
(21)
Asphalt
(31)
Grass-land
+ asphalt
(17 + 37)
r
w
y
y
r
w
w
b
r
r
w
y
b
r
w
Dia 2448
8/095
Dia 2448
9/013
under-exp.
Dia 2448
10/027
cloudy
Dia SO-397
11/018
Dia SO-397
12/034
under-exp.
Color neg.
16/112
Color IR
17/020
Color IR
17/025
under-exp.

Figure 18 b)

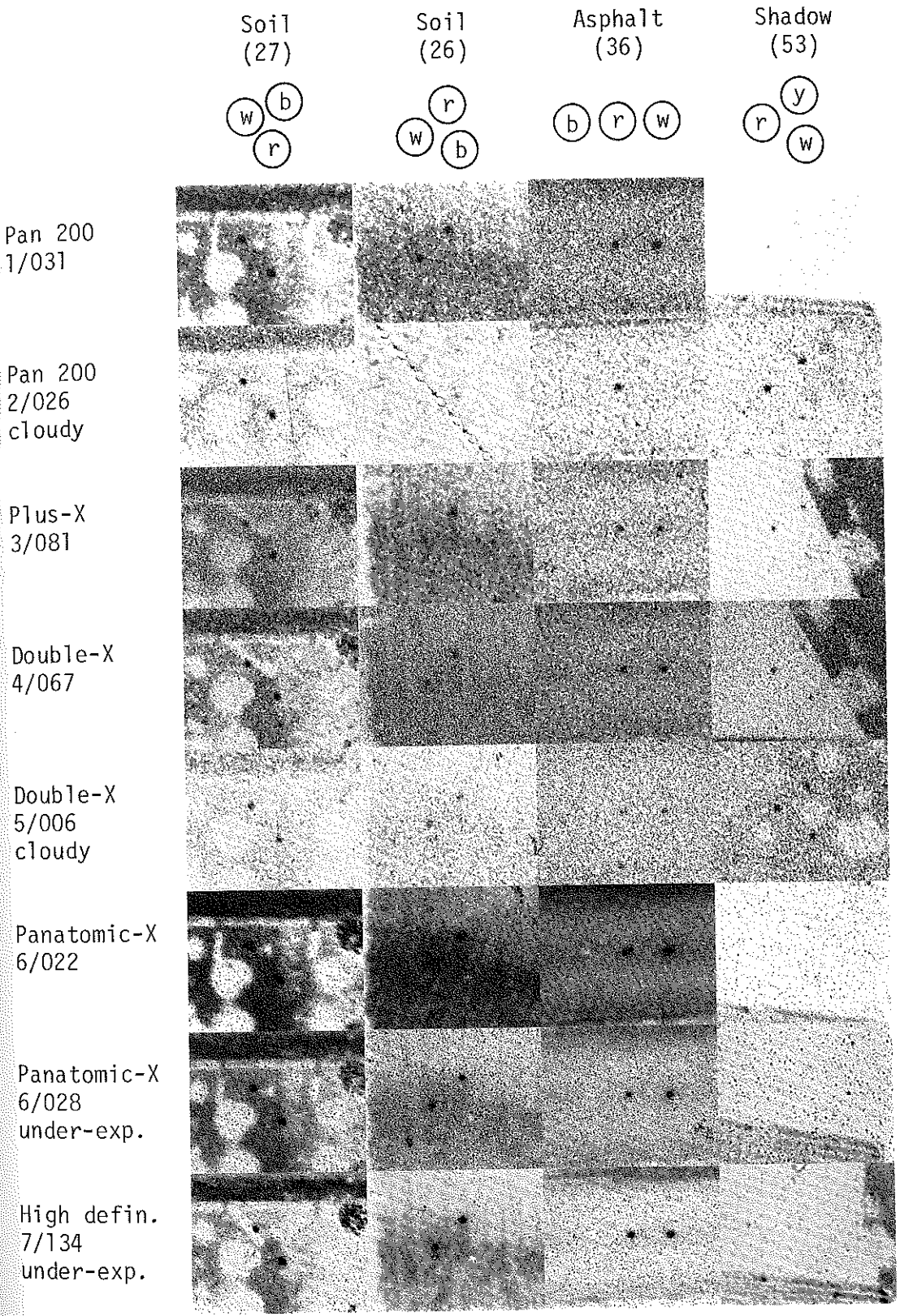
Soil
(27)
w b r
Soil
(26)
r w b
Asphalt
(36)
b r w
Shadow
(53)
r y w
Pan 200
1/031
Pan 200
2/026
cloudy
Plus-X
3/081
Double-X
4/067
Double-X
5/006
cloudy
Panatomic-X
6/022
Panatomic-X
6/028
under-exp.
High defin.
7/134
under-exp.

Figure 18 c)

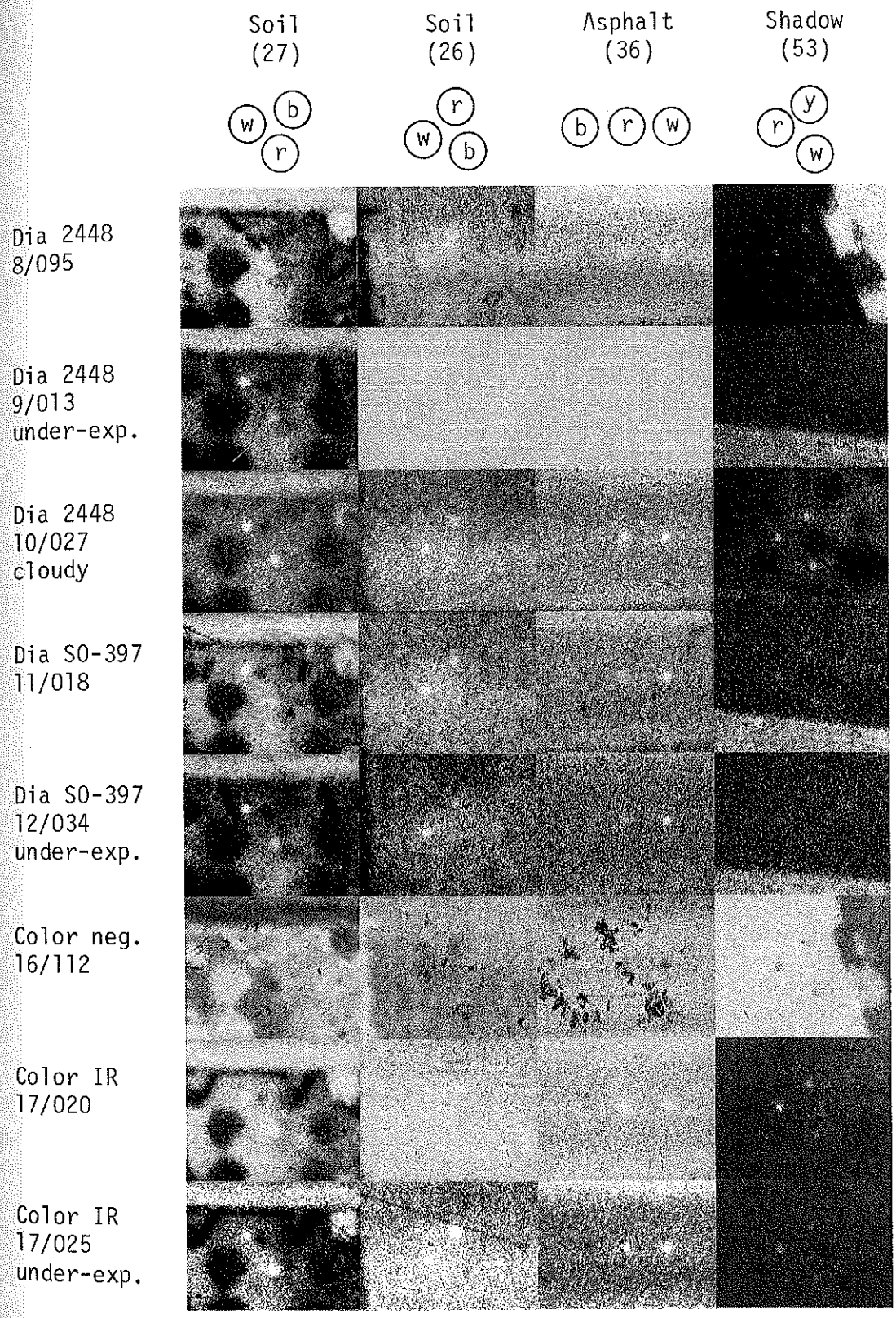
Soil
(27)
Soil
(26)
Asphalt
(36)
Shadow
(53)
w b r
w r b
b r w
r y w
Dia 2448
8/095
Dia 2448
9/013
under-exp.
Dia 2448
10/027
cloudy
Dia SO-397
11/018
Dia SO-397
12/034
under-exp.
Color neg.
16/112
Color IR
17/020
Color IR
17/025
under-exp.

Figure 18 d)

References

[1] *Kölbl, O.:* Vergleichende Analyse von Aufnahmekammern. — Vermessung/Photogrammetrie/Kulturtechnik 9/85, S. 322—330.

[2] *Zeth, U.; Voss, G.:* Some Aspects of Forward Motion Compensation in an Aerial Camera. — ISPRS, Rio de Janeiro 1984, Commission I.

4 Density control of the photographs

Apart from the resolution, photographic density plays a decisive role in quality evaluation of aerial photographs. The intention was to give recommendations for the optimum exposure of aerial photographs. As mentioned in the preceding chapter, it is extremely important to include the characteristics of the restitution instruments in the consideration of optics and illumination. Beside these objective quality criteria, the experience of the operator, the sensitivity of his eyes and other individual factors should also be included. In order to establish these different factors, the image density in the surroundings of the signals in a selection of aerial photographs was measured with a densitometer Macbeth model TR 524); for black & white films the density was measured with a neutral filter whereas for colour films the transparency in the 3 spectral ranges was determined using status A filters.

The pointing quality was given by the quality code which the operators determined during the measuring process. This quality code runs from 0 to 5:

5 = excellent
4 = good
3 = measurable
2 = hardly measurable
1 = not measurable, although the point is visible
0 = the point cannot be measured, or covered, signal lost or other reasons.

Code 1 was also attributed to points which showed up gross measuring errors. In order to establish a relation between the quality code and the density, these values have been presented graphically for all measurements. Figure 19 gives an example of such a plot for Kodak SO 397 colour film. The figure shows that points on asphalt or bare soil are much more difficult to measure than points on grassland. On the other hand, the surroundings of points in grassland are in general much darker than for points on asphalt. Hence points on asphalt are better measured on underexposed film while the pointing qualities of points in shade will diminish.

In general, one gets the impression that the background of signals on black & white film should have a density between 0.5 and 1.0 whereas for colour films the values should be between 1.0 and 1.75. It is understood that these values must be considered as a rough standard which should be more exactly specified. In this context, the photographs on Panatomic-X film and on infrared false-colour film are of special interest as for both films photographs are available which have been labelled as overexposed, normally exposed or underexposed. These pictures permit investigation of the behaviour of the quality code for varying exposures while all other conditions remain unchanged. Figure 20 to 22 show the range of the quality code and the density values for signals on asphalt

and grassland and for signals in shade, for overexposed, normally exposed and underexposed films (the left rectangle stands for underexposed Panatomic-X film, whereas the right side shows underexposed objects on infrared false-colour reversal film). Signals on roofs and on bare soil have not been included as contrast conditions are rather heterogeneous for these 2 groups. In order to ensure comparable conditions for these quality evaluations, only the results of the measurements by the National Board of Survey, Finland (Helsinki) were used. All these measurements were made on a Zeiss PSK stereo-comparator. From these diagrams it can be seen that Panatomic-X film gives the best measuring results when asphalt streets are exposed to a density of 0.7 to 0.9; points in shadow, however, can barely be measured under these conditions. In order to ensure adequate quality for these points too, a longer exposure is preferable and density values between 1.0 and 1.2 should be the aim for streets. Areas of shadow would then reach densities between 0.3 and 0.4.

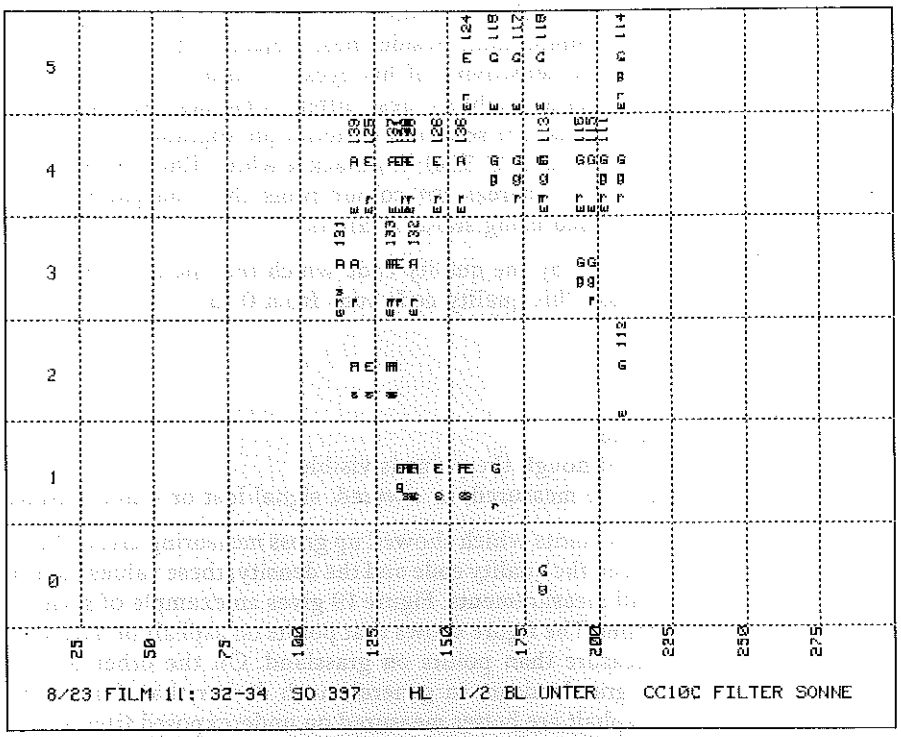

Figure 19 — Comparison of density measurements (abscissa) and quality code (ordinate). In this diagram measurements done by the Survey Board of Finland on the Zeiss stereo-comparator PSK are shown for colour film Kodak SO 397. The density measurements correspond to the red layer of the film and are shown in hundredths. Key: G = signal in grassland, E = signal on bare soil, A = signal on asphalt; w = white, r = red, g = yellow and s = black indicate the colour of the signals. The numbers correspond to the point numbers and for lack of space are only given for values smaller than 160. The corresponding numbers of the other signals must lie on the same abscissa in the diagram as the density values have only been determined once for one group of signals

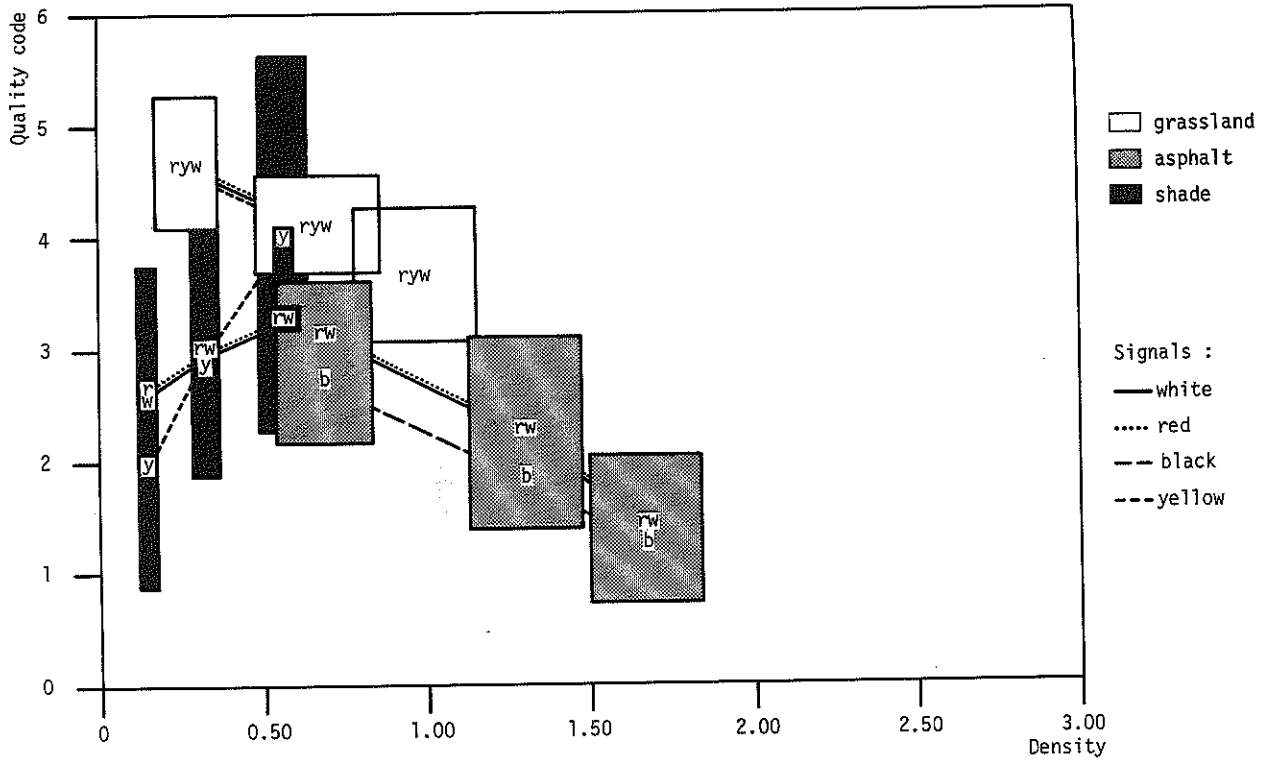

Figure 20 — (Panatomic-X film) Variation in the density of the background of signals and of the quality code when choosing different exposures. The left rectangle represent underexposed film, the middle one normally exposed and the right one overexposed film. The centres of the areas plotted, marked with w = white, r = red, b = black or y = yellow, correspond to the mean value of the group; the right and the left borders indicate the spread computed according to the mean square deviation from the mean value. The tone of the rectangle indicates the background of the signals. The connecting lines show the tendency to variation in the density and the quality code when films are overexposed, normally exposed or underexposed

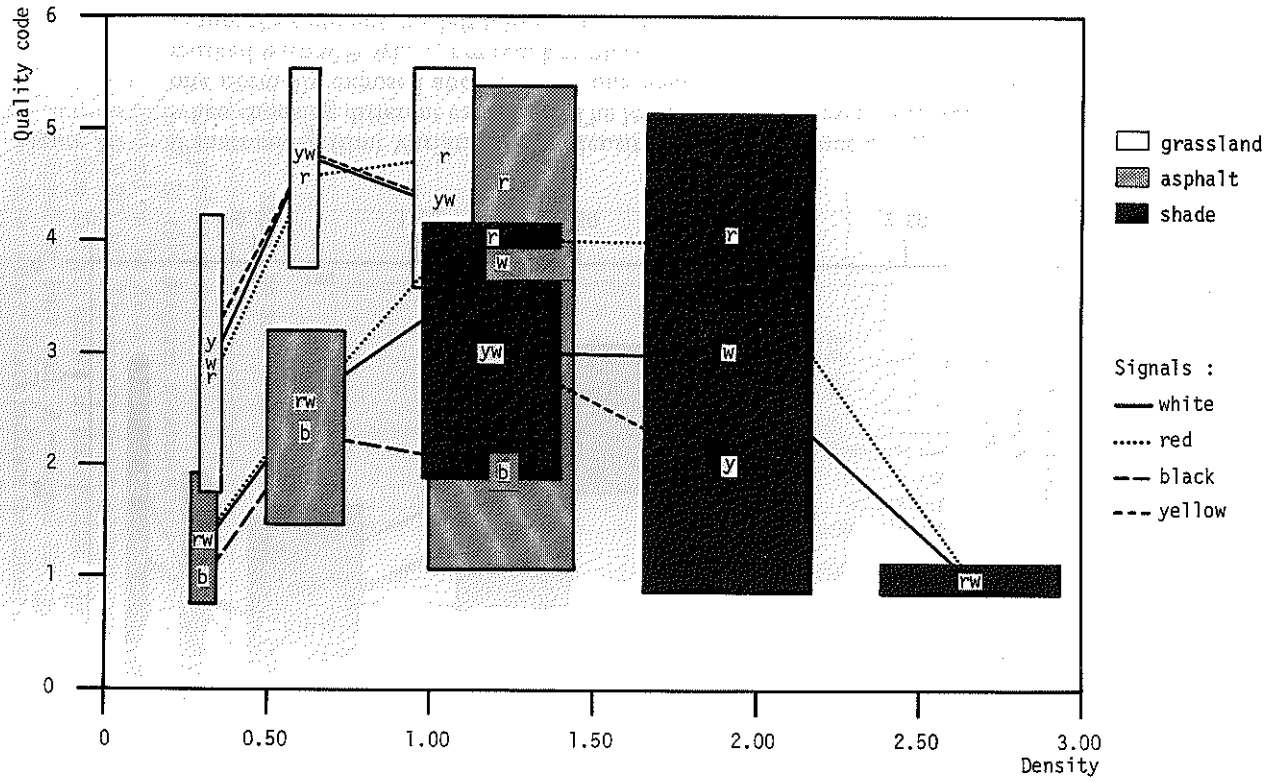

Figure 21 — (False-colour film, infrared sensitive layer, dyed red). Density variation and quality code measured on infrared false-colour film for the infrared sensitive layer

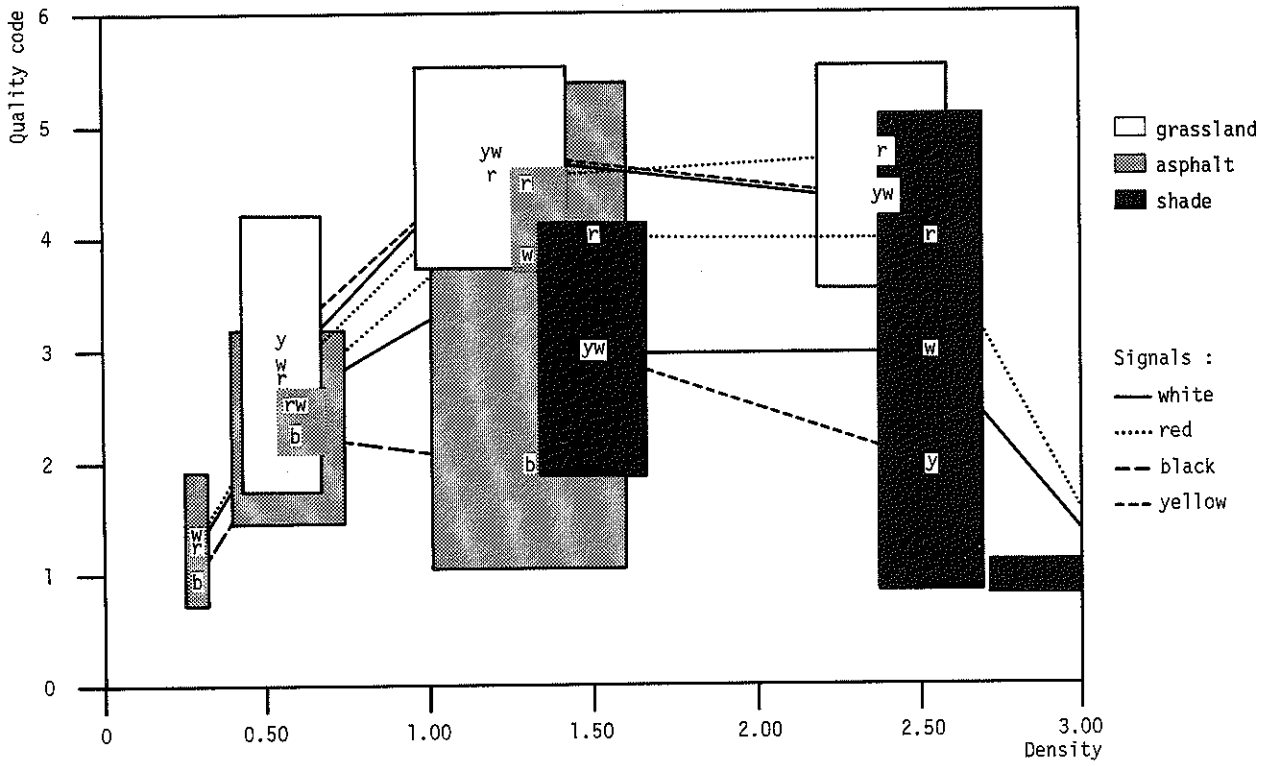

Figure 22 — (False-colour film, green sensitive layer, dyed blue). Density variation and quality code measured on infrared film, green sensitive layer

For false-colour film underexposed photographs are probably best, apart from black signals and signals in shadow; on the other hand, overexposed photographs should be considered generally unusable. Consequently, for roads, a density of between 0.6 and 0.8 should be reached in the infrared sensitive layer (the layer dyed red). Unfortunately the present picture material does not indicate whether different filtering would provide a more favorable colour balance for the various measurements. Previous experiments suggest that optimum filtering requires a good balance between the densities of the infrared sensitive layer and of the green sensitive layer for grassland. This means that about the same densities should be obtained for these 2 layers. Such a balance can be obtained by using an appropriate yellow filter, or alternatively a magenta or cyan filter, depending on the illumination conditions.

It is also possible, with the aid of the quality code, to draw conclusions as to the quality of the observation systems of the different restitution instruments. Again the measuring results by the Survey Board of Finland are used as an example, as this institute has measured a large series of pictures under very similar conditions on two different restitution instruments, namely the Zeiss stereo-comparator PSK and the Kern analytical plotter DSR1. Figure 23 compares the quality code determined in the different measuring series. The lower part of the table gives the mean of the quality code for the different series. The next line shows the differences between the two measuring instruments PSK and DSR1. Negative values indicate where the quality code of the DSR1 was higher on average than that of the PSK. According to these values a considerably higher code was obtained for all black & white films on the DSR1, whereas the reverse was true for colour films. According to this table the optics of the DSR1 have certain advantages for the measurement of signalized points over the PSK at least for black & white films, whereas for colour films the light source seems to have certain disadvantages compared with the PSK. Obviously, such statements must be considered as pure hypothesis and will have to be verified by detailed tests.

5 Investigation into geometrical aspects

5.1 General

The purpose of this part of the test was to study the geometrical accuracy of signalized points on different emulsions using the numerical restitution of the highest precision. Apart from the absolute accuracies achieved with a different emulsion, the optimum combinations of emulsion and target colour, as well as the influence of flying weather, have also been investigated. The main factors used in the test were:

- the emulsion (nine different films);
- the flight weather (sunny or cloudy);
- the target colour (white, red-orange, yellow and black).

In some emulsions it was also possible to study the influence of different exposures on the geometrical accuracy achieved (see 5.5.4).

Difference of numbers between PSK & DSR1	Number of points per model	Difference between PSK & DSR1	Sum of quality codes	1	1	2	3	4	5	111	112	113	114	115	116	211	212	213	214	215	216	Code, picture numbers	Film	
0	107	- 0,37	2,95	2	2	4	5	4	5	4	4	4	4	4	4	4	4	4	4	4	4	1101031033	Agfa	PSK
- 1	73	- 0,76	2,59	2	2	3	3	0	4	0	0	0	4	4	0	0	0	2	4	4	0	1201025027	Agfa	PSK
0	107	- 0,69	2,89	2	2	4	4	4	5	4	4	4	4	4	4	4	4	4	5	4	4	1102082083	Plus-X	PSK
0	107	- 0,81	3,17	3	3	4	4	4	4	4	4	4	4	4	4	4	4	4	4	4	4	1103066067	Double-X	PSK
0	90	- 0,63	2,68	2	2	3	4	0	0	0	2	4	4	4	4	0	3	4	4	4	4	1203004005	Double-X	PSK
0	104	- 0,14	3,31	3	3	4	4	3	4	5	5	5	5	3	5	5	4	3	4	3	3	1106094095	Dia 2448	PSK
0	93	+ 0,55	3,42	2	2	4	3	3	4	0	3	4	5	5	5	0	4	4	4	5	4	1206026027	Dia 2448	PSK
0	105	+ 0,08	3,18	3	3	4	4	5	5	4	2	4	5	4	4	4	4	4	5	3	4	1107032034	Dia SO 397	PSK
+ 1	78	+ 0,15	2,19	2	2	3	3	0	3	0	0	0	3	3	0	0	0	3	3	3	0	1207004005	Dia SO 397	PSK
0	106	- 0,01	3,64	5	5	5	5	5	5	5	5	5	5	5	2	5	5	5	5	5	3	1109023025	Color IR	PSK
0	107	- 0,83	2,15	2	2	4	3	4	4	3	4	4	4	4	3	3	4	3	3	2	3	1108112111	Color neg.	PSK
- 3	107	- 1,12	2,67	1	1	4	4	4	5	4	5	4	5	4	4	4	4	4	5	4	4	1105132133	High def.	PSK
- 1	104	- 0,89	2,95	2	2	4	4	4	5	4	4	4	5	4	4	4	4	4	5	4	4	1104020022	Panatomic-X	PSK
	107		3,32	3	3	4	4	4	4	4	4	4	4	4	4	4	4	4	4	4	4	2101031033	Agfa	DSR1
	74		3,35	3	3	4	4	0	5	0	0	0	4	3	0	0	0	2	4	4	0	2201025027	Agfa	DSR1
	107		3,58	3	3	5	5	5	5	5	4	5	5	5	5	5	4	5	5	5	5	2102082083	Plus-X	DSR1
	107		3,98	4	4	5	5	5	5	4	5	5	5	5	5	5	5	5	5	5	5	2103066067	Double-X	DSR1
	90		3,31	3	3	4	3	0	0	0	2	5	5	5	4	0	4	5	5	5	4	2203004005	Double-X	DSR1
	105		3,84	5	5	5	5	5	5	5	5	5	5	5	5	5	5	5	5	5	5	2104020022	Panatomic-X	DSR1
	107		3,79	2	2	5	5	5	5	5	5	5	5	4	5	5	5	5	5	4	5	2105132133	High def.	DSR1
	104		3,45	2	2	4	5	4	4	4	4	5	5	4	5	4	4	4	5	5	5	2106094095	Dia 2448	DSR1
	93		2,87	3	3	3	3	2	3	0	2	4	4	4	4	0	3	3	3	3	3	2206026027	Dia 2448	DSR1
	105		3,10	3	3	4	3	5	5	4	2	4	5	3	3	4	5	4	3	3	4	2107032034	Dia SO 397	DSR1
	77		2,04	2	2	3	2	0	3	0	0	0	3	3	0	0	0	1	3	3	0	2207004005	Dia SO 397	DSR1
	107		2,98	2	2	3	4	4	4	4	4	4	5	3	4	3	4	3	4	3	3	2108112111	Color neg.	DSR1
	106		3,65	4	4	5	5	5	5	5	5	5	5	5	4	4	5	5	5	5	4	2109023025	Color IR	DSR1
				2.69	2.69	4.00	3.96	4.20	4.42	4.28	3.82	4.41	4.50	4.04	4.14	4.22	4.18	3.81	4.27	3.96	4.00		Sum per point	
				26	26	26	26	20	24	18	22	22	26	26	22	18	22	26	26	26	22		Number of models	

Figure 23 — Comparison of the quality code for different films and measuring instruments; measurements by the National Board of Survey, Finland

Film type	Exposure	Pilot centres										Number	Mean	Variance
		HEL 1 PSK	HEL 2 DRS1	1 Plco	7 Plco	3 Plco	5 Plco	21 Plma	8 Plma	4 AMH	22 A10			
Pan 200	n (S)	2,95	3,32	2,79	2,82	2,79	3,38	2,65			3,04	8	2,97	± 0,09
Pan 200	n (C)	2,59	3,35	2,56					3,65	3,04	2,52	6	2,95	± 0,19
Plus-X	n (S)	2,89	3,58	2,41				2,75				4	2,91	± 0,25
Double-X	n (S)	3,17	3,98	2,52						3,05		4	3,18	± 0,30
Double-X	n (C)	2,68	3,31			2,73	3,44					4	3,04	± 0.20
Panatomic-X	+ D	2,56										1	2,56	
Panatomic-X	n (S)	2,95	3,84	2,89 2,57		2,82			3,37			5	3,14	± 0,21
Panatomic-X	- 1 D (S)	3,60		2,97 2,78	3,51							3	3,33	± 0,23
High defin.	n (S)	2,67	3,79							2,80	2,62	4	2,97	± 0,28
High defin.	- D (S)			3,02 3,28			3,88					2	3,52	± 0,37
Dia 2448	n (S)	3,31	3,45								3,09	3	3,28	± 0,10
Dia 2448	- ½ D (S)			3,13		2,86						2	3,00	± 0,13
Dia 2448	- 1 D (S)							2,74	3,19			2	2,97	± 0,23
Dia 2448	(C)	3,42	2,87		2,70							3	3,00	± 0,22
Dia SO 397	n (S)					2,87		1,94	2,53	2,29		4	2,41	± 0,20
Dia SO 397	- ½ D (S)	3,18	3,10	2,54					3,10			4	2,98	± 0,15
Dia SO 397	- 1 D (S)													
Dia SO 397	n (C)	2,19	2,04	2,02			2,07			2,02		5	2,07	± 0,03
Dia SO 397	- ½ D (C)			2,49								1	2,49	
Dia SO 397	- 1 D (C)				2,72							1	2,72	
Color neg.	n (S)	2,15	2,98	2,58			3,35	3,11				5	2,83	± 0,21
Color IR	+ D (S)	2,12									2,31	2	2,22	± 0,09
Color IR	n (S)	3,27			2,69							2	2,98	± 0,29
Color IR	- 1 D (S)	3,64	3,65	2,98		3,37						4	3,41	± 0,16

Figure 24 — Comparison of the mean of the quality code for different films and pilot centres. An abreviation characterizing the measuring instrument is given below the code of the pilot centre: PSK = Zeiss stereo-comparator, DSR1 = Kern analytical plotter, Plco = Zeiss Planicomp, Plma = Zeiss planimat, AMH = Wild AMH, A10 = Wild A10. In the last column the mean of all values and the mean square deviation referring to the mean are given. The exposure shows: (S) or (C) = sunny or cloudy weather; n = normal exposure; + D = overexposed, without special indications; — 1/2 D or — 1 D = underexposed for 1/2 or 1 diaphragm. Note the strong relation between a high quality code and underexposure of a film

The accuracy was investigated by means of geodetically determined, signalized points set up in the area as follows:

- 20 control points (see 2.3.1);
- 87 check points (see 2.3.2).

The photographic material comprised 54 models (see 2.4.1) of which 13 of a qualitatively and navigationally high level were chosen for the primary investigation. Later seven additional models were chosen so that the test material also included different exposures for some emulsions.

A summary of the processed models is presented in Figure 25.

Flight model	Emulsion	Weather sunny	Weather cloudy	Primary set	Addit. models
1— 31/33	Pan 200	*		*	
2— 25/27	Pan 200		*	*	
3— 82/83	Plus-X	*		*	
4— 66/67	Double-X	*		*	
5— 4/5	Double-X		*	*	
6— 20/22	Panatomic 3412	*		*	
6— 28/30	u Panatomic 3412	*			*
6— 34/36	o Panatomic 3412	*			*
7—132/133	HD 3414	*		*	
8— 94/95	Dia 2448	*		*	
9— 13/15	u Dia 2448	*			*
9— 40/42	Dia 2448	*			*
10— 26/27	Dia 2448		*	*	
12— 32/34	Dia SO 397	*		*	
15— 5/6[1)]	Dia SO 397		*	*	
16—111/112	Negativ 2445	*		*	
17— 18/20	IR 2443	*			*
17— 23/25	u IR 2443	*		*	
17— 24/26	u IR 2443	*			*
17— 29/31	o IR 2443	*			*

[1)] Flight with a single engine aircraft

u = underexposed
o = overexposed

Figure 25 — Flight models included in the geometric part of the test

5.2 *Observations*

The observations of the image coordinates were carried out at the National Board of Survey, Helsinki, with a Zeiss PSK1 stereo-comparator, the accuracy of which was checked with gridplate measurements (ISPRS standard test). The main results were:

	residuals (μm)		double measurements (μm)	
	m_x	m_y	m_x	m_y
left plate	2,5	3,0—3,5	1,5	2,2
right plate	2,5	3,3—3,9	1,6	1,9

The measurements were done with a 12x optical enlargement. The size of the measuring mark was 25 micrometres.

The image coordinate measurements for this test were done by observing the fiducial marks once, the targets with double pointings, and finally the fiducial marks once again. The points were divided into five classes according to their measurability (Appendix 1).

There were an average of 70 to 100 measurable points per model.

5.3 *Computations*

The image coordinates were transformed into the camera coordinates with an affine, 6-parameter transformation using the fiducial marks. The transformed coordinates were the mean values of the double measurements. Before the adjustment the image coordinates were still corrected against the lens distortion according to the calibration certificates. The photogrammetric determination of coordinates for 87 check points was based on the geodetic precise control of 20 stations. The calculations were carried out with block adjustments by bundles. An attempt was made to eliminate the effects of eventual systematic errors by using additional parameters in the calculation [1].

However, as systematics apparently still existed in the residuals of the ground control used, it was decided to approximate them with the finite element technique [2], [3]. The finite element coordinates were calculated separately for the X- and Y-discrepancies, one side of the grid square being 50 metres. In this way, corrected coordinates for check points were used as input data in this part of the study.

Statistics for the bundle block adjustments and the elimination of systematic errors are presented in Figure 26.

For statistical studies the discrepancies between the photogrammetric and geodetic coordinates of the check points were computed. In addition the coordinate system was turned so that the X-axis agreed approximately with the flight direction and the Y-axis perpendicularly against the flight direction.

The absolute values of the discrepancies both in the flight direction (dX), and perpendicularly against it (dY), were chosen as the basis of the statistical investigation. In addition, the discrepancies in planimetry ($dXY = \sqrt{dX^2 + dY^2}$) were used.

Weather: Flight model	Emulsion	Block Adjustment: No. of control points	No. of check points	m_o (µm)	Discrepancies (RMSE) at the control points X (cm)	Y (cm)	Discrepancies (RMSE) at the check points before Corr. of the system. Errors X (cm)	Y (cm)	after X (cm)	Y (cm)
Sun										
Black & white										
1— 31/33	Pan 200	19	71	4.6	1.2	0.9	2.0	2.4	1.4	2.0
3— 82/83	Plus-X	19	69	4.4	1.2	1.3	2.5	2.8	2.2	2.5
4— 66/67	Double-X	20	73	4.1	0.6	0.8	2.1	2.6	1.8	2.2
6— 20/22	Panatomic 3412	17	76	4.4	1.0	1.1	2.3	2.6	1.8	1.9
6— 28/30	u Panatomic 3412	20	84	4.1	0.8	1.1	2.0	2.4	1.6	1.9
6— 34/36	o Panatomic 3412	18	60	4.9	1.3	1.6	2.4	2.7	1.7	2.2
7—132/133	HD 3414	17	53	4.0	1.3	0.8	2.3	2.5	1.7	1.9
Colour										
8— 94/95	Dia 2448	19	73	3.9	1.3	0.8	2.1	2.9	1.7	2.4
9— 13/15	u Dia 2448	15	56	4.0	1.1	0.9	2.5	2.9	1.4	1.7
9— 40/42	Dia 2448	15	63	4.1	0.8	1.1	2.1	2.3	1.6	1.9
12— 32/34	Dia SO 397	20	67	4.7	1.1	1.0	2.2	3.2	1.6	1.9
16—111/112	Negat. 2445	11	52	6.0	0.5	1.4	2.5	3.4	1.9	2.1
17— 18/20	IR 2443	18	74	4.3	0.9	1.2	2.3	2.7	1.7	2.1
17— 23/25	u IR 2443	18	69	3.5	0.9	0.7	1.7	2.5	1.2	2.2
17— 24/26	u IR 2443	12	58	3.3	0.9	0.7	2.3	2.9	1.8	1.7
17— 29/31	o IR 2443	13	44	4.4	1.1	1.5	2.6	3.8	1.9	2.9
Overcast sky										
Black & white										
2— 25/27	Pan 200	14	43	4.7	1.1	1.1	2.8	3.5	2.0	2.8
5— 4/5	Double-X	12	56	5.2	1.0	1.6	2.1	2.2	1.7	1.5
Colour										
10— 26/27	Dia 2448	16	67	5.3	1.9	1.5	3.0	2.4	1.3	1.9
15— 5/6	Dia SO 397	12	41	5.8	1.9	1.8	3.5	4.4	2.7	3.7

o = overexposed
u = underexposed

Figure 26 — Statistics concerning the bundle block adjustments and elimination of systematic errors

5.4 *Statistical investigations*

The aim of the statistical studies was to establish whether significant accuracy differences exist between emulsion/weather condition/target colour/exposures.

Because of the nature of the material and the number of observations, the analysis of variance, the *F*-test of *Fisher*, the Student *t*-test and the nonparametric test of *Mann-Whitney* (Wilcoxon rank sum test) were chosen as the methods of the statistical investigation. A special program package, the SPSS (Statistical Package for the Social Sciences) was chosen for the investigation.

In all tests, 5 %, 1 % and 0.1 % were chosen as the levels of significance (chapter 5.5).

5.4.1 Analysis of variance

In the one-way analysis of variance the dependent variable (*dX*, *dY*, *dXY*) has one factor *A*, which has categories A_i, $i = 1,...,p$.

The factors used in this test were:

- weather condition,
- flight/emulsion,
- target colour,
- exposure.

5.4.2 *t*-tests

The means of two samples were compared with the twotailed Student *t*-test. This test assumes that the sample variances are equal; the *F*-test of *Fisher* was calculated to compare the variances at the 5 % risk level.

Case A) The variances did not differ from each other:

A common *t*-test was applied. A "pooled variance" was calculated from the two samples with sizes k_1 and k_2, means m_1 and m_2 and variances s_1^2 and s_2^2

$$s^2 = \frac{(k_1 - 1)\ s_1^2 + (k_2 - 1)\ s_2^2}{(k_1 - 1) + (k_2 - 1)}$$

with degrees of freedom $k_1 + k_2 - 2$. The *t*-value corresponding to the difference in sample means is

$$t = \frac{m_1 - m_2}{\sqrt{(s^2/k_1) + (s^2/k_2)}}$$

Case B) The variances were unequal:

An approximation for the *t*-value was calculated with the same formula

$$t = \frac{m_1 - m_2}{\sqrt{(s_1^2/k_1) + (s_2^2/k_2)}}$$

which does not follow the t-distribution, but its t-probability can be approximated by treating it as t, but with degrees of freedom

$$df = \frac{((s_1^2/k_1) + (s_2^2/k_2))^2}{(s_1^2/k_1)^2/(k_1 - 1) + (s_2^2/k_2)^2/(k_2 - 1)} .$$

5.4.3 Nonparametric test of *Mann-Whitney*

Because the distribution of the discrepancies was not equal to the normal distribution, and transformations (e. q. logarithmation) did not solve the problem properly, it was decided to compute the nonparametric Mann-Whitney test (Wilcoxon rank sum test) as well.

The Mann-Whitney test can be used to establish whether two samples belong to the same population. The two groups are combined and cases are ranked in order of increasing size. The test statistics U are computed as the number of times a score from group 1 precedes a score from group 2.

From larger groups (more than 30 cases) it can be shown that U is fairly normally distributed (with mean $\frac{1}{2} n_1 n_2$ and variance $\frac{1}{12} n_1 n_2 \ (n_1 + n_2 + 1)$) and U is transformed into normally distributed statistics, Z [4].

5.5 The results of the tests

The tests were calculated separately with X-, Y- and XY-differences (dX, dY, dXY) (see 5.3) when the influence of weather conditions or different flights was studied. When investigating target colour and exposures only XY-differences are used. In the figures of the test results given later the mean (m) and standard deviation (s) for the real discrepancies as well as the same (M, S) for the absolute values are presented.

$$m = \frac{\sum_{i=1}^{N} D_i}{N} \qquad s = \sqrt{\frac{\sum_{i=1}^{N} (D_i - m)^2}{N - 1}}$$

$$M = \frac{\sum_{i=1}^{N} |D_i|}{N} \qquad S = \sqrt{\frac{\sum_{i=1}^{N} (|D_i| - M)^2}{N - 1}}$$

$$D_i = (dX_i,\ dY_i,\ dXY_i).$$

The results of the tests include also the number of observations and the level of significance (see 5.4), which was coded as follows:

$\star$ $= 5\ \% \geqq p > 1\ \%$ = almost significant
$\star\star$ $= 1\ \% \geqq p > 0.1\ \%$ = significant
$\star\star\star$ $= 0.1\ \% \geqq p$ = highly significant.

5.5.1 Flight/Emulsion

In this part of the study all 20 models (Figure 25), both primary and additional, belong to the tested set.

Analysis of variance

The analysis of variance, which was used in the comparison of the models, showed that there were statistically significant differences between them. In a Y-direction the differences were significant, whereas in X- and XY-directions the differences between models were highly significant.

The test parameters (m, s, M, S and the number of check points) are summarized together with the results of the further tests in Figures 27—29.

F-, t- and Mann-Whitney tests

These tests were carried out by comparing the best model with the others.

The Mann-Whitney tests calculated alongside the t-test supported the results of the t- test.

The results of the tests have been compiled in Figures 27—29.

5.5.2 Flight weather

In order to investigate the influence of flight weather four emulsions were selected for the test. These emulsions were Pan 200 and Double-X black & white emulsions and Dia 2448 and Dia SO 397 colour emulsions. The test parameters (m, s, M, S and number of observations) are summarized in Figure 30.

Analysis of variance

The one-way analysis of variance, which was used to compare different types of weather, did not reveal any significant differences between types. However, from a practical point of view we should bear in mind that the number of observed points on cloudy flights is, on average, only 70—75 % of the results of the sunny flights.

Because the analysis of variance did not show any statistically significant differences between the types of weather, other tests were not computed.

5.5.3 Target colour

The purpose of this part of the test was to investigate the influence of different target colours on the geometrical accuracy achieved. This part of the test included only the optimal exposures of each emulsion (see 5.1). The statistical tests were calculated using the XY-discrepancies of the check points.

The one-way analysis of variance showed that there were significant differences between target colours in general. This was supported by further tests, which showed that the black target colour gave highly significantly poorer results than the best one, which was red (Figure 31).

Weather Film	Flight model	Emulsion	No. of check points	Discrepancies at the check points				Level of significance		
				m (cm)	s (cm)	M (cm)	S (cm)	t-test	F-test	M-WH
Sun										
Black & white	1— 31/33	Pan 200	71	−0.1	1.4	1.1	0.9	—	—	—
	3— 82/83	Plus-X	69	−0.1	2.2	1.7	1.3	***	***	***
	4— 66/67	Double-X	73	0.0	1.8	1.3	1.2	**	*	*
	6— 20/22	Panatomic 3412	76	0.0	1.8	1.3	1.3	***	*	—
	6— 28/30	u Panatomic 3412	84	−0.1	1.6	1.1	1.1	*	—	—
	6— 34/36	o Panatomic 3412	60	0.1	1.7	1.3	1.1	—	*	*
	7—132/133	HD 3414	53	−0.1	1.7	1.3	1.1	*	*	*
Colour	8— 94/95	Dia 2448	73	0.0	1.7	1.3	1.1	*	**	*
	9— 13/15	u Dia 2448	56	0.0	1.4	1.0	0.9	—	—	—
	9— 40/42	Dia 2448	63	0.0	1.6	1.3	0.9	—	**	**
	12— 32/34	Dia SO 397	67	0.0	1.6	1.2	1.0	—	*	*
	16—111/112	Negat. 2445	52	0.1	1.9	1.4	1.3	**	**	*
	17— 18/20	IR 2443	74	−0.1	1.7	1.3	1.1	*	*	—
	17— 23/25	u IR 2443	69	0.0	1.2	0.9	0.8	Reference Model		
	17— 24/26	u IR 2443	58	0.0	1.8	1.4	1.2	**	**	*
	17— 29/31	o IR 2443	44	−0.2	1.9	1.5	1.2	*	**	*
Overcast sky										
Black & white	2— 25/27	Pan 200	43	0.0	2.0	1.6	1.2	*	**	**
	5— 4/5	Double-X	56	−0.2	1.7	1.4	0.9	—	**	**
Colour	10— 26/27	Dia 2448	67	−0.1	1.3	1.0	0.8	—	—	—
	15— 5/6	Dia SO 397	41	0.0	2.7	2.1	1.7	***	***	***

o = overexposed
u = underexposed

The level of significance is coded as follows:

* = 5 % $\geqq p >$ 1 % = almost significant
** = 1 % $\geqq p >$ 0.1 % = significant
*** = 0.1 % $\geqq p$ = highly significant

Figure 27 — Results of the statistical tests concerning different flights and models.
Tests calculated with X-discrepancies of the check points

Weather Film	Flight model	Emulsion	No. of check points	Discrepancies at the check points				Level of significance		
				m (cm)	*s* (cm)	*M* (cm)	*S* (cm)	*t*-test	*F*-test	*M-WH*
Sun										
Black & white	1– 31/33	Pan 200	71	0.0	2.0	1.5	1.3	*	*	*
	3– 82/83	Plus-X	69	0.0	2.5	1.7	1.8	***	*	*
	4– 66/67	Double-X	73	0.0	2.2	1.5	1.6	***	—	—
	6– 20/22	Panatomic 3412	76	0.0	1.9	1.3	1.3	*	—	—
	6– 28/30	u Panatomic 3412	84	0.0	1.9	1.4	1.3	*	—	—
	6– 34/36	o Panatomic 3412	60	0.0	2.2	1.6	1.6	***	—	—
	7–132/133	HD 3414	53	0.0	1.9	1.3	1.4	**	—	—
Colour	8– 94/95	Dia 2448	73	0.1	2.4	1.9	1.6	***	**	**
	9– 13/15	u Dia 2448	56	0.0	1.7	1.2	1.1	—	—	—
	9– 40/42	Dia 2448	63	0.0	1.9	1.4	1.2	—	—	—
	12– 32/34	Dia SO 397	67	0.0	1.9	1.5	1.3	*	—	—
	16–111/112	Negat. 2445	52	0.0	2.1	1.4	1.5	**	—	—
	17– 18/20	IR 2443	74	0.0	2.1	1.6	1.4	**	*	—
	17– 23/25	u IR 2443	69	0.0	2.2	1.7	1.4	**	*	*
	17– 24/26	u IR 2443	58	0.0	1.7	1.3	1.1	—	—	—
	17– 29/31	o IR 2443	44	−0.2	2.9	2.0	2.1	***	**	*
Overcast sky										
Black & white	2– 25/27	Pan 200	43	0.0	2.8	1.8	2.2	***	—	—
	5– 4/5	Double-X	56	0.1	1.5	1.1	1.0	Reference Model		
Colour	10– 26/27	Dia 2448	67	0.1	1.9	1.3	1.3	*	—	—
	15– 5/6	Dia SO 397	41	0.0	3.7	2.3	2.3	***	*	*

o = overexposed
u = underexposed

The level of significance is coded as follows:

* = 5 % ≧ p > 1 % = almost significant
** = 1 % ≧ p > 0.1 % = significant
*** = 0.1 % ≧ p = highly significant

Figure 28 — Results of the statistical tests concerning different flights and models.
Tests calculated with Y-discrepancies of the check points

Weather Film	Flight model	Emulsion	No. of check points	Discrepancies at the check points				Level of significance		
				m (cm)	*s* (cm)	*M* (cm)	*S* (cm)	*t*-test	*F*-test	*M-WH*
Sun										
Black & white	1— 31/33	Pan 200	71			2.0	1.4	—	—	—
	3— 82/83	Plus-X	69			2.7	1.9	***	**	**
	4— 66/67	Double-X	73			2.2	1.8	***	—	—
	6— 20/22	Panatomic 3412	76			2.0	1.7	**	—	—
	6— 28/30	u Panatomic 3412	84			2.0	1.5	*	—	—
	6— 34/36	o Panatomic 3412	60			2.2	1.6	**	—	—
	7—132/133	HD 3414	53			2.1	1.5	*	—	—
Colour	8— 94/95	Dia 2448	73			2.5	1.7	**	**	*
	9— 13/15	u Dia 2448	56			1.8	1.1	Reference Model		
	9— 40/42	Dia 2448	63			2.1	1.3	—	—	—
	12— 32/34	Dia SO 397	67			2.1	1.3	—	—	—
	16—111/112	Negat. 2445	52			2.3	1.7	**	—	—
	17— 18/20	IR 2443	74			2.2	1.5	*	—	—
	17— 23/25	u IR 2443	69			2.0	1.5	*	—	—
	17— 24/26	u IR 2443	58			2.0	1.4	—	—	—
	17— 29/31	o IR 2443	44			2.7	2.2	***	*	—
Overcast sky										
Black & white	2— 25/27	Pan 200	43			2.7	2.1	***	**	**
	5— 4/5	Double-X	56			1.9	1.1	—	—	—
Colour	10— 26/27	Dia 2448	67			1.8	1.3	—	—	—
	15— 5/6	Dia SO 397	41			3.4	3.1	***	**	**

o = overexposed
u = underexposed

The level of significance is coded as follows:

* = 5 % $\geqq p >$ 1 % = almost significant
** = 1 % $\geqq p >$ 0.1 % = significant
*** = 0.1 % $\geqq p$ = highly significant

Figure 29 — Results of the statistical tests concerning different flights and models.
Tests calculated with *XY*-discrepancies of the check points

	Clear sky			Overcast sky		
	X	*Y*	*XY*	*X*	*Y*	*XY*
Number of observ.	284	284	284	207	207	207
mean (cm)	0.0	0.0	—	−0.1	0.0	—
standard dev. (cm)	1.6	2.2	—	1.9	2.5	—
M (cm)	1.2	1.6	2.2	1.4	1.6	2.3
S (cm)	1.1	1.5	1.6	1.2	1.9	2.0

Figure 30 — Statistics for the comparison between different types of weather

Target colour	Discrepancies at the check points (cm)		No. of check points	Level of significance		
	M	*S*		*F*-test	*t*-test	M-W
White	2.3	1.9	298	***	—	—
Red	2.1	1.5	307		reference	
Black	2.9	1.3	63	—	***	***
Yellow	2.2	2.0	142	***	—	—

The level of significance is coded as follows:

* = 5 % ≧ p > 1 % = almost significant
** = 1 % ≧ p > 0.1 % = significant
*** = 0.1 % ≧ p = highly significant

Figure 31 — Results of the statistical tests between different target colours

Later it was decided to investigate each target colour separately in order to establish the compatibility of the target colour used for different emulsions. As a result there were very few observations left, especially as far as black and yellow targets were concerned. The results of the tests should therefore be treated with caution. The numbers of observations, mean values (*M*), standard deviations (*S*) and the maximum point errors for each target colour are presented in Figures 32–35.

Weather Flight model	Emulsion	No. of check points	Discrepancies at the check points (cm) *M*	*S*	Max.
Sun					
Black & white					
1— 31/33	Pan 200	25	2.2	2.0	9.4
3— 82/83	Plus-X	26	2.9	1.9	9.9
4— 66/67	Double-X	25	2.7	2.6	13.4
6— 20/22	Panatomic 3412	26	2.2	2.2	12.1
7—132/133	HD 3414	18	2.1	2.1	9.6
Colour					
8— 94/95	Dia 2448	26	2.5	1.8	9.2
12— 32/34	Dia SO 397	27	1.9	1.3	6.3
16—111/112	Negat. 2445	21	2.2	1.8	8.6
17— 23/25	IR 2443	25	2.2	1.9	8.9
Overcast Sky					
Black & white					
2— 25/27	Pan 200	16	2.4	0.8	4.0
5— 4/5	Double-X	21	2.0	1.0	4.1
Colour					
10— 26/27	Dia 2448	25	1.5	0.7	2.9
15— 5/6	Dia SO 397	17	3.1	2.8	11.2

Figure 32 — Accuracy of the white targets on different flights.
XY-discrepancies at the check points

Weather Flight model	Emulsion	No. of check points	Discrepancies at the check points (cm) *M*	*S*	Max.
Sun					
Black & white					
1— 31/33	Pan 200	26	1.9	0.8	3.4
3— 82/83	Plus-X	27	2.3	1.5	7.8
4— 66/67	Double-X	28	1.6	1.0	4.0
6— 20/22	Panatomic 3412	26	2.0	1.4	6.9
7—132/133	HD 3414	19	2.1	1.0	4.0
Colour					
8— 94/95	Dia 2448	26	2.3	1.7	6.8
12— 32/34	Dia SO 397	25	2.1	1.5	7.3
16—111/112	Negat. 2445	18	2.4	1.7	6.3
17— 23/25	IR 2443	25	1.8	1.2	4.4
Overcast Sky					
Black & white					
2— 25/27	Pan 200	19	2.4	1.3	4.2
5— 4/5	Double-X	23	1.6	1.1	4.0
Colour					
10— 26/27	Dia 2448	26	1.9	1.6	8.0
15— 5/6	Dia SO 397	19	2.9	2.4	9.4

Figure 33 — Accuracy of the red targets on different flights.
XY-discrepancies at the check points

Weather Flight model	Emulsion	No. of check points	Discrepancies at the check points (cm) *M*	*S*	Max.
Sun					
Black & white					
1— 31/33	Pan 200	7	2.5	1.5	4.4
3— 82/83	Plus-X	2	2.8	2.6	4.7
4— 66/67	Double-X	7	3.0	0.8	4.3
6— 20/22	Panatomic 3412	10	2.6	1.2	4.2
7—132/133	HD 3414	4	3.1	1.6	4.4
Colour					
8— 94/95	Dia 2448	10	3.1	1.5	5.8
12— 32/34	Dia SO 397	6	2.8	1.3	4.9
16—111/112	Negat. 2445	—	—	—	—
17— 23/25	IR 2443	9	2.8	1.1	4.5
Overcast Sky					
Black & white					
2— 25/27	Pan 200	2	2.9	1.7	4.0
5— 4/5	Double-X	1	4.1	—	4.1
Colour					
10— 26/27	Dia 2448	5	3.3	1.6	5.8
15— 5/6	Dia SO 397	—	—	—	—

Figure 34 — Accuracy of the black targets on different flights.
XY-discrepancies at the check points

Weather Flight model	Emulsion	No. of check points	Discrepancies at the check points (cm) *M*	*S*	Max.
Sun					
Black & white					
1— 31/33	Pan 200	13	1.8	0.9	3.5
3— 82/83	Plus-X	14	2.8	2.5	8.2
4— 66/67	Double-X	13	2.0	1.1	4.0
6— 20/22	Panatomic 3412	14	1.3	0.7	2.8
7—132/133	HD 3414	12	1.7	0.9	3.7
Colour					
8— 94/95	Dia 2448	11	2.2	1.3	5.2
12— 32/34	Dia SO 397	9	2.5	1.1	4.1
16—111/112	Negat. 2445	13	2.1	1.4	4.6
17— 23/25	IR 2443	10	1.3	0.9	3.4
Overcast Sky					
Black & white					
2— 25/27	Pan 200	6	4.5	4.9	14.0
5— 4/5	Double-X	11	2.2	1.0	4.2
Colour					
10— 26/27	Dia 2448	11	1.8	1.1	4.4
15— 5/6	Dia SO 397	5	5.8	5.6	15.3

Figure 35 — Accuracy of the yellow targets on different flights.
XY-discrepancies at the check points

Analysis of variance

The one-way analysis of variance between models was calculated for each target colour. The results showed that only the yellow target colour gave statistically significant differences between models. These differences were highly significant.

F-, *t*- and Mann-Whitney tests

As the results of the analysis of variance showed statistically significant differences between models with yellow targets, the *F*-, *t*- and Mann-Whitney tests were employed for this colour. However, the reliability of the tests is quite poor owing to the small number of observations. The results are presented in Figure 36.

Weather/ Flight model	Emulsion	No. of check points	Level of significance *F*-test	*t*-test	M-WH
SUN					
Black & white					
1— 31/33	Pan 200	13	—	—	—
3— 82/83	Plus-X	14	***	*	—
4— 66/67	Double-X	13	—	—	—
6— 20/22	Panatomic 3412	14			
7—132/133	HD 3414	12	—	—	—
Colour					
8— 94/95	Dia 2448	11	*	—	—
12— 32/34	Dia SO 397	9	—	**	*
16—111/112	Negativ 2445	13	*	—	—
17— 23/25	IR 2443	10	—	—	—
OVERCAST SKY					
Black & white					
2— 25/27	Pan 200	6	***	—	**
5— 4/5	Double-X	11	—	*	*
Colour					
10— 26/27	Dia 2448	11	—	—	—
15— 5/6	Dia SO 397	5	***	—	**

The level of significance is coded as follows:

* = 5 % $\geqq p >$ 1 % = almost significant
** = 1 % $\geqq p >$ 0.1 % = significant
*** = 0.1 % $\geqq p$ = highly significant

Figure 36 — Results of the statistical tests with yellow targets between models

5.5.4 Exposures

Of the test material measured in Helsinki three emulsions had different exposures under similar flight conditions. These emulsions were black & white Panatomic 3412 and Dia 2448 and IR 2443 colour films (Figure 25).

Analysis of variance

The analysis of variance, which was calculated between different exposures for each emulsion, showed that there were statistically significant differences only for the Dia 2448 colour film. The results are presented in Figure 37.

Emulsion	Flight model	Exposure	Discrepancies at the check points (cm) M	S	No. of check points	Analysis of variance
Panatomic 3412	6—20/22	normal	2.0	1.7	76	no.
	6—28/30	−1 Ap.	2.0	1.5	84	signif.
	6—34/36	+1 Ap.	2.2	1.6	60	diff.
Dia 2448	8—94/95	normal	2.5	1.7	73	almost
	9—40/42	normal	2.1	1.3	63	signif.
	9—13/15	−1 Ap.	1.8	1.1	56	diff.
IR 2443	17—23/25	−1 Ap.	2.0	1.5	69	no.
	17—24/26	−1 Ap.	2.0	1.4	58	signif.
	17—18/20	normal	2.2	1.5	74	diff.
	17—29/31	+1 Ap.	2.7	2.2	44	

Figure 37 — Summary of the analysis of variance between different exposures of the emulsion under similar flight conditions

F-, *t*- and Mann-Whitney tests

F-, *t*- and Mann-Whitney tests were calculated between the different exposures of Dia 2448 emulsion. These tests indicated that model 8—94/95 differed significantly in terms of its standard deviation and mean according to *F*- and *t*-tests, and almost significantly according to the Mann-Whitney test.

5.6 *Summary*

From studies of the geometrical accuracy of the measurements done in Helsinki, we may conclude:

- Under optimal conditions there are no significant differences in measurability between emulsions in terms of geometrical quality.

  However, from the practical point of view the number of measurable points varies considerably between emulsions and models.

  Compared with the restitution of other emulsions the observations of Colour Negative Film 2445 in particular were influenced by the exceptional colours and the instrument used for the restitution.
- According to this test flight weather has no significant effect on the geometrical quality of the images, but it has great influence on the measurability of the targets.
- The statistical tests showed that there were significant differences between target colours in general. The black target colour gave highly significantly poorer results than the others.

  According to these tests the accuracy achieved with yellow targets is affected by the emulsion employed, but owing to the small number of observations this result is not very reliable.

  Coverally it was noticed that the capacity of the source of illumination in PSK-1 was not high enough on some occasions, especially when observing dark objects.

References

[1] *Ebner, H.:* Self Calibrating Block Adjustment. — ISP, Helsinki 1976, Commission III.

[2] *Ebner, H.:* Zwei neue Interpolationsverfahren und Beispiele für ihre Anwendung. — Bildmessung und Luftbildwesen 47, 1979, pp. 15—27.

[3] *Haljala, S.:* Transformations of National Plane Coordinate Systems by using the Method of Finite Elements. — Nordic Geodetic Commission, Gävle 1982.

[4] *Malik, H.J.; Mulle, K.:* A First Course in Probability and Statistics. — Addison-Westley 1973.

6 Analysis of the measuring precision of the signalized points

The photographs from the "Steinwedel" test-field were measured at 19 different centres. This wide range of measurements allows some conclusions to be drawn about the most appropriate photographic material; another result is an interesting survey of the measuring capacity of the different centres and particularly of the quality of the photogrammetric instruments used. An overview of the measuring results of the different centres is given in Figure 39 and a detailed view of the measuring results of the individual models in Figure 38. Figure 39 shows the mean observation errors of the model measurements, the mean deviation from the control points before and after correction of systematic error components, and the total number of measured points per model. The latter figure is of considerable importance when comparing the measuring results as the quality of the points differ considerably, and centres which eliminated all points which did not appear optimal might have considerably improved the final results. Of course all the values show a marked variation from model to model. This spread is also given in the table by the mean square error, so that this variation can be included in the analysis of the results.

It is very clear that the measuring precision is determined mainly by the choice of the restitution instrument. Precision was lowest with the Wild A8. It is poorer than the group with all the other analog plotters, the Zeiss Planimat, Wild A10 and AMH; another group is formed by the analytical plotters which give about 50 % higher precision. From this group of analytical instruments 4 centres stand out as they give precision higher by another 30 %. Two Zeiss Planicomps and the AC1 and BC1 analytical plotters of the Wild factory were used in these cases.

6.1 Compensation of systematic error components

A detailed study of the measuring precision of aerial photographs requires a distinction to be made between systematic error components and random errors. This distinction is of special importance when the influence of image quality on measuring precision is analysed. The individual centres have calculated a Helmert transformation with the 20 given control points after measurement on the photogrammetric instruments. It was not expected that higher order transformations should be used to correct for affinity for example.

As in [2] (cf. reference chapter 5), a computing algorithm for finite elements was chosen to distinguish between the 2 error components. The errors in X and Y were approximated independently using correction surfaces of finite elements with a side length of 50 m. For the determination of the correction surfaces, all control points (point numbers 111—454) have been used. In a sense, this deviated from the principle that only control points should be used for the orientation. This procedure was, however, required as it seemed necessary to use a rather dense net of reference points for this transformation. Furthermore, the model coordinates of the control points measured by the individual centres were not registered on an electronic storage device.

It is evident that for such a strip transformation the number of degrees of freedom has to be considered when computing the standard deviation. Taking into account the relatively large side length of the surfaces of finite elements and the clustering of the points, the redundancy after correction of the systematic errors was estimated by taking n-15, where n is the total number of control points.

	Flight number	Film type	Exposure	Density	Picture numbers	Centre	Mean quality codes	Total of points	Pointing precision						Co-ordinate residuals before correction of systematic errors					Co-ordinate residuals after correction of systematic errors					Number
									1	2	3	4	5	Total	2	3	4	5	Total	2	3	4	5	Total	
1	1	Pan 200	n(S)	0,92	17/19	22	3,01	114	3	2,2/46	1,6/26	1,9/25	2,2/14	1,99	3,7	2,3	3,0	3,4	3,28	2,7	2,0	1,8	1,7	2,25	83
2	1	Pan 200	n(S)	0,92	17/19	34	2,82	114	16	1,1/23	0,8/24	0,5/51		0,78	2,6	1,7	1,8		1,96	2,2	1,4	1,2		1,50	72
3	1	Pan 200	n(S)	0,92	25/27	3	2,69	113	6	1,6/42	1,4/42	1,4/18	1,2/ 5	1,46	3,2	3,2	2,0	1,9	2,94	2,7	2,0	1,6	1,6	2,24	79
4	1	Pan 200	n(S)	0,92	25/27	5	3,19	113	20	1,2/22	1,5/16	1,0/26	1,0/29	1,14	3,2	2,4	2,1	1,7	2,34	1,9	2,0	1,1	1,0	1,47	63
5	1	Pan 200	n(S)	0,92	25/27	35	3,24	113	7	1,0/31	0,7/19	0,5/40	0,5/16	0,74	2,8	2,5	1,9	1,6	2,28	1,9	1,5	1,2	0,9	1,46	79
6	1	Pan 200	n(S)	0,92	31/33	1	2,72	113	10	1,7/37	1,1/41	0,9/25		1,31	3,5	3,3	2,8		3,26	2,6	1,8	1,5		2,04	77
7	1	Pan 200	n(S)	0,92	31/33	7	2,81	113	19	1,5/22	1,3/34	0,8/38		1,20	1,9	2,0	1,5		1,76	1,5	1,5	1,2		1,37	67
8	1	Pan 200	n(S)	0,92	31/33	9	2,81	113	29	2,0/17	1,6/25	1,6/30	1,4/12	1,68	2,9	3,2	3,3	2,7	3,11	2,5	2,4	2,0	1,6	2,16	71
9	1	Pan 200	n(S)	0,92	31/33	21	2,39	113	35	1,8/24	1,4/29	1,2/25		1,47	2,7	2,5	3,5		3,03	2,2	1,9	2,0		2,05	65
10	2	Pan 200	n(C)	1,05	14/16	4	3,06	83	6	1,5/16	1,9/28	2,1/33		1,91	5,5	4,4	3,4		4,37	3,7	2,7	2,2		2,79	54
11	2	Pan 200	n(C)	1,03	24/26	22	2,37	93	16	3,1/36	2,7/32	3,2/ 9		2,93	3,6	3,1	6,2		3,55	3,3	2,6	2,4		2,95	54
98	15	Dia SO397	n(C)	0,93	3/ 4	25	2,59	87	28	2,4/11	2,2/17	1,8/31		2,04	19,8	15,7	15,7		16,74	6,6	3,9	3,2		4,46	38
99	15	Dia SO397	n(C)	0,93	5/ 6	1	1,99	85	22	1,7/42	1,3/21			1,56	3,4	2,7			3,19	2,4	1,9			2,27	45
100	15	Dia SO397	n(C)	0,93	5/ 6	6	2,39	85	28	3,3/10	2,5/33	1,7/14		2,48	5,7	3,3	2,6		3,73	5,0	2,8	2,2		3,19	37
101	15	Dia SO397	n(C)	0,93	7/ 8	4	2,01	85	23	2,4/38	2,5/24			2,44	5,7	2,8			4,91	3,5	3,0			3,32	41
102	16	Color neg.	n(S)	1,02	111/112	1	2,57	113	10	1,9/32	1,2/68	1,1/ 3		1,45	3,2	3,0	3,8		3,12	2,8	2,0	2,3		2,30	77
103	16	Color neg.	n(S)	1,02	111/112	5	3,21	113	10	1,7/22	1,7/32	1,1/32	1,0/17	1,44	3,3	2,7	2,2	1,8	2,60	2,1	1,6	1,3	1,4	1,61	77
104	16	Color neg.	n(S)	1,02	111/112	21	2,75	113	32	1,6/15	1,7/25	1,3/31	1,3/10	1,49	2,5	3,5	2,2	4,1	3,00	2,1	2,8	1,8	3,3	2,44	73
105	16	Color neg.	n(S)	1,02	111/112	26	2,83	113	12	1,5/18	1,1/61	0,7/21	0,7/ 1	1,09	3,6	2,3	2,6	2,5	2,59	2,7	1,7	1,1	1,9	1,77	74
106	16	Color neg.	n(S)		113/114	24				3,3/21	2,7/68	3,2/ 6		2,85	9,3	7,1	9,8		7,94	4,0	3,3	5,3		3,71	69
107	16	Color neg.	n(S)		113/114	25				3,8/17	2,7/41	1,9/36	2,6/ 6	2,67	7,5	6,1	5,0	6,4	5,98	5,5	3,9	3,0	5,1	4,06	77
108	17	Color IR	n(S)	0,76	13/15	2	3,41	113	1	1,8/27	1,4/32	1,4/31	1,0/22	1,45	3,5	3,0	1,9	2,6	2,78	2,7	2,1	1,3	1,2	1,89	85
109	17	Color IR	n(S)	0,76	13/15	7	2,58	113	15	1,4/44	0,8/28	0,6/26		1,06	2,9	1,8	2,0		2,39	2,2	1,7	1,2		1,75	73
110	17	Color IR	n(S)		18/20	35				1,1/56	0,9/28	0,5/19	0,5/ 1	0,96	2,5	1,7	1,8	1,9	2,16	2,1	1,3	1,1	0,9	1,73	80
111	17	Color IR	-1D(S)	1,35	23/25	1	2,82	113	17	1,3/26	0,8/31	0,8/38	0,3/ 1	0,96	2,6	2,1	2,4	2,7	2,37	2,2	1,7	1,3	0,7	1,72	75
112	17	Color IR	-1D(S)	1,35	23/25	3	3,31	113	7	1,7/24	1,5/28	1,0/35	0,9/19	1,32	3,4	2,2	1,8	1,5	2,32	3,1	1,9	1,4	1,2	1,99	83
113	17	Color IR	-1D(S)	1,35	23/25	23	2,48	113	45	2,7/ 8	2,4/21	2,3/39		2,40	3,9	4,3	3,3		3,73	3,3	1,6	1,4		1,76	55
114	17	Color IR	(S)		24/26	9				2,6/ 9	2,2/14	2,0/30	2,3/16	2,18	3,5	3,5	3,5	3,4	3,48	3,1	2,6	2,4	2,1	2,47	62
115	17	Color IR	+D (S)	0,40	29/31	1	2,04	113	39	1,4/40	1,0/25	0,8/ 9		1,23	2,8	2,4	2,9		2,66	2,2	1,6	1,4		1,87	58
116	17	Color IR	+D (S)	0,40	29/31	22	2,29	113	33	3,0/41	2,1/22	1,3/ 7	1,2/10	2,45	4,8	4,0	2,0	3,3	4,11	3,9	3,6	1,7	3,1	3,47	61

Figure 38 — Summary of coordinate residual errors before and after correction of systematic errors. The table gives the pointing precision and the coordinate residuals divided into quality codes. Under column 1 of the pointing precision only the number of points is given, as points with quality code "1" were not measured. The following column gives the root mean square error referring to the mean of the 2 measurements, and after the slash the number of points measured. In the column "total" the weighted mean for all points measured is given; for the coordinate residuals only the mean square error is shown and the total of points used for the section analysed is given in the column "number". The first part of the table gives information on exposure, film number and density. The abbreviations for the exposure are the same as in Figure 24. In the following column the mean density of the background of points measured is given. Points with a rather heterogeneous background have been omitted. Beside the more or less subjective interpretation of the exposure, the mean density gives an objective measure of the overall density of the picture. In the column under "centre", the number of the pilot centre and the type of plotting instrument are given (abbreviation as in Figure 24). The mean quality code characterizes the average pointing quality of the signalized points for all the measurements (all measuring results are given in centimetres, referring to terrain co-ordinates, picture scale 1 : 4000)

m e	Exposure	Density	Picture numbers	Centre	Mean quality codes	Total of points	Pointing precision						Co-ordinate residuals before correction of systematic errors					Co-ordinate residuals after correction of systematic errors					Number
							1	2	3	4	5	Total	2	3	4	5	Total	2	3	4	5	Total	
0	n(S)	0,92	17/19	22	3,01	114	3	2,2/46	1,6/26	1,9/25	2,2/14	1,99	3,7	2,3	3,0	3,4	3,28	2,7	2,0	1,8	1,7	2,25	83
0	n(S)	0,92	17/19	34	2,82	114	16	1,1/23	0,8/24	0,5/51		0,78	2,6	1,7	1,8		1,96	2,2	1,4	1,2		1,50	72
0	n(S)	0,92	25/27	3	2,69	113	6	1,6/42	1,4/42	1,4/18	1,2/ 5	1,46	3,2	3,2	2,0	1,9	2,94	2,7	2,0	1,6	1,6	2,24	79
0	n(S)	0,92	25/27	5	3,19	113	20	1,2/22	1,5/16	1,0/26	1,0/29	1,14	3,2	2,4	2,1	1,7	2,34	1,9	2,0	1,1	1,0	1,47	63
0	n(S)	0,92	25/27	35	3,24	113	7	1,0/31	0,7/19	0,5/40	0,5/16	0,74	2,8	2,5	1,9	1,6	2,28	1,9	1,5	1,2	0,9	1,46	79
0	n(S)	0,92	31/33	1	2,72	113	10	1,7/37	1,1/41	0,9/25		1,31	3,5	3,3	2,8		3,26	2,6	1,8	1,5		2,04	77
0	n(S)	0,92	31/33	7	2,81	113	19	1,5/22	1,3/34	0,8/38		1,20	1,9	2,0	1,5		1,76	1,5	1,5	1,2		1,37	67
0	n(S)	0,92	31/33	9	2,81	113	29	2,0/17	1,6/25	1,6/30	1,4/12	1,68	2,9	3,2	3,3	2,7	3,11	2,5	2,4	2,0	1,6	2,16	71
0	n(S)	0,92	31/33	21	2,39	113	35	1,8/24	1,4/29	1,2/25		1,47	2,7	2,5	3,5		3,03	2,2	1,9	2,0		2,05	65
0	n(C)	1,05	14/16	4	3,06	83	6	1,5/16	1,9/28	2,1/33		1,91	5,5	4,4	3,4		4,37	3,7	2,7	2,2		2,79	54
0	n(C)	1,03	24/26	22	2,37	93	16	3,1/36	2,7/32	3,2/ 9		2,93	3,6	3,1	6,2		3,55	3,3	2,6	2,4		2,95	54
0	n(C)	1,03	24/26	34	2,60	93	23	1,2/18	0,7/25	0,8/27		0,91	2,1	2,0	1,6		1,94	2,2	1,4	1,3		1,65	49
0	n(C)	1,04	25/27	1	2,58	85	8	1,5/22	1,3/53	1,8/ 2		1,37	3,2	2,4	0,6		2,66	3,0	1,7	0,9		2,20	50
0	n(C)	1,04	25/27	8	3,47	85	5	1,7/ 9	2,1/12	1,5/59		1,63	3,6	3,5	3,8		3,73	2,9	2,8	1,8		2,20	53
0	n(C)	1,04	25/27	23	2,25	85	26	1,6/12	1,7/47			1,65	3,5	2,9			3,02	2,5	2,0			2,14	38
	n(S)		80/81	24				3,4/11	2,7/32	4,5/24		3,56	15,8	5,7	5,1		6,17	16,3	3,3	3,7		4,66	51
	n(S)		80/81	25				3,1/16	3,5/12	2,8/11	2,6/32	2,92	6,8	3,8	4,3	3,7	4,65	3,5	4,1	3,6	3,0	3,36	52
	n(S)	0,87	82/83	1	2,35	113	17	1,4/44	1,3/48	0,8/ 4		1,29	3,4	2,7	1,5		2,98	3,0	1,8	1,6		2,36	72
	n(S)	0,87	82/83	6	3,16	113	25	2,6/17	2,8/18	2,2/21	2,0/32	2,35	6,1	3,0	3,6	3,2	3,85	5,1	2,9	2,7	2,9	3,31	66
	n(S)	0,87	82/83	21	2,48	113	39	1,9/19	1,8/23	1,4/26	1,4/ 6	1,69	4,0	3,5	3,8	3,6	3,71	3,3	2,7	2,1	1,9	2,59	65
	n(S)	0,87	82/83	29	2,95	113	28	2,6/12	1,9/28	1,6/28	1,1/17	1,78	4,0	2,1	2,8	2,9	2,86	3,7	1,8	2,1	1,8	2,33	61
-X	n(S)		64/65	26				1,9/20	1,6/25	0,9/37	1,1/14	1,37	3,7	2,8	2,6	1,5	2,67	3,8	1,8	1,2	1,2	1,91	71
-X	n(S)	0,63	66/67	1	2,43	113	13	1,5/42	1,2/54	0,7/ 4		1,33	2,7	2,5	2,4		2,59	2,5	1,6	1,8		2,03	79
-X	n(S)	0,63	66/67	4	3,06	113	13	3,0/23	2,6/32	2,5/34	2,2/11	2,61	2,9	4,1	2,8	3,4	3,34	2,9	3,0	2,2	2,0	2,59	73
-X	n(S)	0,63	66/67	23	2,11	113	58	1,9/ 6	1,6/28	1,5/21		1,59	3,3	3,8	4,2		3,97	3,7	2,0	1,8		2,10	45
-X	n(C)	0,98	4/ 5	3	2,71	105	13	2,0/26	1,5/44	1,3/22		1,64	3,2	2,3	1,8		2,56	2,7	1,8	1,4		2,07	69
-X	n(C)	0,98	4/ 5	5	3,42	105	18	1,5/10	1,0/13	0,8/38	0,7/26	0,93	4,2	2,0	1,8	2,1	2,29	4,0	1,6	1,2	0,9	1,78	62
-X	n(C)	0,98	4/ 5	29	2,89	105	26	2,8/ 5	1,7/32	1,6/39	1,9/ 3	1,76	6,1	2,7	3,1		3,35	4,7	2,0	2,0		2,35	58
-X	n(C)	0,98	6/ 7	2	3,51	104	24	2,7/ 9	1,8/ 6	1,4/20	1,4/45	1,65	4,3	1,9	3,0	2,4	2,76	3,1	2,5	2,4	1,5	2,05	60
-X	n(C)	0,98	6/ 7	35	2,86	104	19	1,3/15	1,0/32	0,6/38		0,90	3,2	2,6	2,7		2,76	1,8	1,6	1,2		1,45	62
-X	(C)		8/ 9	25				2,8/15	2,4/19	2,6/40	1,4/ 1	2,59	6,4	6,3	5,3	3,2	5,77	4,0	3,4	3,1	1,5	3,38	56
mic-X	n(S)		15/17	25				4,3/ 9	3,8/26	3,4/34	3,9/28	3,74	9,6	4,7	6,1	5,1	5,95	8,2	3,1	3,2	3,6	4,07	71
mic-X	n(S)	0,90	16/18	3	2,79	114	5	1,6/39	1,6/45	1,4/25		1,56	3,0	3,2	2,7		3,03	2,1	1,7	1,5		1,80	82
mic-X	n(S)	0,90	16/18	8	3,26	114	8	2,3/18	2,1/36	2,2/40	2,0/12	2,14	3,2	3,1	2,6	3,4	3,03	2,3	2,3	1,9	1,7	2,08	82
mic-X	n(S)	0,90	20/22	1	2,49	114	7	1,6/52	1,1/47	1,1/ 8		1,37	5,2	1,9	1,8		3,90	2,5	1,5	1,1		2,03	78
mic-X	n(S)	0,90	20/22	1	2,75	114	10	2,0/42	2,1/29	1,2/33		1,83	3,4	2,5	2,1		2,72	2,4	1,6	1,5		1,90	79
mic-X	n(S)	0,90	20/22	6	3,58	114	9	2,3/17	2,4/21	2,4/33	1,8/34	2,17	3,9	3,1	2,6	2,4	2,88	3,1	2,2	2,3	1,6	2,21	78
mic-X	-1D (S)		28/30	9				1,7/18	1,5/12	1,3/30	1,2/27	1,41	3,4	4,4	2,3	4,0	3,50	2,2	1,8	1,9	1,4	1,79	75
mic-X	-1D (S)		28/30	29				1,5/19	1,7/ 4	1,4/31	1,5/45	1,49	2,8	1,5	2,3	2,2	2,34	2,3	1,3	2,2	1,6	1,98	78
mic-X	-1D (S)	0,43	29/31	1	2,93	113	14	1,5/15	1,3/49	1,1/35		1,23	2,9	3,7	2,7		3,26	1,8	2,3	1,5		1,92	77
mic-X	-1D (S)	0,43	29/31	1	2,72	113	11	1,3/35	1,1/42	1,0/25		1,14	2,6	2,3	2,9		2,63	1,9	1,8	1,5		1,70	72
mic-X	-1D (S)	0,43	29/31	7	3,40	113	10	1,3/20	0,9/19	0,9/43	0,8/21	0,99	2,4	1,9	2,1	2,8	2,32	1,7	1,6	1,1	1,1	1,35	78
mic-X	-1D (S)	0,43	29/31	35	4,21	113	2	0,3/ 5	0,7/28	0,6/10	0,6/68	0,60	3,9	2,1	1,8	2,0	2,02	2,9	1,3	0,8	0,9	1,04	84
mic-X	+2/3 (S)		34/36	1				1,7/16	1,2/43	0,9/51		1,19	2,2	3,1	2,6		2,78	2,0	1,9	1,6		1,77	80
mic-X	+2/3 (S)		34/36	34				3,0/18	1,0/37	0,7/32	0,5/11	1,51	4,8	2,9	1,5	3,4	3,18	3,7	1,6	1,0	1,3	2,09	75
Def.	n(S)		130/131	4	2,73	114	28	3,2/24	2,7/22	3,2/31	3,3/ 9	3,12	4,5	3,7	5,4	2,9	4,42	3,5	1,6	1,7	1,7	2,36	68
Def.	n(S)		130/131	26	2,79	114	15	2,3/28	1,8/43	1,1/22	1,0/ 6	1,80	4,1	2,4	1,9	4,5	3,05	3,7	1,4	2,0	3,8	2,57	72
Def.	n(S)		132/133	22	2,59	114	20	2,1/48	1,4/16	1,4/19	1,2/11	1,79	3,1	3,1	2,9	3,2	3,08	2,9	2,8	1,8	2,0	2,60	72
Def.	-D(S)		134/135	2	3,76	113	19	2,8/10	2,7/12	3,1/10	1,9/62	2,28	1,9	2,7	2,7	2,4	2,42	1,3	1,5	2,0	1,5	1,58	71
Def.	-D(S)		134/135	5	3,76	113	21	0,9/ 6	0,6/10	0,6/18	0,6/58	0,64	2,0	2,3	2,9	2,7	2,66	1,1	1,5	1,0	1,0	1,05	71
Def.	-D(S)		134/135	29	3,44	113	22	2,6/ 9	2,2/17	2,3/27	1,8/38	2,15	3,2	2,7	2,7	2,8	2,79	2,9	2,5	1,9	2,0	2,14	72
Def.	-D(S)		136/137	1	2,97	113	15	2,0/15	1,2/43	1,0/38	1,3/ 2	1,27	2,3	3,2	2,3	2,6	2,72	1,3	2,1	1,6	0,9	1,80	76
Def.	-D(S)	0,97	268/269	1	3,11	101	9	1,1/13	1,5/39	1,0/38	1,0/ 2	1,22	2,4	2,9	1,9	2,6	2,46	1,9	1,8	1,5	1,4	1,66	74

98	15	Dia SO397	n(C)	0,93	3/ 4	25	2,59	87	28	2,4/11	2,2/17	1,8/31		2,04	19,8	15,7	15,7		16,74	6,6	3,9	3,2		4,46	30
99	15	Dia SO397	n(C)	0,93	5/ 6	1	1,99	85	22	1,7/42	1,3/21			1,56	3,4	2,7			3,19	2,4	1,9			2,27	45
100	15	Dia SO397	n(C)	0,93	5/ 6	6	2,39	85	28	3,3/10	2,5/33	1,7/14		2,48	5,7	3,3	2,6		3,73	5,0	2,8	2,2		3,19	37
101	15	Dia SO397	n(C)	0,93	7/ 8	4	2,01	85	23	2,4/38	2,5/24			2,44	5,7	2,8			4,91	3,5	3,0			3,32	41
102	16	Color neg.	n(S)	1,02	111/112	1	2,57	113	10	1,9/32	1,2/68	1,1/ 3		1,45	3,2	3,0	3,8		3,12	2,8	2,0	2,3		2,30	77
103	16	Color neg.	n(S)	1,02	111/112	5	3,21	113	10	1,7/22	1,7/32	1,1/32	1,0/17	1,44	3,3	2,7	2,2	1,8	2,60	2,1	1,6	1,3	1,4	1,61	77
104	16	Color neg.	n(S)	1,02	111/112	21	2,75	113	32	1,6/15	1,7/25	1,3/31	1,3/10	1,49	2,5	3,5	2,2	4,1	3,00	2,1	2,8	1,8	3,3	2,44	73
105	16	Color neg.	n(S)	1,02	111/112	26	2,83	113	12	1,5/18	1,1/61	0,7/21	0,7/ 1	1,09	3,6	2,3	2,6	2,5	2,59	2,7	1,7	1,1	1,9	1,77	74
106	16	Color neg.	n(S)		113/114	24				3,3/21	2,7/68	3,2/ 6		2,85	9,3	7,1	9,8		7,94	4,0	3,3	5,3		3,71	69
107	16	Color neg.	n(S)		113/114	25				3,8/17	2,7/41	1,9/36	2,6/ 6	2,67	7,5	6,1	5,0	6,4	5,98	5,5	3,9	3,0	5,1	4,06	77
108	17	Color IR	n(S)	0,76	13/15	2	3,41	113	1	1,8/27	1,4/32	1,4/31	1,0/22	1,45	3,5	3,0	1,9	2,6	2,78	2,7	2,1	1,3	1,2	1,89	85
109	17	Color IR	n(S)	0,76	13/15	7	2,58	113	15	1,4/44	0,8/28	0,6/26		1,06	2,9	1,8	2,0		2,39	2,2	1,7	1,2		1,75	73
110	17	Color IR	n(S)		18/20	35				1,1/56	0,9/28	0,5/19	0,5/ 1	0,96	2,5	1,7	1,8	1,9	2,16	2,1	1,3	1,1	0,9	1,73	80
111	17	Color IR	-1D(S)	1,35	23/25	1	2,82	113	17	1,3/26	0,8/31	0,8/38	0,3/ 1	0,96	2,6	2,1	2,4	2,7	2,37	2,2	1,7	1,3	0,7	1,72	75
112	17	Color IR	-1D(S)	1,35	23/25	3	3,31	113	7	1,7/24	1,5/28	1,0/35	0,9/19	1,32	3,4	2,2	1,8	1,5	2,32	3,1	1,9	1,4	1,2	1,99	83
113	17	Color IR	-1D(S)	1,35	23/25	23	2,48	113	45	2,7/ 8	2,4/21	2,3/39		2,40	3,9	4,3	3,3		3,73	3,3	1,6	1,4		1,76	55
114	17	Color IR	(S)		24/26	9				2,6/ 9	2,2/14	2,0/30	2,3/16	2,18	3,5	3,5	3,5	3,4	3,48	3,1	2,6	2,4	2,1	2,47	62
115	17	Color IR	+D (S)	0,40	29/31	1	2,04	113	39	1,4/40	1,0/25	0,8/ 9		1,23	2,8	2,4	2,9		2,66	2,2	1,6	1,4		1,87	58
116	17	Color IR	+D (S)	0,40	29/31	22	2,29	113	33	3,0/41	2,1/22	1,3/ 7	1,2/10	2,45	4,8	4,0	2,0	3,3	4,11	3,9	3,6	1,7	3,1	3,47	61

Figure 38 — Summary of coordinate residual errors before and after correction of systematic errors. The table gives the pointing precision and the coordinate residuals divided into quality codes. Under column 1 of the pointing precision only the number of points is given, as points with quality code "1" were not measured. The following column gives the root mean square error referring to the mean of the 2 measurements, and after the slash the number of points measured. In the column "total" the weighted mean for all points measured is given; for the coordinate residuals only the mean square error is shown and the total of points used for the section analysed is given in the column "number". The first part of the table gives information on exposure, film number and density. The abbreviations for the exposure are the same as in Figure 24. In the following column the mean density of the background of points measured is given. Points with a rather heterogeneous background have been omitted. Beside the more or less subjective interpretation of the exposure, the mean density gives an objective measure of the overall density of the picture. In the column under "centre", the number of the pilot centre and the type of plotting instrument are given (abbreviation as in Figure 24). The mean quality code characterizes the average pointing quality of the signalized points for all the measurements (all measuring results are given in centimetres, referring to terrain co-ordinates, picture scale 1 : 4000)

Centre	Number of Models	Observation errors Residuals Mean	Variance	Co-ordinate residuals before correction Mean	Variance	after correction Mean	Variance	Number of points Mean	Variance
24 A8	5	3.5	± 0.8	8.4	± 3.6	3.3	± 0.5	61	± 12
25 A8	10	2.9	± 0.9	7.2	± 3.9	3.1	± 0.3	62	± 13
8 Plma	5	1.7	± 0.3	3.5	± 0.3	2.0	± 0.3	66	± 14
9 Plma	5	1.8	± 0.3	3.4	± 0.3	2.0	± 0.3	62	± 17
21 Plma	5	1.6	± 0.1	3.4	± 0.4	2.2	± 0.3	63	± 10
22 A10	5	2.3	± 0.4	3.5	± 0.4	2.4	± 0.4	68	± 11
4 AMH	5	2.7	± 0.6	4.2	± 0.6	2.3	± 0.3	56	± 13
1 Plco	22	1.2	± 0.2	2.7	± 0.4	1.7	± 0.2	72	± 11
2 Plco	6	1.5	± 0.5	2.7	± 0.2	1.7	± 0.2	71	± 8
3 Plco	6	1.5	± 0.1	2.8	± 0.8	1.8	± 0.1	77	± 6
6 Plco	5	2.0	± 0.5	3.2	± 0.5	2.1	± 0.5	65	± 16
29 Plco	9	1.5	± 0.4	3.4	± 0.3	1.7	± 0.2	60	± 12
23 Traster	3	1.9	± 0.5	3.6	± 0.5	1.7	± 0.2	47	± 8
26 DSR1	5	1.2	± 0.1	2.7	± 0.2	1.8	± 0.2	66	± 15
Hel DSR1	13	–	–	2.6	± 0.5	2.0	± 0.4	72	± 12
Hel PSK	19	–	–	2.3	± 0.5	1.8	± 0.2	60	± 11
5 Plco	5	1.0	± 0.3	2.4	± 0.2	1.4	± 0.3	62	± 15
7 Plco	5	1.1	± 0.2	2.3	± 0.6	1.4	± 0.5	63	± 15
34 AC1	5	1.1	± 0.3	2.4	± 0.5	1.4	± 0.2	56	± 16
35 BC1	5	0.8	± 0.2	2.4	± 0.3	1.4	± 0.3	76	± 8

Figure 39 — Summary of the precision of the different centres with different instruments: The table gives the arithmetic means of the root mean square errors of the measurements as they are shown in Figure 38 under "total". In addition to the arithmetic mean, the mean square error referring to the mean is given, under "variance" (1st group: analog plotter with rather low precision; 2nd group: precision analog plotter; 3rd group: analytical plotter with floating mark greater than 40 µm; 4th group: analytical plotter with variable floating mark; 5th group: analytical plotter with floating mark smaller than 30 µm)

6.2 *Discussion of the measuring results*

It is deduced that measurements on analytical plotters (Planicomp) as well as on the different analog restitution instruments are affected by systematic errors of about 40 %. For the Planicomp, the mean residual coordinate error was reduced from 2.7 cm to ± 1.8 cm corresponding to ± 7µm and ± 5 µm; for the analog restitution instruments, the original value of ± 3.7 cm was reduced to 2.7 cm corresponding to ± 10 and ± 7 µm. It is noticeable that a good coincidence is achieved between the pointing precision and the residual coordinate errors only after correction of the systematic error components; on average, the pointing precision is only 30—40 % better than the residual measuring error, whereas this deviation is nearly twice the pointing precision before error correction. Further, after this correction, a strong correlation is observed between the residual coordinate errors and the quality code for the individual classes. On an average the residual coordinate errors vary by nearly 20 % from one class of quality code to the next. This proves that the quality code has a real meaning and that use of these values is fully justified in judging different photographs.

6.3 *Influence of film type and signal colour on measuring precision*

The residual errors obtained after correction of systematic error components can now be used to analyse the influence of film type and the colour of the signals on the measuring precision. It may even be possible to find which particular colour is most appropriate for a particular land surface (asphalt, bare soil, meadow). To obtain an overview of the optimal film types to be used, the mean square errors of the residuals of all measurements have been grouped according to the film type used. Figure 40 gives an overview of the results obtained. As in the preceding tables, variances of the standard deviations are also shown. This table implies that colour film and infrared colour film give a slightly higher precision than black & white films. The differences are slight and rarely exceed 10 % but nevertheless seem to be significant. The same analysis of the results obtained with stereorestitution instruments with floating marks of 25µm (4th group of instruments) gives just the opposite result, which at first glance seems to be a contradiction. But it is quite easy to find an explanation for this phenomenon. The resolution of the colour film and of the false-colour film resulted in the signalized points beeing slightly larger than 40µm in the image, whereas with black & white films and especially with Panatomic-X film, the signalized points are slightly smaller than 40 µm. During the measurement the very small points on this black & white film are completely covered by the floating mark and consequently the pointing is less precise than with instruments which have a properly adopted floating mark.

The colour of the signals has little influence on the measuring precision as shown in Figures 41—43. Only black signals give considerably poorer precision than all the other signals. For yellow signals it should be taken into account that practically all points with this colour were in meadows and only 2 points were on bare soil. In all these cases very favourable contrast conditions were obtained and measuring results were optimal for all signals. As only two yellow signals were on bare soil it did not seem appropriate to continue the investigation for the colour of the signal. Furthermore, the differences in precision between white and red signals are minima and therefore better results are obtained for red signals in shade, whereas white signals are better in meadows or on bare soil.

It must be concluded that under optimal conditions the black & white film gives slightly better results than the colour film, the colour of the signal is of minor importance but the most limiting factor for precision measurements are still the plotting instruments. Of great importance are also the image quality and the signal reproduction. It seems therefore appropriate to continue establishing norm for the quality requirements of the film as for density, contrast and resolution.

Flight number	Film	Co-ordinate residuals: All analytical plotters Mean	Variance		Only analytical plotters with floating mark 30 µm Mean	Variance		
Black & white films								
1	Pan 200 (sunny)	1,46	± 0,15	(6)	1,29	± 0,04	(4)	1,29 ± 0,06
2–5	Pan 200 (cloudy) Plus-X Double-X	1,81	± 0,15	(10)	1,32	± 0,01	(3)	
6	Panatomic-X	1,69	± 0,07	(10)	1,34	± 0,17	(4)	
7	High def.				0,93	-	(1)	
Colour films								
8–10	Dia 2448	1,58	± 0,08	(12)	1,42	± 0,20	(4)	1,55 ± 0,09
11–15	Dia SO-397	1,88	± 0,08	(16)	1,71	± 0,22	(4)	
16	Color neg.				1,45	-	(1)	
17	Color IR	1,61	± 0,04	(7)	1,55	± 0,01	(3)	

Figure 40 — Residual errors and variances (in cm) in signalized points for analytical plotters according to film type. The number in brackets indicate the number of models measured

Ground cover	Colour of signals											
	White			Red			Black			Yellow		
	Mean	Variance		Mean	Variance		Mean	Variance		Mean	Variance	
Meadow	1.06	± 0.14	(8)	0.92	± 0.10	(9)				0.97	± 0.10	(9)
Soil	1.10	± 0.09	(9)	1.29	± 0.13	(9)	1.72	± 0.29	(6)	1.63	± 0.24	(2)
Asphalt	1.26	± 0.12	(8)	1.51	± 0.39	(8)	1.91	± 0.22	(8)			
Shade	1.53	± 0.36	(2)	1.56	± 0.52	(2)				1.50	± 0.48	(2)

Figure 41 — Residual errors and variances (in cm) for signalized points according to the colour of the signals and the ground cover. The numbers in brackets indicate the number of points analysed. The table gives a synthesis of all measurements (black & white and colour films) made in centres 5, 7, 34, 35 (analytical plotters, floating mark smaller than30 μm)

a)

Black & white films			
Colour of signals :	Red (2)	White (1)	Black (3)
Yellow	6 ± 3	16 ± 3	73 ± 1
Red		12 ± 3	47 ± 4
White			32 ± 5

b)

Colour films			
Colour of signals :	Red (2)	White (1)	Black (3)
Yellow	11 ± 3	11 ± 3	45 ± 5
Red		2 ± 2	43 ± 5
White			45 ± 5

c)

Infrared colour films			
Colour of signals :	Red (2)	White (1)	Black (3)
Yellow	8 ± 2	13 ± 2	66 ± 8
Red		6 ± 2	69 ± 3
White			39 ± 3

Figure 42 — Reduction of the measuring precision of the signalized points as for the colour of the signals when analysing all the measurements done on analytical plotters. The values give the mean reduction of measuring precision and the corresponding variance (in %) from left to right (for example: red is 6 % lower than yellow for black & white film)

a)

Black & white films			
	Shade (5)	Ground (2)	Asphalt (3)
Meadow	6 ± 4	16 ± 3	27 ± 3
Shade		12 ± 5	24 ± 6
Ground			7 ± 3

b)

Colour films			
	Ground (2)	Asphalt (3)	Shade (5)
Meadow	15 ± 2	18 ± 2	22 ± 5
Ground		1 ± 3	5 ± 5
Asphalt			3 ± 5

c)

Infrared colour films			
	Shade (5)	Ground (2)	Asphalt (3)
Meadow	15 ± 3	15 ± 2	20 ± 2
Shade		3 ± 4	10 ± 4
Ground			4 ± 2

Figure 43 — Reduction of measuring precision of the signalized points for the ground cover for all analytical plotters. The table is to be read in the same manner as Figure 42

7 Reliability of photogrammetric plotting with different emulsions

7.1 Aims of investigation of the reliability of image-interpretation

In large scale photogrammetry two questions are of prior importance:

1. How r e l i a b l e can a complete and correct interpretation of features be expected to be, using "aerial photography"?
2. How p r e c i s e can the photogrammetric plotting of signalized points be expected to be?

An answer has been sought to the second question for the past 30 years, for instance by the Commission C of the OEEPE, not only with respect to the precision of signalized points in conventional black & white films (Oberriet, Reichenbach) but also with respect to topographical features (roof points) in black & white films (Dordrecht, Wien). In Chapter 5 a detailed account of the geometrical precision of measuring points is given. In this chapter only investigations of the reliability of plotting in different emulsions, will be described.

The most important criterias of reliability in photogrammetric plotting are:

- a given point must be found easily and must be identified and interpreted in a correct way;
- the point must be measured within given tolerances, in a "secure way".

If these criteria are n o t met, the photographic material will be unreliably to some extent.

These criteria have been applied when investigating signalized and topographical points; all restitutions of the different models with different emulsions have been inspected for "missing of points", i. e.:

- the point was not to be seen , was not perceptible, or
- the point was measured with a gross error.

To establish the reliability of the different flight-dispositions the percentage of "missing of points" has been determined.

7.2 Description of the present plotting results

The investigations were based initially on the results of the restitutions of the 17 flights, as described in chapter 2.4.1. Because of differences in illumination of the test-field and in film exposure, the emulsions were divided into groups as follows. There are 11 flights in sunshine:

3 with standard black & white emulsions,

4 with standard colour emulsions,

2 with special black & white emulsions,

2 with special colour emulsions.

There are 5 flights under overcast conditions:

2 with standard black & white emulsions,

3 with standard colour emulsions,

and 1 flight severe overexposure.

This photographic material — in total 54 models — was restituted by the 18 participant groups (see Figure 7) with:

11 analytical plotters (Planicomp, AC1, etc.),

5 analog instruments, e. g. Planimat, A10,

2 analog instruments e. g. A8.

On first examination of the restitutions it was found that the proportion of missing points with the A8 instruments was about 20 % higher, and that the standard deviations of the coordinates were even about 100 % higher with respect to the analytical plotters. Similarly the other five analog plotters also gave differing results: the precision variation for roof points was about 20 %, the level of missing of roof points and signalized points was not significant.

For the sake of uniformity, the following discussion and analysis of results use only the results from the 11 analytical instruments; the number of the restituted models and of the restitutions are shown in columns 4 and 5 of Figure 44. Altogether, the following results are based on 76 restitutions of 54 models, that is, an average of about 4—5 restitutions per flight.

The results of the seven older instruments were not taken into consideration with good reason; the results of the restitutions using the seven older instruments vary much more than those using the analytical instruments. If they were included in the whole analysis, they would strengthen the result, that no significant difference at all is to be found between the different emulsions.

The results were derived in the following way:

a) The average percentage of missing points (of the total number of points plotted per model):
   - Points, which were visible from the air on the day of the photo flight and should actually be measurable, but were not in fact measured — often without any obvious reason. It is assumed that those points which were damaged on the day of the photo flight, and those which were hidden from view or were outside the limits of the model, were not included;
   - points with gross errors, i. e. exceeding four times the standard deviation of the coordinates:

     for signalized points and roof points 20 cm,

     for topographical points 70 cm.

b) For measuring precision the standard deviations of the coordinates from the "true" terrestrial values are indicated; the accuracy of the terrestrial coordinates is ± 1 cm. The photogrammetrically produced coordinates were obtained through the normal Helmert-Transformation from the models using the 20 corresponding terrestrial control points; systematic errors were not eliminated.

7.3 Missing signalized points

The precision of the determination of coordinates of signalized points is discussed in Chapter 5; in this chapter only the results of the investigations of the reliability of signalized points in different emulsions are given.

The question of reliability of interpretation and identification is interesting in several respects:

- differences between the emulsions in general, without distinction between of the points,
- the reliability of signalized points, first with respect to different target colours, but also with respect to the background,
- differences with respect to several combinations of target colour/background.

7.3.1 Missing points in different emulsions in general

If we do not differentiate between target colour and the background, we can derive the following conclusions from the investigation (Figure 44, right column):

- The percentages of missing points range up to 4 % overall, i. e., out of 100 virtually measurable points there were 4 points which were not measurable at all (the black targets are not included here). The absolute value of 4 % has little significance, but this value is rather high in relation to careful signalization in the field and the precise location of all points in the grid-reference map. But it should be noted that a number of points were located in extreme positions (bright asphalt and concrete, bright soil, shadow, unsuitable target colour etc.) in order to test signalized points in extreme circumstances as well.

  The actual quota of missing points for the different flight-emulsion-dispositions is of primary importance.

- The target colour "black" (Figure 44, column 9) results in a missing point rate of about 30 % in sunshine, and as much as 50 % or so under overcast conditions; thus we can conclude that "black" is not suitable as a target colour, not even for bright surfaces such as asphalt or concrete. Panatomic-X and infrared colour film gave more positive results; we can conclude that these emulsions have a higher sensitivity than the others to black targets. The black targets are not included in the following discussion in order to avoid distortion of the results.

- Generally, in sunshine, we can say that standard black & white films show a slightly higher percentage of missing points (5 %) than standard colour films (3 %); this difference, however, is not significant if we consider the variation in results within the two groups of emulsions

black & white	3—8 %,
colour	2—6 %;

  these are for flights in sunshine, arranged in groups for different target colours.

Sun

Emulsion	Flight No.	Number of		in % of total numbers of sign. points				
				Target colour				Mean (without black)
		models	resti-tutions	white	red	yellow	black	
Standard								
Black & white		7	11	6	4	5	37	5
Pan 200	1	3	6	5	4	4	30	4
Plus-X	3	2	2	8	4	3	40	6
Double-X	4	2	3	6	4	7	23	6
Colour		13	17	3	3	4	31	3
Dia 2448	8	2	2	4	5	6	24	5
Dia 2448	9	4	6	3	3	5	35	3
Dia SO 397	11	4	6	3	3	3	33	3
Dia SO 397	12	3	3	2	2	3	41	2
Special								
Black & white								
Panatomic-X	6	6	10	3	3	3	6	3
High Definition	7	4	6	4	6	6	21	5
Colour								
Negative	16	2	3	2	1	2	35	2
Infrared	17	5	6	3	2	3	9	2.5
	Σ	37	53	4	3.5	4	28	3

Overcast Sky

Standard								
Black & white		6	8	7	7	6	33	7
Pan 200	2	3	3	5	7	9	26	7
Double-X	5	3	5	8	6	3	40	6
Colour		8	11	6	6	5	60	6
Dia 2448	10	2	3	6	4	3	45	5
Dia SO 397	14	3	5	9	7	6	65	7
Dia SO 397	15	3	3	5	6	6	70	5
	Σ	14	19	6	6	6	50	6

Overexposed

Standard								
Colour								
Dia SO 397	13	3	5	15	12	10	60	12

Figure 44 — Missing signalized points

- Of the special emulsions, colour negative film surprisingly shows the best result; also black & white Panatomic film is characterized by relatively few missing points, at least if we compare it with standard black & white films, although here we have to stress that the differences between the different emulsions are not very significant.
- Under overcast conditions there is no significant difference between the emulsions used: nevertheless, one a definite conclusion can be drawn, namely that an overcast sky — and hence considerably less light — produces an increase in the percentage of missing points; some rates are twice as high as in sunshine.
- Even worse than loss of light under overcast conditions is overexposure; this greatly reduces the reliability of interpretation and identification of signalized points and effects signalized points more strongly than nonsignalized points (Chapters 7.4 and 7.5).

7.3.2 Missing points for different target colours and different backgrounds

Signalized points are characterized by:

- their colour (white, red, yellow, black);
- their background (grassland, soil, asphalt, roof, shadow).

An analysis of the results of all restitutions gives the following conclusions:

- Apart from black targets (Chapter 7.3.1), and without distinguishing between backgrounds, we can discover no significant difference between the three target colours (Figure 45, columns 6—8): this is as valid for standard films as for special films, and is not dependent on light conditions. Disregarding the background, we may conclude that all three target colours — white, red, yellow — give results of the same quality.
- If we analyse the five different backgrounds (Figure 45), areas of shadow generally produce very bad results, as could be expected. Significant differences, however, are seen for missing points in shadow with standard black & white films on the one hand and the new colour diapositiv film SO 397 and the two special emulsions on the other.
- Besides shadow, asphalt is definitely not suitable as a background (column 6). The reason for the bad results is the overillumination of the targets by the bright asphalt and concrete. For all emulsions the only way to avoid this is by adding a dark contrasting strip round the targets.
- It is surprising that targets on roofs produce the best results; obviously the dark red colour of roofs provides an optimal contrast with the target colours used (column 7).
- Overexposure increases the number of missing points, particularly with bright backgrounds (soil, asphalt); unfortunately there is no corresponding improvement in recognition in areas of shadow.
- If we consider just the points in shadow for infrared colour films — the photographic material generally shows bad results — this particular film has the lowest percentage of missing points. Infrared colour film is the most effective one for reliability of interpretation, and this applies to signalized points as well.

Sun

Emulsion	Flight No.	in % of all points					Mean (without black)
		Grass-land	Soil	Asphalt Concrete	Roof	Shadow	
Standard							
Black & white		2	4	5	1	17	5
Pan 200	1	2	3	5	2	13	4
Plus-X	3	1	5	8	0	18	6
Double-X	4	2	3	3	1	20	6
Colour		2	2	3	1	8	3
Dia 2448	8	3	3	4	1	12	5
Dia 2448	9	1	1	1	0	14	3
Dia SO 397	11	2	3	3	1	4	3
Dia SO 397	12	2	2	3	1	4	2
Special							
Black & white							
Panatomic-X	6	2	1	3	1	6	3
High Definition	7	0	3	9	6	(54)	5
Colour							
Negative	16	0	1	2	0	5	2
Infrared	17	0	1	1	0	10	2.5
	Σ	2	3	4	1	9	3

Overcast sky

Standard							
Black & white		6	10	12	3	1	7
Pan 200	2	11	14	9	0	0	7
Double-X	5	0	6	14	6	1	6
Colour		6	6	8	2	5	6
Dia 2448	10	3	6	9	2	2	5
Dia SO 397	14	8	8	7	3	7	7
Dia SO 397	15	5	5	8	2	6	5
	Σ	5	8	9	3	3	6

Overexposed

Standard							
Colour							
Dia SO 397	13	4	17	20	6	10	12

Figure 45 — Missing signalized points on different backgrounds

— Figure 46 shows a matrix distribution of the missing points for all possible target-colour/background combinations; in this figure Plus-X black & white film is used as an example representing average film quality. Apart from the results already seen the figure shows that the rarely used combination "yellow on a roof" gives the best results; for the combinations used in practice, the combination "yellow on grassland" gives the best results. The matrix shows the white targets to be somewhat unreliable. Red targets give the best results for areas in shadow. An overillumination by asphalt or concrete cannot be avoided with any target colour, not even with "black".

Missing points in % — Example: PLUS X

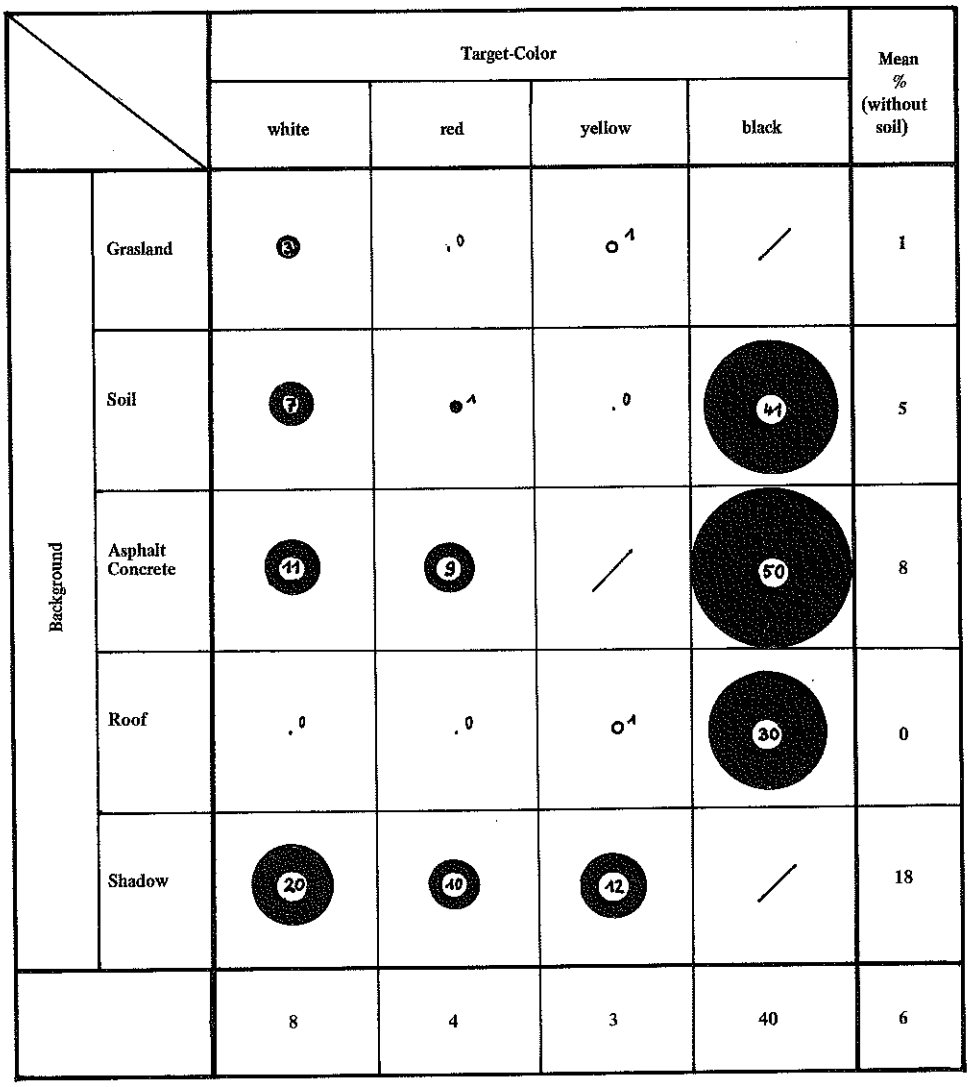

Figure 46 — Target colour/Background

7.4 Missing and precision of roof points

The precision of roof points was the subject of the OEEPE test, "Dordrecht" (OEEPE Publication No. 13: *Timmermann, Roos, Schürer, Förstner*, "On the Accuracy of Photogrammetric Measurements of Buildings").

The "Steinwedel" test does not discuss accuracy and precision of roof points in general but deals with potential differences in reliability and precision of roof-point measurements with different emulsions (see also Chapter 2.3.4).

The results of the restitutions are given in Figure 47. It is generally noted that the rate of missing roof points is substantially lower than that of signalized and topographical points. This is obvious from the fact that buildings are the most easy to identify even in bad aerial photos, and that measurement of roof points is possible here — even though the results are poorer.

The figure first shows the standard deviations of coordinates from the calculated values for the roof points; the next column shows the standard deviation of photogrammetrically derived roof distances (between parallel roof edges).

The roof corners and roof distances have a similar precision; the precision of the roof distances, which is better by 10—20 %, indicates that short distances do not include systematic image deformations. Because of the small variation and greater clarity in demonstrations it may be possible to state a "mean" value for the precision of photogrammetrically determined roof points in general.

The results imply the following conclusions:

As with signalized points:

- measurements with colour films are slightly — but not significantly — better than with black & white films;
- under overcast sky conditions the precision is about 50 % poorer and the level of reliability (missing points) is poorer still;
- no emulsion gives significantly different results from the other emulsions;
- because the precision of the roof distances is almost unaffected by systematic image deformation, these roof distances clearly imply that there are no significant differences between nine emulsions.

7.5 Missing and precision of topographical points

Thirty-two topographical points of different types were distributed in the test field (see Chapter 2.3.5), (Figure 48 and 49). In a first analysis of all the restitution results (Figure 50), all the points were analysed. A second analysis used only three selected groups of points with a similar shape:

6 foot points of walls and buildings,
5 corners of green vegetation (grassland, hedges),
6 borders between water and grassland.

Sun

Emulsion	Flight No.	Missing of points %	Precision [cm]		
			σ_k corners	σ_k distances	Mean
Standard					
Black & white		1	6	5	5
Pan 200	1	1	5.8	4.2	5
Plus-X	3	2	6.6	5.3	6
Double-X	4	1	5.3	3.9	5
Colour		2	5	4	4
Dia 2448	8	2	5.1	3.9	4
Dia 2448	9	1	5.0	3.3	4
Dia SO 397	11	2	5.6	4.1	5
Dia SO 397	12	2	5.3	3.4	4
Special					
Black & white					
Panatomic-X	6	0.5	5.9	4.0	5
High Definition	7	2	4.6	4.4	4
Colour					
Negative	16	1	4.4	4.5	4
Infrared	17	1	5.2	4.9	5
	Σ	1	5	4	5

Overcast sky

Standard					
Black & white		5	7	5	6
Pan 200	2	5	6.7	6.0	6
Double-X	5	5	6.7	4.2	6
Colour		4	7	7	8
Dia 2448	10	1	6.7	7.1	7
Dia SO 397	14	4	7.8	7.7	8
Dia SO 397	15	5	8.5	6.7	8
	Σ	4	7	6	7

Overexposed

Standard					
Colour					
Dia SO 397	13	7	6	6	6

Figure 47 — Missing and precision of roof points

For a l l points the following conclusions can be drawn:

- In sunshine the topographical points are equally perceptible and measurable for all emulsions; the number of missing points is the same for all emulsions. High Definition film is an exception, because this emulsion gives high contrast and thus "swallows" many details.
- In sunshine precision seems to be lower for black & white films, but not significantly, as there are only small differences between the emulsions, and these are greater than those between black & white and colour films.
- The best results of all are produced with infrared colour film.
- Under overcast conditions, there is a clear deterioration of the total result: the precision is worse by about 50 %, and the number of missing points increases by up to five times as many. Definite proof is lacking, however, that the better results with colour films are due to the colour emulsions.

From the s p e c i f i c investigation of the three selected groups of points (Figure 51) we can say:

- The results are similar to those of the general investigation.
- The results for the special emulsions (without High Definition) seem to be very good. Infrared colour film gives
  - as could be expected — a good result, especially for the borders between water and grassland. Even infrared colour film does not give better results than the other emulsions for green vegetation points.

SUNSHINE
Black & white Pan 200

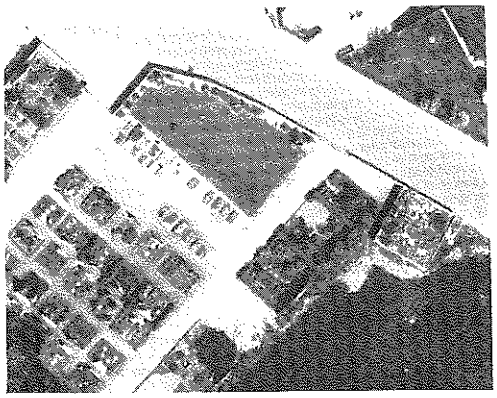

Colour Diapositiv 2448

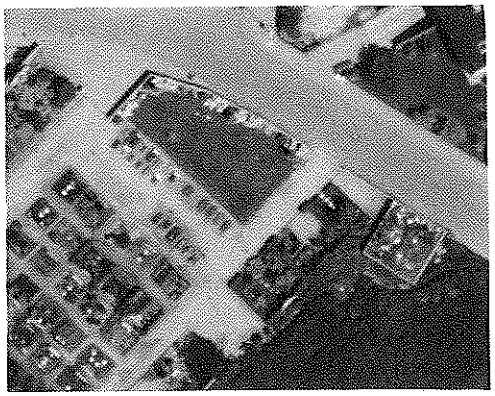

Panatomic-X

Colour infrared

OVERCAST SKY
Black & white Pan 200

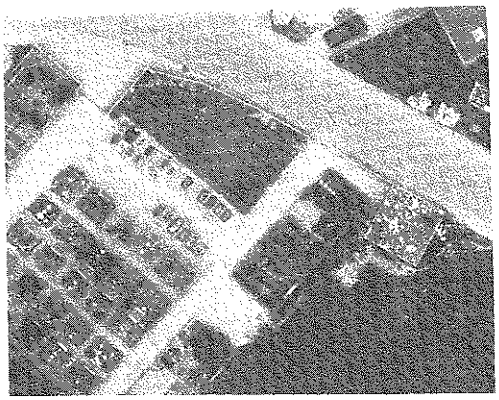

Colour Diapositiv 2448

Figure 48 — Topography in large-scale photographs, Type "Grassland corner"

SUNSHINE

Black & white Pan 200

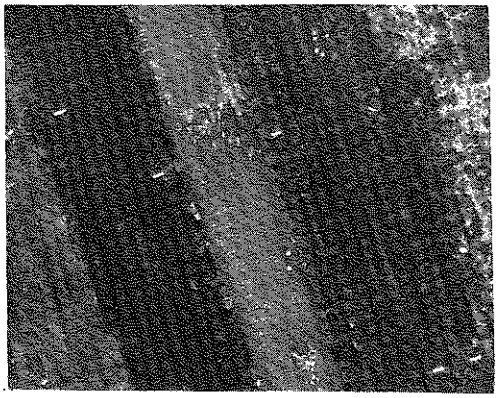

Colour Diapositiv 2448

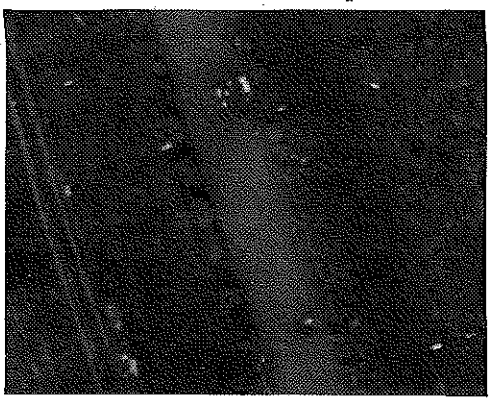

Panatomic-X

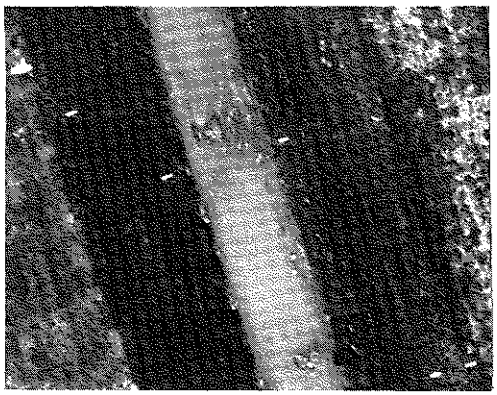

Colour infrared

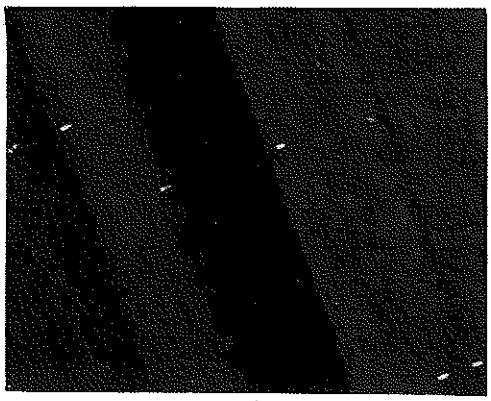

OVERCAST SKY

Black & white Pan 200

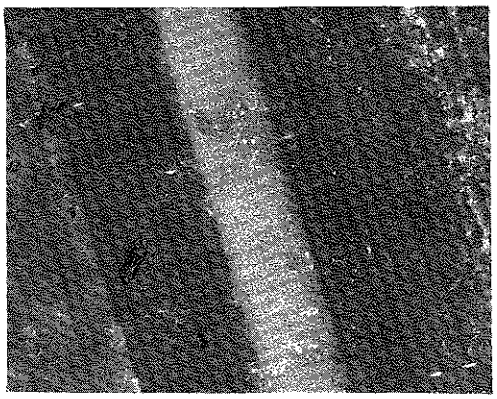

Colour Diapositiv 2448

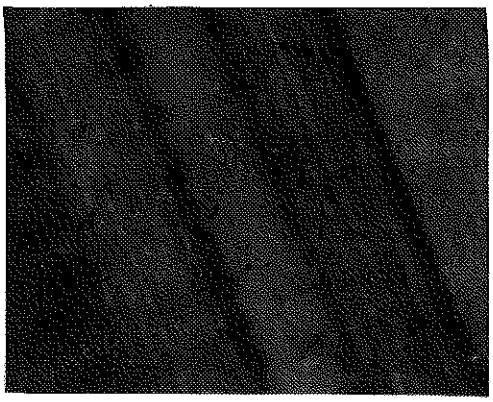

Figure 49 — Type "Water borderline"

Sun 

Emulsion	Flight No.	Number of		Missing points %	Precision σ_k [cm]
		models	resti-tutions		
Standard					
Black & white		7	11	3	17.5
Pan 200	1	3	6	2	19.8
Plus-X	3	2	2	3	15.2
Double-X	4	2	3	4	17.0
Colour		13	17	3	14.3
Dia 2448	8	2	2	3	12.7
Dia 2448	9	4	6	3	12.7
Dia SO 397	11	4	6	3	17.6
Dia SO 397	12	3	3	3	14.1
Special					
Black & white					
Panatomic-X	6	6	10	2	15.8
High Definition	7	4	6	6	17.0
Colour					
Negative	16	2	3	2	14.4
Infrared	17	5	6	1	13.0
	Σ	37	53	2	15

Overcast sky 

Standard					
Black & white		6	8	16	21.2
Pan 200	2	3	3	17	22.0
Double-X	5	3	5	15	20.2
Colour		8	11	11	23.3
Dia 2448	10	2	3	8	18.3
Dia SO 397	14	3	5	13	22.5
Dia SO 397	15	3	3	13	29.5
	Σ	14	19	13	22

Overexposed 

Standard					
Colour					
Dia SO 397	13	3	5	10	24.0

Figure 50 — Missing and precision of topographical points

Sun

Emulsion	Flight No.	Wall corners		Grassland-corners		Water-edges	
		%	σ_k [cm]	%	σ_k [cm]	%	σ_k [cm]
Standard							
Black & white		9	8	5	8	8	20
Pan 200	1	6	8	4	7	5	18
Plus-X	3	10	7	6	11	8	23
Double-X	4	12	8	5	7	10	21
Colour		7	7	7	9	7	19
Dia 2448	8	5	6	8	9	4	20
Dia 2448	9	10	6	10	9	10	18
Dia SO 397	11	6	8	4	10	5	23
Dia SO 397	12	8	7	7	9	6	17
Special							
Black & white							
Panatomic-X	6	4	6	0	6	2	18
High Definition	7	4	7	4	11	4	21
Colour							
Negative	16	8	6	3	8	0	18
Infrared	17	10	6	4	8	0	16
	Σ	8	7	6	8	6	19

Overcast sky

Standard							
Black & white		21	9	18	11	10	32
Pan 200	2	20	8	16	11	15	40
Double-X	5	22	10	20	11	5	25
Colour		25	9	12	12	13	38
Dia 2448	10	15	9	10	9	3	26
Dia SO 397	14	35	8	15	12	20	40
Dia SO 397	15	25	9	12	14	15	48
	Σ	23	9	15	11	12	35

Overexposed

Standard							
Colour							
Dia SO 397	13	40	12	5	11	35	35

Figure 51 — Missing and precision of selected topographical points

7.6 Summary of all results

This summary gives a general view of all the investigations of reliability of the "Steinwedel" test. For this the results for the films used and restituted are summarized and combined into groups (Figure 52).

The general view allows a comparison between black & white films and colour films, and a further comparison between standard films (black & white, colour) and special films. High Definition film is of no interest here, because it gives results which differ considerably from the average for the other films.

7.7 Conclusions for further investigations

- The photogrammetrical results of the "Steinwedel" test are not very uniform; as presented they will not provide further information about the differences in quality of different emulsions;

  this is true at least for black & white films and for standard film material colour films.

- If there are to be further restitutions, the specifications for plotting instruments and methods should be much more restricted; only analytical plotters should be used.

- In spite of the lack of significance in the differences in quality between black & white and the colour films, it is still not known whether there are economic advantages in for instance using colour films, or in finding topographical points by a quicker method than with colour films.

- Further investigations should be made of special emulsions. When setting up further tests with these emulsions the use of Forward Motion Compensation cameras should be tried.

- Also further interest is the question of what differences will be found between several flights using the same emulsion but different test fields of the same conception and arrangement.

- There are still no precise and definite criteria for judging the reliability of interpretation and identification.

- When awarding contracts for photo flights to companies and institutes more precise and rigorous conditions for exposure and film development should be prescribed.

Sun

Emulsion	Number of resti-tutions	Reliability missing points in %			Precision σ_k [cm]	
		Sign.	Roof	Top.	Roof	Top.
Standard						
Black & white	11	5	1	3	5	18
Colour	17	3	2	3	4	14
Special						
Black & white						
Panatomic	10	3	0.5	2	5	16
Colour						
Negativ	3	2	1	2	4	14
Infrared	6	2.5	1	1	5	13

Overcast sky

Standard						
Black & white	8	7	5	16	6	21
Colour	11	6	4	11	8	23

Overexposed

Standard						
Colour						
Dia SO 397	5	12	7	10	6	24

Figure 52 — General view of results

Light	General	Emulsions		
		Black & white films	Colour films	Special emulsions
Sun	With good illumination and with correct exposure there are no significant differences between the different emulsions. Special emulsions give certain advantages.	No significant difference between black & white and colour films. Colour films give slightly higher reliability for signalized points.		Special emulsions give at least as good results as black & white films; some are even better than colour films.
Overcast sky	Under overcast conditions the results are 2—4 times poorer. Points with a poorer structure suffer mostly from reduced light.	No significant difference between black & white and colour films. Colour films give slightly higher reliability; their precision seems to be slightly poorer than that of black & white films.		
Overexposed	Overexposure gives even poorer results than overcast conditions.			

Figure 53 — Summary of results

Appendix I

OEEPE-TEST "STEINWEDEL"

Instructions for restitution

1 General information

A test on "Optimal Emulsions for Large Scale Mapping" was included in the test programme of the OEEPE in 1981. The main objective of the test is to investigate whether or not there are significant overall differences, advantages and/or disadvantages in the use of different emulsions for the purpose of large scale mapping. The pre-studies and preparations for the test were carried out during the winter of 1981—1982. The test area "Steinwedel" (near Hannover, West Germany) was ready for use in May 1982. Details of the test field, such as lay-out, number and planimetric accuracy of the ground control points, groups of coloured targets, roof corners and topographic features, are shown in the map.

Aerial photographs were taken at a scale of 1 : 4000 (f= 30 cm) with nine different emulsions in May—June 1982. Most of the emulsions were used in both sunny and overcast weather. The detailed list of photographic material, as it can be made available for this test, is given.

The aim of this part of the investigation is to study the measuring accuracy of different targets and topographic features in large-scale photography using different emulsions, and to study their interpretation quality.

In addition, the influence of various colours used for targeting will be analysed. The first part of the investigation is carried out at two separate pilot centres:

- The photographic-physical quality of the photogrammetric material is studied at the EPF, Lausanne.
- The geometric quality of the film material and the measuring precision as a function of the imaging quality is treated by the National Board of Survey, Helsinki (measurements by stereo-comparator).

2 Restitution

2.1 The measuring instruments

The measurements should be carried out on precision stereo-plotters (analog instruments or analytical plotters) with numerical registration devices (not comparators). The size of the floating mark should not exceed 30 μm in photo scale.

Before measurements, the measuring instruments should be checked by grid-plate measurements. The calibration statutes have to be proved by monocular-grid-plate measuring (15—25 points, point spacing 5 cm).

2.2 *Observation procedure*

An total of 222 points should be measured stereoscopically in two independent series. A series of measurements consists, as a rule, of:

- 20 control points
- 114 signalized points
- 20 roof corners
- 34 roof edges
- 32 topographic features.

As a rule, the measuring sequence is free; nevertheless it is recommended that the indications in the joint map at a scale of 1 : 1000, be followed.

In particular it should be noticed that the topographic points Numbers 881—886 and 891—894 have to be measured a second time with numbers 635—644 as shown in the index map.

881	635	883	637	885	639	891	641	893	643
882	636	884	638	886	640	892	642	894	644

2.3 *Point number*

The point number are composed of three digits, e. g. 248, according to the following principles:

1. digit: 0 = Control point (in Planicomp it can be 9)
   1—4 = Signalized point (colour)
   5 = Roof corner
   6 = Roof edge
   8 = Topographical feature.
2. digit: According to the background of a target
   1 = Meadow
   2 = Bar soil
   3 = Asphalt or concrete
   4 = Red roof
   5 = Shadow.
3. digit: The high numbers marked on the 1 : 1000 map are the group numbers according to the location of the point and refer only to the signalized points.

2.4 *Quality judgement*

In the first measuring series, each point should be evaluated according to the pointing quality (according to its appearance in stereovision) by coding with a number placed immediately before the point number:

1 = not measurable
2 = hardly measurable
3 = measurable
4 = good
5 = excellent.

The points with quality code 1 will not be registered but they should be listed in special list attached (general remarks on the restitution).

The point number of the first series consequently has the following format:

2436: 2 = quality code,
436 = point number.

For the second serie the number has only 3 digits, e. g. 436.

2.5 *Transformation*

The coordinates measured should be transformed into ground coordinates by the Helmert transformation. The transformation has to be done separately for the two series of measurements. The transformed coordinates should be listed in the following form:

No	x	y	h
2147	442,601	639,633	7,219 (1. round)

In addition, the residuals, as well as the standard deviations of the control point coordinates after the Helmert transformation, should be listed.

The transformed coordinates should preferably be sent on magnetic tape in the following form:

1. Line (record): The combined check number (see 2.6).
2. Following lines (records): transformed coordinates: No, x, y, h

   Format: (I 13, 3F 12.3)

   Note: In each model, which consists of two rounds, the first point number is the combined check number with arbitrary x, y, h-coordinates (which will be eliminated later).

   Last records: grid-plate measurements, same format as before.

Tape marking: without label
9 channels
1600 BPI
EBCDIC—Code
records and blocks fixed
lenght: 1 block = 1 record = 80 characters
end two TAPE MARKS

2.6 The combined check number

The combined check number includes information on the operative centre, flight and model. It should be printed in the first row (see 2.5) and is composed of 12 digits in three parts:

1. part	: digits 1 and 2	: A code for each operative centre Hannover e. g. "01"
	3. digit	: Zero
2. part	: digits 4 and 5	: The flight number 01 . . . . 17 (see App.)
	6. digit	: Zero
3. part	: digits from 7 to 12:	The model number, e. g. 023025

Example: 010130023025

3 Communication

Each operative centre should complete the restitution work within about three weeks. After restitution and transformation the results are to be sent to the Pilot Centre:

Dr. *W. Brindöpke*
Landesvermessung
Warmbüchenkamp 2
D-3000 Hannover 1
Tel.: 05 11/16 73-260 or
/16 73-0

The package should include:

- 1 magnetic tape (see 2.5)
- Documentation of the transformations (see 2.5)
- Photographic material
- General information about the restitution
- Information on the state of calibration.

LIST OF THE OEEPE PUBLICATIONS

State — August 1985

A. Official publications

1 *Trombetti, C.:* „Activité de la Commission A de l'OEEPE de 1960 à 1964" — *Cunietti, M.:* „Activité de la Commission B de l'OEEPE pendant la période septembre 1960—janvier 1964" — *Förstner, R.:* „Rapport sur les travaux et les résultats de la Commission C de l'OEEPE (1960—1964)" — *Neumaier, K.:* „Rapport de la Commission E pour Lisbonne" — *Weele, A.J. v. d.:* „Report of Commission F." — Frankfurt a. M. 1964, 50 pages with 7 tables and 9 annexes.

2 *Neumaier, K.:* „Essais d'interprétation de »Bedford« et de »Waterbury«. Rapport commun établi par les Centres de la Commission E de l'OEEPE ayant participé aux tests" — „The Interpretation Tests of »Bedford« and »Waterbury«. Common Report Established by all Participating Centres of Commission E of OEEPE" — „Essais de restitution »Bloc Suisse«. Rapport commun établi par les Centres de la Commission E de l'OEEPE ayant participé aux tests" — „Test »Schweizer Block«. Joint Report of all Centres of Commission E of OEEPE." — Frankfurt a. M. 1966, 60 pages with 44 annexes.

3 *Cunietti, M.:* „Emploi des blocs de bandes pour la cartographie à grande échelle — Résultats des recherches expérimentales organisées par la Commission B de l'O.E.E.P.E. au cours de la période 1959—1966" — „Use of Strips Connected to Blocks for Large Scale Mapping — Results of Experimental Research Organized by Commission B of the O.E.E.P.E. from 1959 through 1966." — Frankfurt a. M. 1968, 157 pages with 50 figures and 24 tables.

4 *Förstner, R.:* „Sur la précision de mesures photogrammétriques de coordonnées en terrain montagneux. Rapport sur les résultats de l'essai de Reichenbach de la Commission C de l'OEEPE" — „The Accuracy of Photogrammetric Co-ordinate Measurements in Mountainous Terrain. Report on the Results of the Reichenbach Test Commission C of the OEEPE." — Frankfurt a. M. 1968, Part I: 145 pages with 9 figures; Part II: 23 pages with 65 tables.

5 *Trombetti, C.:* „Les recherches expérimentales exécutées sur de longues bandes par la Commission A de l'OEEPE." — Frankfurt a. M. 1972, 41 pages with 1 figure, 2 tables, 96 annexes and 19 plates.

6 *Neumaier, K.:* „Essai d'interprétation. Rapports des Centres de la Commission E de l'OEEPE." — Frankfurt a. M. 1972, 38 pages with 12 tables and 5 annexes.

7 *Wiser, P.:* „Etude expérimentale de l'aérotriangulation semi-analytique. Rapport sur l'essai »Gramastetten«." — Frankfurt a. M. 1972, 36 pages with 6 figures and 8 tables.

8 „Proceedings of the OEEPE Symposium on Experimental Research on Accuracy of Aerial Triangulation (Results of Oberschwaben Tests)"
Ackermann, F.: „On Statistical Investigation into the Accuracy of Aerial Triangulation. The Test Project Oberschwaben" — „Recherches statistiques sur la précision de l'aérotriangulation. Le champ d'essai Oberschwaben" — *Belzner, H.:* „The Planning. Establishing and Flying of the Test Field Oberschwaben" — *Stark, E.:* Testblock Oberschwaben, Programme I. Results of Strip Adjustments" — *Ackermann, F.:* „Testblock Oberschwaben, Program I. Results of Block-Adjustment by Independent Models" — *Ebner, H.:* Comparison of Different Methods of Block Adjustment" — *Wiser, P.:* „Propositions pour le traitement des erreurs non-accidentelles" — *Camps, F.:* „Résultats obtenus dans le cadre du project Oberschwaben 2A" — *Cunietti, M.; Vanossi, A.:* „Etude statistique expérimentale des erreurs d'enchaînement des photogrammes" — *Kupfer, G.:* „Image Geometry as Obtained from Rheidt Test Area Photography" — *Förstner, R.:* „The Signal-Field of Baustetten. A Short Report" — *Visser, J.; Leberl, F.; Kure, J.:* „OEEPE Oberschwaben Reseau Investigations" — *Bauer, H.:* „Compensation of Systematic Errors by Analytical Block Adjustment with Common Image Deformation Parameters." — Frankfurt a. M. 1973, 350 pages with 119 figures, 68 tables and 1 annex.

9 *Beck, W.:* „The Production of Topographic Maps at 1 : 10,000 by Photogrammetric Methods. — With statistical evaluations, reproductions, style sheet and sample fragments by Landesvermessungsamt Baden-Württemberg, Stuttgart." — Frankfurt a. M. 1976, 89 pages with 10 figures, 20 tables and 20 annexes.

10 „Résultats complémentaires de l'essai d'«Oberriet» de la Commission C de l'OEEPE — Further Results of the Photogrammetric Tests of «Oberriet» of the Commission C of the OEEPE"
Härry, H.: „Mesure de points de terrain non signalisés dans le champ d'essai d'«Oberriet» — Measurements of Non-Signalized Points in the Test Field «Oberriet» (Abstract)" — *Stickler, A.; Waldhäusl, P.:* „Restitution graphique des points et des lignes non signalisés et leur comparaison avec des résultats de mesures sur le terrain dans le champ d'essai d'«Oberriet» — Graphical Plotting of Non-Signalized Points and Lines, and Comparison with Terrestrial Surveys in the Test Field «Oberriet»" — *Förstner, R.:* „Résultats complémentaires des transformations de coordonnées de l'essai d'«Oberriet» de la Commission C de l'OEEPE — Further Results from Co-ordinate Transformations of the Test «Oberriet» of Commission C of the OEEPE" — *Schürer, K.:* „Comparaison des distances d'«Oberriet» — Comparison of Distances of «Oberriet» (Abstract)." — Frankfurt a. M. 1975, 158 pages with 22 figures and 26 tables.

11 „25 années de l'OEEPE"
Verlaine, R.: „25 années d'activité de l'OEEPE" — „25 Years of OEEPE (Summary)" — *Baarda, W.:* „Mathematical Models." — Frankfurt a. M. 1979, 104 pages with 22 figures.

12 *Spiess, E.:* „Revision of 1 : 25,000 Topographic Maps by Photogrammetric Methods." — Frankfurt a. M. 1985, 228 pages with 102 figures and 30 tables.

13 *Timmerman, J.; Roos, P. A.; Schürer, K.; Förstner, R.:* On the Accuracy of Photogrammetric Measurements of Buildings – Report on the Results of the Test "Dordrecht", Carried out by Commission C of the OEEPE. – Frankfurt a. M. 1982, 144 pages with 14 figures and 36 tables.

14 *Thompson, C. N.:* Test of Digitising Methods. – Frankfurt a. M. 1984, 120 pages with 38 figures and 18 tables.

B. Special publications

— Special Publications O.E.E.P.E. — Number I

Solaini, L.; Trombetti, C.: Relation sur les travaux préliminaires de la Commission A (Triangulation aérienne aux petites et aux moyennes échelles) de l'Organisation Européenne d'Etudes Photogrammétriques Expérimentales (O.E.E.P.E.). I^{ère} Partie: Programme et organisation du travail. — *Solaini, L.; Belfiore, P.:* Travaux préliminaires de la Commission B de l'Organisation Européenne d'Etudes Photogrammétriques Expérimentales (O.E.E.P.E.) (Triangulations aériennes aux grandes échelles). — *Solaini, L.; Trombetti, C.; Belfiore, P.:* Rapport sur les travaux expérimentaux de triangulation aérienne exécutés par l'Organisation Européenne d'Etudes Photogrammétriques Expérimentales (Commission A et B). — *Lehmann, G.:* Compte rendu des travaux de la Commission C de l'O.E.E.P.E. effectués jusqu'à présent. — *Gotthardt, E.:* O.E.E.P.E. Commission C. Compte-rendu de la restitution à la Technischen Hochschule, Stuttgart, des vols d'essai du groupe I du terrain d'Oberriet. — *Brucklacher, W.:* Compte-rendu du centre «Zeiss-Aerotopograph» sur les restitutions pour la Commission C de l'O.E.E.P.E. (Restitution de la bande de vol, groupe I, vol. No. 5). — *Förstner, R.:* O.E.E.P.E. Commission C. Rapport sur la restitution effectuée dans l'Institut für Angewandte Geodäsie, Francfort sur le Main. Terrain d'essai d'Oberriet les vols No. 1 et 3 (groupe I). — I.T.C., Delft: Commission C, O.E.E.P.E. Déroulement chronologique des observations. — Photogrammetria XII (1955—1956) 3, Amsterdam 1956, pp. 79—199 with 12 figures and 11 tables.

— Publications spéciales de l'O.E.E.P.E. — Numéro II

Solaini, L.; Trombetti, C.: Relations sur les travaux préliminaires de la Commission A (Triangulation aérienne aux petites et aux moyennes échelles) de l'Organisation Européenne d'Etudes Photogrammétriques Expérimentales (O.E.E.P.E.). 2^{e} partie. Prises de vues et points de contrôle. — *Gotthardt, E.:* Rapport sur les premiers résultats de l'essai d'«Oberriet» de la Commission C de l'O.E.E.P.E. — Photogrammetria XV (1958—1959) 3, Amsterdam 1959, pp. 77—148 with 15 figures and 12 tables.

— *Trombetti, C.:* Travaux de prises de vues et préparation sur le terrain effectuées dans le 1958 sur le nouveau polygone italien pour la Commission A de l'OEEPE. — Florence 1959, 16 pages with 109 tables.

— *Trombetti, C.; Fondelli, M.:* Aérotriangulation analogique solaire. — Firence 1961, 111 pages, with 14 figures and 43 tables.

— Publications spéciales de l'O.E.E.P.E. — Numéro III

Solaini, L.; Trombetti, C.: Rapport sur les résultats des travaux d'enchaînement et de compensation exécutés pour la Commission A de l'O. E. E. P. E. jusqu'au mois de Janvier 1960. Tome 1: Tableaux et texte. Tome 2: Atlas. — Photogrammetria XVII (1960—1961) 4, Amsterdam 1961, pp. 119—326 with 69 figures and 18 tables.

— „OEEPE — Sonderveröffentlichung Nr. 1"

Gigas, E.: „Beitrag zur Geschichte der Europäischen Organisation für photogrammetrische experimentelle Untersuchungen" — *N. N.:* „Vereinbarung über die Gründung einer Europäischen Organisation für photogrammetrische experimentelle Untersuchungen" — „Zusatzprotokoll" — *Gigas, E.:* „Der Sechserausschuß" — *Brucklacher, W.:* „Kurzbericht über die Arbeiten in der Kommission A der OEEPE" — *Cunietti, M.:* „Kurzbericht des Präsidenten der Kommission B über die gegenwärtigen Versuche und Untersuchungen" — *Förstner, R.:* „Kurzbericht über die Arbeiten in der Kommission B der OEEPE" — „Kurzbericht über die Arbeiten in der Kommission C der OEEPE" — *Belzner, H.:* „Kurzbericht über die Arbeiten in der Kommission E der OEEPE" — *Schwidefsky, K.:* „Kurzbericht über die Arbeiten in der Kommission F der OEEPE" — *Meier, H.-K.:* „Kurzbericht über die Tätigkeit der Untergruppe „Numerische Verfahren" in der Kommission F der OEEPE" — *Belzner, H.:* „Versuchsfelder für internationale Versuchs- und Forschungsarbeiten." — Nachr. Kt.- u. Vermesss.-wes., R. V, Nr. 2, Frankfurt a. M. 1962, 41 pages with 3 tables and 7 annexes.

— *Rinner, K.:* Analytisch-photogrammetrische Triangulation eines Teststreifens der OEEPE. — Österr. Z. Vermess.-wes., OEEPE-Sonderveröff. Nr. 1, Wien 1962, 31 pages.

— *Neumaier, K.; Kasper, H.:* Untersuchungen zur Aerotriangulation von Überweitwinkelaufnahmen. — Österr. Z. Vermess.-wes., OEEPE-Sonderveröff. Nr. 2, Wien 1965, 4 pages with 4 annexes.

— „OEEPE — Sonderveröffentlichung Nr. 2"

Gotthardt, E.: „Erfahrungen mit analytischer Einpassung von Bildstreifen." — Nachr. Kt.- u. Vermess.-wes., R. V, Nr. 12, Frankfurt a. M. 1965, 14 pages with 2 figures and 7 tables.

— „OEEPE — Sonderveröffentlichung Nr. 3"

Neumaier, K.: „Versuch »Bedford« und »Waterbury«. Gemeinsamer Bericht aller Zentren der Kommission E der OEEPE" — „Versuch »Schweizer Block«. Gemeinsamer Bericht aller Zentren der Kommission E der OEEPE." — Nachr. Kt.- u. Vermess.-wes., R. V, Nr. 13, Frankfurt a. M. 1966, 30 pages with 44 annexes.

— *Stickler, A.; Waldhäusl, P.:* Interpretation der vorläufigen Ergebnisse der Versuche der Kommission C der OEEPE aus der Sicht des Zentrums Wien. — Österr. Z. Vermess.-wes., OEEPE-Sonderveröff. (Publ. Spēc.) Nr. 3, Wien 1967, 4 pages with 2 figures and 9 tables.

— „OEEPE — Sonderveröffentlichung Nr. 4"

Schürer, K.: „Die Höhenmeßgenauigkeit einfacher photogrammetrischer Kartiergeräte. Bemerkungen zum Versuch »Schweizer Block« der Kommission E der OEEPE." — Nachr. Kt.- u. Vermess.-wes., Sonderhefte, Frankfurt a. M., 1968, 25 pages with 7 figures and 3 tables.

— „OEEPE — Sonderveröffentlichung Nr. 5"

Förstner, R.: „Über die Genauigkeit der photogrammetrischen Koordinatenmessung in bergigem Gelände. Bericht über die Ergebnisse des Versuchs Reichenbach der Kommission C der OEEPE." — Nachr. Kt.- u. Vermess.-wes., Sonderhefte, Frankfurt a. M. 1969, Part I: 74 pages with 9 figures; Part II: 65 tables.

— „OEEPE — Sonderveröffentlichung Nr. 6"

Knorr, H.: „Die Europäische Organisation für experimentelle photogrammetrische Untersuchungen — OEEPE — in den Jahren 1962 bis 1970." — Nachr. Kt.- u. Vermess.-wes., Sonderhefte, Frankfurt a. M. 1971, 44 pages with 1 figure and 3 tables.

— „OEEPE — Sonderveröffentlichung Nr. D–7"

Förstner, R.: „Das Versuchsfeld Reichenbach der OEEPE." — Nachr. Kt.- u. Vermess.-wes., Sonderhefte, Frankfurt a. M. 1972, 191 pages with 49 figures and 38 tables.

— „OEEPE — Sonderveröffentlichung Nr. D–8"

Neumaier, K.: „Interpretationsversuch. Berichte der Zentren der Kommission E der OEEPE." — Nachr. Kt.- u. Vermess.-wes., Sonderhefte, Frankfurt a. M. 1972, 33 pages with 12 tables and 5 annexes.

— „OEEPE — Sonderveröffentlichung Nr. D–9"

Beck, W.: „Herstellung topographischer Karten 1 : 10 000 auf photogrammetrischem Weg. Mit statistischen Auswertungen, Reproduktionen, Musterblatt und Kartenmustern des Landesvermessungsamts Baden-Württemberg, Stuttgart." — Nachr. Kt.- u. Vermess.-wes., Sonderhefte, Frankfurt a. M. 1976, 65 pages with 10 figures, 20 tables and 20 annexes.

— „OEEPE — Sonderveröffentlichung Nr. D–10"

Weitere Ergebnisse des Meßversuchs „Oberriet" der Kommission C der OEEPE. *Härry, H.:* „Messungen an nicht signalisierten Geländepunkten im Versuchsfeld «Oberriet»" — *Stickler, A.; Waldhäusl, P.:* „Graphische Auswertung nicht signalisierter Punkte und Linien und deren Vergleich mit Feldmessungsergebnissen im Versuchsfeld «Oberriet»" — *Förstner, R.:* „Weitere Ergebnisse aus Koordinatentransformationen des Versuchs «Oberriet» der Kommission C der OEEPE" — *Schürer, K.:* „Streckenvergleich «Oberriet»." — Nachr. Kt.- u. Vermess.-wes., Sonderhefte, Frankfurt a. M. 1975, 116 pages with 22 figures and 26 tables.

— „OEEPE — Sonderveröffentlichung Nr. D–11"

Schulz, B.-S.: „Vorschlag einer Methode zur analytischen Behandlung von Reseauaufnahmen." — Nachr. Kt.- u. Vermess.-wes., Sonderhefte, Frankfurt a. M. 1976, 34 pages with 16 tables.

— „OEEPE — Sonderveröffentlichung Nr. D–12"

Verlaine, R.: „25 Jahre OEEPE." — Nachr. Kt.- u. Vermess.-wes., Sonderhefte, Frankfurt a. M. 1980, 53 pages.

— „OEEPE — Sonderveröffentlichung Nr. D–13"

Haug, G.: „Bestimmung und Korrektur systematischer Bild- und Modelldeformationen in der Aerotriangulation am Beispiel des Testfeldes „Oberschwaben." — Nachr. Kt.- u. Vermess.-wes., Sonderhefte, Frankfurt a. M. 1980, 136 pages with 25 figures and 51 tables.

— „OEEPE — Sonderveröffentlichung Nr. D—14"

Spiess, E.: „Fortführung der Topographischen Karte 1 : 25 000 mittels Photogrammetrie" (in Vorbereitung).

— „OEEPE — Sonderveröffentlichung Nr. D—15"

Timmerman, J.; Roos, P. A.; Schürer, K.; Förstner, R.: „Über die Genauigkeit der photogrammetrischen Gebäudevermessung. Bericht über die Ergebnisse des Versuchs Dordrecht der Kommission C der OEEPE." — Nachr. Kt.- u. Vermess.-wes., Sonderhefte, Frankfurt a. M. 1983, 131 pages with 14 figures and 36 tables.

C. Congress reports and publications in scientific reviews

— *Stickler, A.:* Interpretation of the Results of the O.E.E.P.E. Commission C. — Photogrammetria XVI (1959—1960) 1, pp. 8—12, 3 figures, 1 annexe (en langue allemande: pp. 12—16).

— *Solaini, L.; Trombetti, C.:* Results of Bridging and Adjustment Works of the Commission A of the O.E.E.P.E. from 1956 to 1959. — Photogrammetria XVI (1959—1960) 4 (Spec. Congr.-No. C), pp. 340—345, 2 tables.

— *N. N.:* Report on the Work Carried out by Commission B of the O.E.E.P.E. During the Period of September 1956—August 1960. — Photogrammetria XVI (1959—1960) 4 (Spec. Congr.-No. C), pp. 346—351, 2 tables.

— *Förstner, R.:* Bericht über die Tätigkeit und Ergebnisse der Kommission C der O.E.E.P.E. (1956—1960). — Photogrammetria XVI (1959—1960) 4 (Spec. Congr.-No. C), pp. 352—357, 1 table.

— *Bachmann, W. K.:* Essais sur la précision de la mesure des parallaxes verticales dans les appareils de restitution du I^{er} ordre. — Photogrammetria XVI (1959—1960) 4 (Spec. Congr.-No. C), pp. 358—360).

— *Wiser, P.:* Sur la reproductibilité des erreurs du cheminement aérien. — Bull. Soc. Belge Photogramm., No. 60, Juin 1960, pp. 3—11, 2 figures, 2 tables.

— *Cunietti, M.:* L'erreur de mesure des parallaxes transversales dans les appareils de restitution. — Bull. Trimestr. Soc. Belge Photogramm., No. 66, Décembre 1961, pp. 3—50, 12 figures, 22 tables.

— „OEEPE — Arbeitsberichte 1960/64 der Kommissionen A, B, C, E, F"

Trombetti, C.: „Activité de la Commission A de l'OEEPE de 1960 à 1964" — *Cunietti, M.:* „Activité de la Commission B de l'OEEPE pendant la période septembre 1960—janvier 1964" — *Förstner, R.:* „Rapport sur les travaux et les résultats de la Commission C de l'OEEPE (1960—1964)" — *Neumaier, K.:* „Rapport de la Commission E pour Lisbonne" — *Weele, A. J. van der:* „Report of Commission F." — Nachr. Kt.- u. Vermess.-wes., R. V. Nr. 11, Frankfurt a. M. 1964, 50 pages with 7 tables and 9 annexes.

— *Cunietti, M.; Inghilleri, G.; Puliti, M.; Togliatti, G.:* Participation aux recherches sur les blocs de bandes pour la cartographie à grande échelle organisées par la Commission B de l'OEEPE. Milano, Centre CASF du Politecnico. — Boll. Geod. e Sc. affini (XXVI) 1, Firenze 1967, 104 pages.

— *Gotthardt E.:* Die Tätigkeit der Kommission B der OEEPE. — Bildmess. u. Luftbildwes. 36 (1968) 1, pp. 35—37.

— *Cunietti, M.:* Résultats des recherches expérimentales organisées par la Commission B de l'OEEPE au cours de la période 1959—1966. Résumé du Rapport final. — Présenté à l'XI^{e} Congrès International de Photogrammétrie, Lausanne 1968, Comm. III (en langues française et anglaise), 9 pages.

- *Förstner, R.:* Résumé du Rapport sur les résultats de l'essai de Reichenbach de la Commission C de l'OEEPE. — Présenté à l'XI[e] Congrès International de Photogrammétrie, Lausanne 1968, Comm. IV (en langues française, anglaise et allemande), 28 pages, 2 figures, 2 tables.
- *Timmerman, J.:* Proef „OEEPE-Dordrecht". — ngt 74, 4. Jg., Nr. 6, Juni 1974, S. 143—154 (Kurzfassung: Versuch „OEEPE-Dordrecht". Genauigkeit photogrammetrischer Gebäudevermessung. Vorgelegt auf dem Symposium der Kommission IV der I.G.P., Paris, 24.—26. September 1974).
- *Timmerman, J.:* Report on the Commission C. "OEEPE-Dordrecht" Experiment. — Presented Paper for Comm. IV, XIII[th] Congress of ISP, Helsinki 1976.
- *Beck, W.:* Rapport de la Commission D de l'OEEPE sur l'établissement de cartes topographiques au 1/10 000 selon le procédé photogrammétrique. — Presented Paper for Comm. IV, XIII[th] Congress of ISP, Helsinki 1976.
- *Verlaine, R.:* La naissance et le développement de l'OEEPE — Festschrift — Dr. h. c. *Hans Härry*, 80 Jahre — Schweizerische Gesellschaft für Photogrammetrie und Wild Heerbrugg AG, Bern 1976.
- *Förstner, R.:* Internationale Versuche (Essais contrôlés) — Festschrift — Dr. h. c. *Hans Härry*, 80 Jahre. — Schweizerische Gesellschaft für Photogrammetrie und Wild Heerbrugg AG, Bern 1976.
- *Baj, E.; Cunietti, M.; Vanossi, A.:* Détermination Expérimentale des Erreurs Systématiques des Faisceaux Perspectifs. — Société Belge de Photogrammétrie, Bulletin trimestriel, Brüssel 1977, pp 21—49.
- *Timmerman, J.:* Fotogrammetrische stadskaartering de OEEPE-proef Dordrecht. — Geodesia 19, Amsterdam 1977, pp. 291—298.
- *Waldhäusl, P.:* The Vienna Experiment of the OEEPE/C. Proceedings — Standards and Specifications for Integrated Surveying and Mapping Systems. — Schriftenreihe HSBw, Heft 2, München 1978.
- *Bachmann, W. K.:* Recherches sur la stabilité des appareils de restitution photogrammétriques analogiques. — Vermessung, Photogrammetrie, Kulturtechnik, Zürich 1978, pp. 265—268.
- *Parsic, Z.:* Untersuchungen über den Einfluß signalisierter und künstlicher Verknüpfungspunkte auf die Genauigkeit der Blocktriangulation. — Vermessung, Photogrammetrie, Kulturtechnik, Zürich 1978, pp. 269—278.
- *Waldhäusl, P.:* Der Versuch Wien der OEEPE/C. — Geowissenschaftliche Mitteilungen der Studienrichtung Vermessungswesen der TU Wien, Heft 13, Wien 1978, pp. 101—124.
- *Waldhäusl, P.:* Ergebnisse des Versuches Wien der OEEPE/C. — Presented Paper for Comm. IV, XIV[th] Congress of ISP, Hamburg 1980.
- *Timmerman, J.; Förstner, R.:* Kurzbericht über die Ergebnisse des Versuchs Dordrecht der Kommission C der OEEPE. — Presented Paper for Comm. IV, XIV[th] Congress of ISP, Hamburg 1980.

— *Bachmann, W. K.:* Elimination des valeurs erronées dans un ensemble de mesures controlées. — Papers written in honor of the 70th birthday of Professor *Luigi Solaini* — Richerche di Geodesia Topografia e Fotogrammetria, Milano 1979, pp. 27—39.

— *Visser, J.:* The European Organisation for Experimental Photogrammetric Research (OEEPE) — The Thompson Symposium 1982. — The Photogrammetric Record, London 1982, pp. 654—668.

— *Spiess, E.:* Revision of Topographic Maps: Photogrammetric and Cartographic Methods of the Fribourg Test. — The Photogrammetric Record, London 1983, pp. 29—42.

— *Jerie, H.G. and Holland, E.W.:* Cost model project for photogrammetric processes: a progress report. — ITC Journal, Enschede 1983, pp. 154—159.

— *Ackermann, F. E.* (Editor): Seminar — Mathematical Models of Geodetic/Photogrammetric Point Determination with Regard to Outliers and Systematic Errors — Working Group III/1 of ISP — Commission A of OEEPE. — Deutsche Geodätische Kommission bei der Bayerischen Akademie der Wissenschaften, Reihe A, Heft Nr. 98, München 1983.

— *Brindöpke, W., Jaakkola, M., Noukka, P., Kölbl, O.:* Optimal Emulsions for Large Scale Mapping — OEEPE—Commission C. — Presented Paper for Comm. I, XVth Congress of ISPRS, Rio de Janeiro 1984.

— *Ackermann, F.:* Report on the Activities of Working Group III/1 During 1980—84. — Comm. III, XVth Congress of ISPRS, Rio de Janeiro 1984.

— *Förstner, W.:* Results of Test 2 on Gross Error Detection of ISP WG III/1 and OEEPE. — Comm. III, XVth Congress of ISPRS, Rio de Janeiro 1984.

— *Gros, G.:* Modèles Numériques Altimétriques — Lignes Characteristiques — OEEPE Commission B. — Comm. III, XVth Congress of ISPRS, Rio de Janeiro 1984.

— *Ducher, G.:* Preparation d'un Essai sur les Ortho- et Stereo-Orthophotos. — Comm. IV, XVth Congress of ISPRS, Rio de Janeiro 1984.

— *van Zuylen, L.:* The influence of reproduction methods on the identification of details in orthophoto maps. — ITC Journal, Enschede 1984, pp. 219—226.

— *Brindöpke, W., Jaakkola, M., Noukka, P., Kölbl, O.:* Optimale Emulsionen für großmaßstäbige Auswertungen. — Bildmess. u. Luftbildw. 53 (1985) 1, pp. 23—35.

The official publications and the special publications issued in Frankfurt a. M. are for sale at the

Institut für Angewandte Geodäsie
— Außenstelle Berlin —

Stauffenbergstraße 11—13, D-1000 Berlin 30

Organisation Européenne d'Etudes Photogrammétriques Expérimentales

Publications officielles

Content